

University of Nebraska - Lincoln

DigitalCommons@University of Nebraska - Lincoln

---

Public Access Theses and Dissertations from the  
College of Education and Human Sciences

Education and Human Sciences, College of (CEHS)

---

Winter 12-1-2015

# Mechanisms by which dietary ellagic acid attenuates obesity and obesity-mediated metabolic complications

Inhae Kang

University of Nebraska-Lincoln, [ihkang0224@huskers.unl.edu](mailto:ihkang0224@huskers.unl.edu)

Follow this and additional works at: <http://digitalcommons.unl.edu/cehsdiss>

 Part of the [Digestive, Oral, and Skin Physiology Commons](#), [Endocrinology, Diabetes, and Metabolism Commons](#), [Food Science Commons](#), [Human and Clinical Nutrition Commons](#), [Medical Nutrition Commons](#), [Molecular, Genetic, and Biochemical Nutrition Commons](#), [Nutritional and Metabolic Diseases Commons](#), [Nutritional Epidemiology Commons](#), [Other Medical Specialties Commons](#), and the [Other Medicine and Health Sciences Commons](#)

---

Kang, Inhae, "Mechanisms by which dietary ellagic acid attenuates obesity and obesity-mediated metabolic complications" (2015). *Public Access Theses and Dissertations from the College of Education and Human Sciences*. 252. <http://digitalcommons.unl.edu/cehsdiss/252>

This Article is brought to you for free and open access by the Education and Human Sciences, College of (CEHS) at DigitalCommons@University of Nebraska - Lincoln. It has been accepted for inclusion in Public Access Theses and Dissertations from the College of Education and Human Sciences by an authorized administrator of DigitalCommons@University of Nebraska - Lincoln.

MECHANISMS BY WHICH DIETARY ELLAGIC ACID ATTENUATES OBESITY  
AND OBESITY-MEDIATED METABOLIC COMPLICATIONS

by

Inhae Kang

A DISSERTATION

Presented to the Faculty of

The Graduate College at the University of Nebraska

In Partial Fulfillment of Requirements

For the Degree of Doctor of Philosophy

Major: Interdepartmental Area of Nutrition

Under the Supervision of Professor Soonkyu Chung

Lincoln, Nebraska

November, 2015

MECHANISMS BY WHICH DIETARY ELLAGIC ACID ATTENUATES OBESITY  
AND OBESITY-MEDIATED METABOLIC COMPLICATIONS

Inhae Kang, Ph.D.

University of Nebraska, 2015

Advisor: Soonkyu Chung

Ellagic acid (EA) is a polyphenol found in various fruits and plants, such as berries, pomegranates, muscadine grapes, nuts and bark of oak tree. EA has been known to exhibit anti-inflammatory and anti-proliferative effects in various types of cancer. However, little is known about the effects of EA on obesity. Herein, 1) the lipid-lowering role of EA was identified in primary human adipose stem cells (*hASCs*) and human hepatoma Huh7 cells; 2) the molecular mechanisms by which EA attenuates adipogenesis by epigenetic modification were identified; 3) the effects of EA on high fat and high sucrose-mediated obesity was determined in young C57BL/6J mice; and 4) the potential role of urolithins (Uro), metabolites of EA, in attenuating adipogenesis and lipogenesis of adipocytes were investigated.

In this dissertation research, I firstly identified the novel inhibitory roles of EA on hypertrophic (increase in fat cell size) or hyperplastic (new fat cell formation) adipocyte expansion. 10  $\mu\text{M}$  of EA treatment significantly repressed hypertrophic lipid accumulation by inhibiting *de novo* lipogenesis of fatty acid in mature adipocytes. The anti-lipogenic effects of EA was also confirmed in Huh7 cells. EA were able to reverse the exogenous fatty acid-induced hepatic triglyceride (TG) accumulation by increasing  $\beta$ -oxidation. These results suggested that EA exerts TG-lowering effects both in adipose

tissue and liver. Intriguingly, EA were also able to repress adipogenic conversion of *hASCs* by blocking early adipogenic markers. Since epigenetic modification has been recently revealed to be a key mechanism regulating adipocyte differentiation, chromatin modifying enzymes were measured. Inhibition of adipogenic conversion of EA was accompanied with augmentation of histone deacetylase (HDAC) 9 and reduction of histone methyltransferase (coactivator associated arginine methyltransferase 1, CARM1) activity. Next, we confirmed lipid-lowering effects of EA *in vivo*. High fat and high sucrose diet for 12 weeks resulted in a significantly increase in; 1) body weight, 2) plasma cholesterol and TG levels, 3) hepatic endoplasmic reticulum (ER)/oxidative stress, and 4) adipose inflammation, which were normalized by EA-containing raspberry seed flour (RSF) supplementation without altering food intake. Furthermore, systemic levels of glucose and insulin tolerance and hepatic insulin sensitivity were improved by RSF. Finally, to determine whether Uro, gut microbiota-derived metabolites from of EA, displays anti-adipogenic and anti-lipogenic effects of EA in adipocytes, UroA, B, C, D, and iso-UroA were added to differentiating and differentiated *hASCs*. UroA, C and D are biologically active gut metabolites of EA exerting potent lipid-lowering effects in adipocyte similar to EA. Overall, these data suggest that EA is a potent dietary factor to attenuate obesity and Uro may be novel metabolites manifesting EA's effects.

## ACKNOWLEDGEMENTS

I would like to express my sincere appreciation to Dr. Soonkyu Chung for providing me the opportunity to extend my education. Dr. Chung not only provided me great number of bio-techniques, but also, most importantly, taught me the way of critical thinking and abilities to learn new technologies, optimize protocols and solve problems. I also want to extend appreciation to my committee members for their valuable contribution to my dissertation work: Dr. Janos Zemleni, Dr. Qiaozhu Su, and Dr. Jaekwon Lee.

In addition to the important role Dr. Chung played in my training, many others were crucial for my growth as a researcher. All lab members at UF and UNL that have helped me in different ways and are in need of recognition are Jung-Heun Ha, Lu Zhao, Meshail Okla, MeeAe Lee, Wei Wang, Ji-Young Kim, YongEun Kim, Teresa Buckner, and Mohammed Alquraishi.

Finally, I express my deepest gratitude to the most important people in my life, my parents, husband Jaeyoon, and son who inspire me with endless love.

Inhae Kang

November, 2015

# TABLE OF CONTENTS

<b>LIST OF FIGURES</b>	<b>VII</b>
<b>LIST OF TABLES</b>	<b>X</b>
<b>I. INTRODUCTION: REVIEW LITERATURES</b>	<b>1</b>
<i>Bioavailability of EA</i>	4
EFFECTS OF EA ON OBESITY	6
<i>In vitro evidence</i>	6
<i>In vivo evidence</i>	8
<i>Mechanisms involved in anti-obesity effects of EA</i>	15
IMPLICATIONS AND CONCLUSION	20
REFERENCES	22
<b>HYPOTHESIS AND SPECIFIC AIMS</b>	<b>27</b>
<b>II. CHAPTER I: ELLAGIC ACID MODULATES LIPID ACCUMULATION IN PRIMARY HUMAN ADIPOCYTES AND HUMAN HEPATOMA HUH7 CELLS VIA DISTINCT MECHANISMS</b>	<b>29</b>
ABSTRACT	30
1. INTRODUCTION	31
2. MATERIALS AND METHODS	32
3. RESULTS	37
4. DISCUSSION	42
REFERENCES	55

<b>III. CHAPTER II: ELLAGIC ACID INHIBITS ADIPOCYTE DIFFERENTIATION THROUGH COACTIVATOR ASSOCIATED ARGININE METHYLTRANSFERASE 1-MEDIATED CHROMATIN MODIFICATION</b>	<b>58</b>
ABSTRACT	59
1. INTRODUCTION	60
2. MATERIALS AND METHODS	62
3. RESULTS	67
4. DISCUSSION	70
REFERENCES	82
<b>IV. CHAPTER III: RASPBERRY SEED FLOUR ATTENUATES HIGH SUCROSE DIET-MEDIATED HEPATIC STRESS AND ADIPOSE TISSUE INFLAMMATION</b>	<b>86</b>
ABSTRACT	87
1. INTRODUCTION	88
2. MATERIALS AND METHODS	89
3. RESULTS	95
4. DISCUSSION	101
REFERENCES	124
<b>V. CHAPTER IV: UROLITHIN A, C AND D, BUT NOT ISO-UROLITHIN A AND UROLITHIN B, ATTENUATE TRIGLYCERIDE ACCUMULATION IN PRIMARY CULTURES OF HUMAN ADIPOCYTES</b>	<b>128</b>
1 INTRODUCTION	130

2 MATERIALS AND METHODS	131
3 RESULTS	135
4 DISCUSSION	138
REFERENCES	154
<b>OUTLOOK</b>	<b>159</b>

## LIST OF FIGURES

### I. INTRODUCTION: REVIEW LITERATURES

- Figure I-1 Schematic diagram showing that factors affect the pathogenesis of obesity. Obesity is accompanied by oxidative stress, inflammation, and dyslipidemia, which synergistically progress to obesity-related diseases, type 2 diabetes and NAFLD..... 2
- Figure I-2 Yearly number of publications related to EA from 1964-2015. Data were obtained from PubMed. Data for the year 2015 shows the numbers of publications available up through July 31, 2015. .... 3
- Figure I-3 Chemical structures of EA and Uro. A series of metabolites called “Urolithins” are formed from EA via enzymatic activation of gut microbes..... 5

### II. CHAPTER I: Ellagic acid modulates lipid accumulation in primary human adipocytes and human hepatoma Huh7 cells via distinct mechanisms

- Figure II-1 MGP supplementation attenuated fat mass and adipocyte size..... 48
- Figure II -2 NAc constituents of MGP were associated with a decrease of adipocyte differentiation..... 49
- Figure II -3 EA suppressed adipogenesis of *hASCs*..... 50
- Figure II -4 EA decreased triglyceride accumulation in mature human adipocytes. A. Experimental scheme. .... 51
- Figure II -5 MGP supplementation decreased hepatic lipid accumulation..... 52
- Figure II -6 EA decreased triglyceride accumulation in human hepatoma Huh7 cells. ... 53

### III. CHAPTER II: Ellagic acid inhibits adipocyte differentiation through coactivator associated arginine methyltransferase 1-mediated chromatin modification

- Figure III-1 EA alters HDAC9 expression during adipocyte differentiation. .... 76

Figure III -2 EA alters HDAC activity during adipocyte differentiation.....	77
Figure III -3 Depletion of HDAC9 in <i>hASCs</i> has minimal impact on EA-mediated inhibition of adipogenesis. ....	78
Figure III -4 EA inhibits H3R17me2 without affecting CARM1 expression levels. ....	79
Figure III -5 Rescue of CARM1 activity by delivering CPP- CARM1 partially reverses EA-mediated adipogenesis of <i>hASCs</i> .....	80
Figure III -6 Epigenetic modification of adipogenesis by EA through the mechanism involved in CARM1 inhibition in <i>hASCs</i> .....	81
<b>IV. CHAPTER III: Raspberry seed flour attenuates high sucrose diet-mediated hepatic stress and adipose tissue inflammation</b>	
Figure IV -1 Identification of ellagic acid and its derivatives after hydrolysis of RSF..	111
Figure IV-2 RSF supplementation ameliorated glucose and insulin tolerance in C57BL/6 mice against HS diet. ....	112
Figure IV -3 RSF supplementation attenuated hepatic ER stress and insulin sensitivity against HS diet. ....	113
Figure IV -4 RSF supplementation reduced hepatic oxidative stress against HS diet....	115
Figure IV -5 RSF supplementation attenuated visceral adipocyte hypertrophy and adipose inflammation against HS diet.....	116
<b>V. CHAPTER IV: Urolithin A, C and D, but not iso-Urolithin A and Urolithin B, attenuate triglyceride accumulation in primary cultures of human adipocytes</b>	
Figure V -1 Metabolism of EA to produce Uro and the effects of Uro on cell viability in primary human adipocytes.....	145
Figure V -2 Uro, but not iso-UroA, suppressed adipogenesis in <i>hASCs</i> .....	146

Figure V -3 Uro, but not iso-UroA, suppressed lipogenesis in mature human adipocytes. .....	147
Figure V -4 Uro regulated lipid metabolisms in human adipocytes. ....	149
Figure V -5 Uro, but not iso-UroA, regulated lipid mechanisms in human hepatoma Huh7 cells. ....	150

## LIST OF TABLES

### I. INTRODUCTION: REVIEW LITERATURES

Table I-1 <i>In vitro</i> studies carried out with plant extracts rich in EA in relation to obesity and its metabolic complication .....	11
Table I-2 <i>In vivo</i> studies carried out using EA or EA-containing plants in relation to obesity and its metabolic complications .....	12
Table I-3 Effect of ellagic acid (EA)-containing diet from different sources intake on improvement of lipid profiles in small animals <sup>1</sup> .....	15

### IV. CHAPTER III

Table IV-1 Main phenolic compounds identified in RSF.....	109
Table IV-2 Food intake, metabolic parameters and blood lipid profiles * .....	110

## I. INTRODUCTION: REVIEW LITERATURES

Obesity has reached epidemic proportions in the United States and worldwide [1, 2]. A systemic analysis for Global Burden of Disease Study reported that the prevalence of obesity has increased from ~30 % to 40 % during 1980-2013 worldwide underlining the urgent need of global action to intervene obesity [3]. The major cause of obesity is likely attributed to the obesogenic diets, although other factors such as lack of exercise, unhealthy eating habits, and genetic preposition expedite the onset of obesity and/or exacerbate severity of obesity [4]. Obesity develops from chronic positive energy imbalance when food intake exceeds the energy expenditure [5]. The progression of obesity is initiated by adipose tissue expansion by depositing surplus energy into the form of triglyceride (TG). Adipose tissue expansion occurs by forming new fat cell formation (hyperplasia, adipogenesis) or by enlarging its size to aggrandize TG storage capacity (hypertrophy) [6]. Several studies have clearly demonstrated that high fat (HF) diet triggers visceral fat expansion through adipocyte hyperplasia as well as adipocyte hypertrophy [7]. The increased visceral adiposity is accompanied by an increase of immune cell infiltration into adipose tissue, basal (or non-stimulatory) lipolysis, and defective adipokine secretion [6, 8]. These immunological and endocrinological changes of adipose tissue during pathogenesis of obesity are positively associated with hepatic steatosis and systemic levels of glucose intolerance and insulin resistance (**Figure I-1**) [9, 10]. Thus, there is an imminent need to devise dietary regimens to disconnect the vicious link between diet-induced adipocyte expansion and metabolic dysfunction.

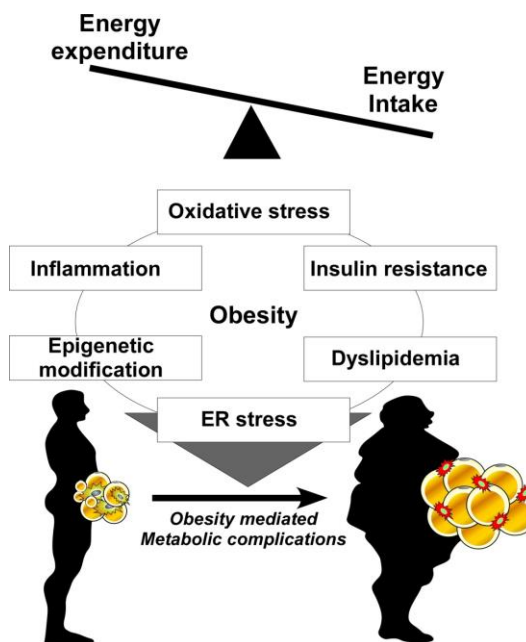


**Figure I-1 Schematic diagram showing that factors affect the pathogenesis of obesity.** Obesity is accompanied by oxidative stress, inflammation, and dyslipidemia, which synergistically progress to obesity-related diseases, type 2 diabetes and NAFLD.

The increased intake of fruits and vegetables (FV) has been shown to inversely correlate with incidence of obesity [11, 12]. In addition to the benefits from fiber consumption, dietary polyphenolic compounds in FV have attracted attention due to its biochemical ability to modulate signaling pathways of lipid and glucose metabolism. Among numerous polyphenolic compounds, we and others have recently recognized that ellagic acid (EA), abundant polyphenolic compound found in various berries and nuts, as one of promising dietary candidate to control obesity and its associated metabolic complications. Besides to its anti-proliferative function of EA in cancer, there is accumulating evidence that EA decreases chronic metabolic diseases such as dyslipidemia, insulin resistance and non-alcoholic fatty liver diseases. This review

comprised of three sections to provide a novel insight into 1) bioavailability of EA, 2) *in vitro* and *in vivo* evidence that EA is capable to regulate lipid and glucose metabolism, and 3) mode of action that EA counteracts obesity-associated metabolic diseases. According to literature search in NCBI Pubmed on July 2015, 1,721 articles have been published regarding EA since 1964 (**Figure I-2**). However, the molecular mechanisms by which EA exerts anti-obesogenic effects by modulating lipid and glucose metabolisms remain unclear.

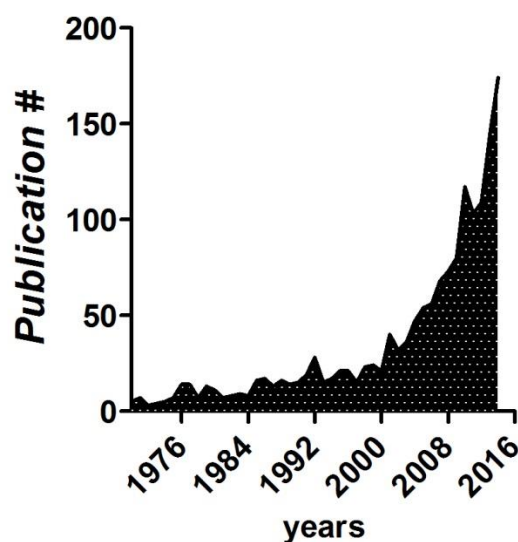


**Figure I-2** Yearly number of publications related to EA from 1964-2015. Data were obtained from PubMed. Data for the year 2015 shows the numbers of publications available up through July 31, 2015.

In this review, I thoroughly discuss the emerging evidence that EA alters gene expression, cell signaling, and metabolism to reduce overweight and obesity *in vitro* and *in vivo*. I also comprehensively review the molecular mechanisms by which dietary EA attenuates obesity driven-health abnormality, and propose dietary EA as a promising polyphenolic compound to combat obesity.

## Bioavailability of EA

EA (2,3,7,8-tetrahydroxy [1]-benzopyranol [5,4,3-cde]benzopyran-5,10-dion) was firstly discovered by Braconnot in 1831 [13]. EA is a highly thermostable molecule (melting point 350 °C), with molecular weight of 302.194 g mol<sup>-1</sup>. EA consists of the lipophilic part with four rings and the hydrophilic part with four hydroxyl group and two lactone groups [14]. The strong hydrogen-bonding network act as an electron acceptor, which in turn enables EA to participate in a number of reactions [15]. EA is naturally present in numerous fruits and vegetables including strawberries, blackberries, red and black raspberries, and nuts including walnuts, pistachio, cashew nuts, oak acorns and pecans [16, 17] in the form of hydrolysable ellagitannins (ETs). ETs are also abundant in pomegranates and muscadine grapes especially in seed and skin [18-20]. Following oral administration of EA-containing foods, ET is hydrolyzed to form free EA. Subsequently, majority of EA undergoes metabolic conversion by intestinal gut microbes resulting in generation of urolithins (Uro, dibenzopyran-6-one metabolites) through reduction of one of the two lactone groups and decarboxylation and dihydroxylation (UroD → UroC → UroA or iso-UroA → UroB) (**Figure I-3**) [21]. Besides its microbial conversion into Uro, free EA undergoes phases II reactions that are conjugation processes of glucuronidation, sulfation and methylation at the large intestine. In physiological condition, virtually very low EA can be found in plasma or tissues based on human clinical trials [22] as well as on studies with rodents and other small mammals [23, 24]. More specifically, upon ingestion, peak plasma concentration of free EA is no more than 100 nM in plasma. However, Uro and its conjugated form can reach micromolar concentrations in plasma [25]. Furthermore, EA is found only a trace amount in the peripheral tissues, whereas Uro

and its conjugates accumulate in the prostate, intestine, and colon [26]. Glucuronides and methyl glucuronide of EA, UroA, and UroD present in the bile through enterohepatic circulation [27]. Phase II reactions of EA also affect EA uptake in hepatocytes and additional metabolism in liver [28]. However, specific bacterial strains that convert EA or its intermediate metabolites into UroA, B and D have not been identified yet.

Likewise to the many other polyphenolic compounds, low bioavailability is the major limiting factor for dietary EA to exhibit metabolic activities *in vivo*. Noticeably, however, the most recent study by González-Sarrías et al. reports that EA could be found higher concentration than previously reported [29]. Apparently bioavailability of EA is regulated by multiple factors including conjugation with tannin, microbial conversion into Uro, metabolism in hepatocytes, and phase II reaction. Nonetheless of these limited bioavailability, pure EA or EA-containing food seem to effective in normalizing obesity and obesity-mediated metabolic dysfunction as we summarize in following sections.

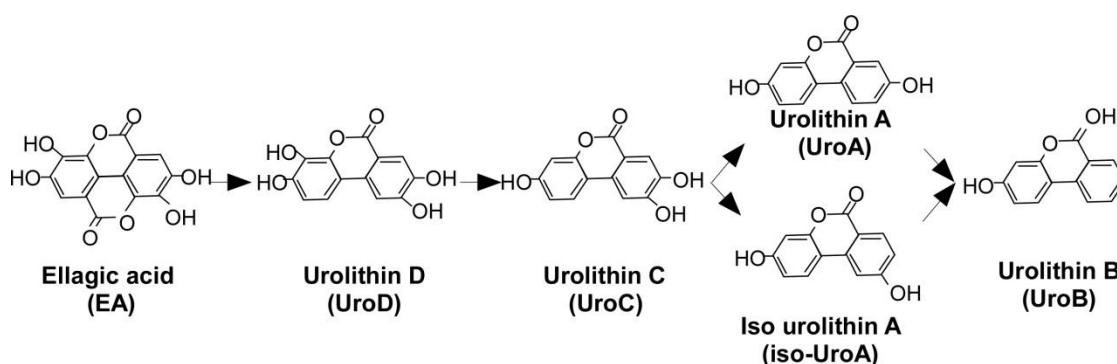


**Figure I-3 Chemical structures of EA and Uro.** A series of metabolites called “Urolithins” are formed from EA via enzymatic activation of gut microbes.

## Effects of EA on obesity

### *In vitro* evidence

There are several studies having directly or indirectly investigated the potential role of EA in adiposity control using adipocyte cell models (**Table I-1**). The most popular cell used to identify the anti-adipogenic effects is 3T3-L1 cell, a well-established murine pre-adipocyte cell line. Using 3T3-L1 cells, Mejia-Meza et al. first reported that EA-containing food alter adipocyte differentiation [30]. In their study, it is demonstrated that 250 µg/mL of fresh and dried red raspberries, which contain a large amount of EA (around 3.7 mg/g dry basis) as well as other polyphenolic compounds, inhibit adipogenesis and reduces lipid accumulation in 3T3-L1 cells. Wang et al. found that 15-20 µM of the concentration of EA significantly reduced adipogenesis through inhibition of cell cycle progression from G1→S transition without causing apoptosis in 3T3-L1 cells [31]. Consistently, Woo et al. also demonstrated EA significantly reduced lipid accumulation and early adipogenic markers such as kruppel-like factor 4 (KLF4), KLF5, Krox20 as well as peroxisome proliferator-activated receptor  $\gamma$  (PPAR $\gamma$ ), and CCAAT/enhancer binding protein  $\alpha$  (C/EBP $\alpha$ ) via cell cycle arrest [32]. These initial results that EA decreases adipocyte differentiation in 3T3-L1 cells were confirmed and obtained human relevance by the following studies from primary cultures of human adipocytes. Primary human adipogenic stem cells (*hASCs*), isolated from scavenged adipose tissue after liposuction or abdominoplasty surgery [33], have been extensively used to investigate adipocyte lipid metabolism in humans. Okla et al. [34] reported that muscadine grape polyphenols (MGP), which contains 18.2 mg/g of free EA were able to reduce lipid accumulation during adipogenesis in *hASCs*. Among the polyphenolic

constituents of MGP, authors identified that EA (~10  $\mu$ M) was the responsible polyphenol that exclusively represses the adipogenesis by decreased the expression of adipogenic genes, i.e., PPAR $\gamma$ , fatty acid synthase (Fas), adipocyte protein 2 (aP2), and C/EBP $\alpha$  [34, 35].

Most *in vitro* studies were focused on investigating the role of EA in inhibiting new fat cell formation and few studies investigate the role of EA on terminal stage of differentiation or lipogenesis. Interestingly, Okla et al. showed that 3 day incubation of EA (10  $\mu$ M) in cultures of mature human adipocytes effectively reduces lipogenesis as well as in human hepatocytes. By using the radiolabeled precursor, it has been demonstrated that EA significantly reduced *de novo* lipogenesis, TG esterification, while enhanced FA oxidation. These TG-lipid lowering effects of MGP supplementation were confirmed in HF-fed C57BL mice showing that both hepatic TG contents and adipose tissue mass are reduced. The reduction of TG in liver was associated with increased hepatic FA oxidative gene expressions [34] implicating that decreased TG accumulation is linked with energy expenditure. The activation of AMP-activated kinase (AMPK) is likely involved in this link, since AMPK activation has shown to regulate energy homeostasis [36] by inhibiting adipogenesis, *de novo* TG synthesis, and by augmenting FA oxidation [37]. Supporting this notion, Poulouse et al. demonstrated that only 100 nM EA treatment for 30 minutes induced AMPK activation in fully differentiated 3T3-L1 cells [38]. Consistently, Kang et al also showed that activation of AMPK is triggered by EA and UroA, C, and D in primary cultured of human adipocytes inhibiting differentiation of *hASC* into adipocytes (under review). Therefore, further analysis is required to validate these possibilities.

In addition to anti-adipogenic/lipogenic effects of EA, Chinese sweet leaf tea extract containing 10 µg/ml of EA attenuated angiogenic gene expression of vascular endothelial growth factor (VEGF) in 3T3-L1 [39]. Another studies reported that EA containing pomegranate fruit extract (10-100 µg/ml of EA) or pure EA (20-70 µM) treatment in 3T3-L1 cells reduce resistin release, an anti-insulin sensitizing adipokine [40]. There are also another set of evidence that EA not only affects TG metabolism in adipocyte and hepatocytes, but also regulate cholesterol metabolism in macrophages. In J774A macrophage cell line, treatment of 5 µM of EA for 18 hours showed reduced cholesterol ester (CE) accumulation by presumably reduced scavenger receptor class B member 1 (SR-B1) induction for oxLDL uptake, but increased cholesterol efflux [41]. This study implicates that EA may be involved in reverse cholesterol transport process from the plaque area for attenuation of cardiovascular diseases risk.

### ***In vivo* evidence**

The TG-lowering function of EA observed in *in vitro* studies is well supported by animal studies establishing physiological role of EA against the pathogenesis of obesity. A general consensus has found that EA-containing foods are effective in attenuating adiposity, plasma markers of metabolic syndrome although the attenuated fat mass were variable depending on the source and content of EA as well as supplementation duration (**Table I-2**). The dietary supplementation studies using ‘EA-containing whole foods’ such as pomegranate peel extract (6 mg EA/kg BW) [42], blueberry extracts (150 mg of EA/kg BW) [43], Chinese sweet leaf tea (220 mg EA/kg BW) [39], mango (1 or 10 % in diet) [44] and chestnut inner shell extract (150 mg/kg BW) [45], significantly reduced body weight as well as white adipose tissue mass in rodents. Moreover, despite same BW

changes, loss of visceral fat mass were found in some study such as 0.4% of MGP supplementation in C57BL/6 mice [18] and 30 mg/kg BW of Pomegranate fruit extract (PFE)-fed ovariectomized ddY female mice [40]. Pomegranate flower at a concentration of 0.5% in the diet was also able to reduce epididymal fat mass in aged ddY mice [46]. The loss of body weight and/or fat mass are accompanied by the improvement of plasma lipid profiles (reduced elevated FFA, TG, total cholesterol (TC), LDL, VLDL but increased HDL) and glycemic index (reduced hyperglycemia and hyperinsulinemia).

Instead of EA-containing whole foods, it is also showed that “pure EA” is also able to attenuate obesity or obesity-mediated metabolic complications in animals. Furthermore, supplementation of 0.1% EA in KK-Ay mice, a type 2 diabetes mice model, ameliorated dysregulation of serum lipid profiles and resistin, and upregulated apolipoprotein A-I (ApoA-1), lipoprotein receptor (LDLr), carnitine palmitoyltransferase (CPT), and PPAR $\gamma$  gene expressions in hepatic tissue resulting in improved hepatic steatosis [47]. Panchal et al. and Kannan et al. showed that EA (0.8 g/kg diet and 15 mg/kg BW respectively) not only ameliorates lipid and glucose metabolisms but also attenuates obesity-associated myocardial dysfunction and cardiovascular remodeling by altered myocardial necrosis and upregulation of nuclear factor erythroid 2–related factor 2 (Nrf2) and CPT1 expressions in heart and liver [48, 49]. Ahad et al. demonstrated that low-dose streptozotocin (STZ) injection with HF-diet triggered the diabetic nephropathy in Wistar albino rats, which was significantly prevented by oral administration of EA (40 mg/kg BW for 16 weeks) attenuating dyslipidemia and onset of diabetic nephropathy [50] presumably through inactivation of renal nuclear factor-kappaB (NF- $\kappa$ B) activation. Collectively, these studies suggest that EA may be beneficial to diabetes-associated

microvascular diseases such as cardiovascular diseases and diabetic kidney by decreasing chronic inflammation.

In our effort to obtain a general impact of EA supplementation against pathogenesis of obesity, we conducted small meta-analysis using published data from 10 animal studies with EA supplementation (**Table I-3**). It is noticeable that experimental groups with EA consumption reduced approximately 25% of dyslipidemia (decreased in TG) without altering food intake. The improvement of plasma lipid profile was more evident than measurable differences in total BW and/or adipose tissue mass. It might be attributed to the variable EA bioavailability depending on the source of EA. Further research is warranted whether intake of EA with other phytochemicals facilitates the EA uptake at the intestinal epithelium barrier. Moreover, future studies to determine appropriate dose of EA and the upper limit of safety as well as the underlying mechanisms of toxicity are necessary.

**Table I-1 *In vitro* studies carried out with plant extracts rich in EA in relation to obesity and its metabolic complication**

Test material	Test model	Dose/Duration	Cell responses	Physiological effects	References
EA	3T3-L1 preadipocytes	5,25, and 50 $\mu$ M, 6-8 days	$\downarrow$ lipid accumulation, PPAR $\gamma$ , C/EBP $\alpha$ , $\downarrow$ early adipogenic markers KLF4, KLF5, Krox20, C/EBP $\beta$ within 24 hours	Anti-adipogenesis	Woo et al. (2015)
EA	Human liver cell line Huh7 cells	10 $\mu$ M, 2 days	$\downarrow$ <i>de novo</i> TG synthesis and TG esterification, $\uparrow$ FA oxidation	Anti-lipogenesis	Okla and Kang et al. (2015)
EA	Differentiated <i>hASCs</i>	10 $\mu$ M, 3 or 7 days	Inhibits <i>de novo</i> lipogenesis	Anti-lipogenesis	Okla and Kang et al. (2015)
EA	<i>hASCs</i>	10 $\mu$ M, 7 days	$\downarrow$ adipogenic genes and protein (PPAR $\gamma$ , C/EBP $\alpha$ , aP2, Fas), alters epigenetic markers ( $\uparrow$ HDAC9, $\downarrow$ CARM1 enzyme activity)	Anti-adipogenesis	Kang et al. (2014)
EA	3T3-L1 preadipocytes	20 $\mu$ M, 2 days	$\downarrow$ early day 2–4 of differentiation, $\downarrow$ clonal expansion, block the cell cycle at the G1/S transition and Cyclin A and Rb phosphorylation	Anti-adipogenesis	Wang et al. (2013)
EA	Macrophage-like cell line J774A1 with oxidized LDL	5 $\mu$ M, 18 hours	$\downarrow$ lipid accumulation and SR-B1 induction, $\downarrow$ macrophage lipid uptake to block foam cells and $\uparrow$ cholesterol efflux	Anti-atherogenesis	Park et al. (2011)
Chinese sweet leaf tea extract (GER)	3T3-L1 preadipocytes	10 $\mu$ g/ml of GER	$\downarrow$ the expression of VEGF	Anti-angiogenesis	Koh et al. (2011)
3,3'-di-O-methylellagic acid and EA	3T3-L1 adipocytes	1,3,10 $\mu$ M	$\downarrow$ TG, and GPDH activity	Anti-adipogenesis	Yang et al. (2011)
Pomegranate fruit extract and EA	3T3-L1 preadipocytes	10-100 $\mu$ g/ml of PFE, 20-70 $\mu$ M of EA	$\downarrow$ resistin release	Degradation of intracellular resistin	Makino-Wakagi et al. (2012)

*Abbreviation:* EA, ellagic acid; PPAR $\gamma$ , Peroxisome proliferator-activated receptor gamma; C/EBP $\alpha$ , CCAAT/enhancer binding protein alpha; KLF4, Kruppel-like factor 4; TG, triglyceride; *hASCs*, human adipogenic stem cells, Fas, Fatty acid synthetase; HDAC9, histone deacetylase 9; CARM1, co-activator arginine methyltransferase 1; SR-B1, Scavenger receptor class B member 1; VEGF, Vascular endothelial growth factor; GPDH, Glycerol-3-phosphate dehydrogenase

**Table I-2 *In vivo* studies carried out using EA or EA-containing plants in relation to obesity and its metabolic complications**

Test material	Test model	Dose/Duration	Results			Physiological effects	References
			$\Delta$ BW	$\Delta$ Fat	Cell responses		
EA	HFD+STZ induced type 2 diabetic Wistar albino rats	EA (40 mg/kg BW/day) for 16 weeks	-	-	-↓levels of TC, LDL-C, VLDL-C, FFA and TG, -↑ the levels of HDL-C	Protection of diabetic nephropathy	Ahad et al (2014)
EA	albino Wistar+isoproterenol (oxidative stress)	EA (7.5 and 15mg/kg BW) orally for 10 days	-	-	-Restores arrhythmias, ventricular hypertrophy, lipid peroxidation, -Altered lipid profile and myocardial necrosis	Prevention of myocardial infarction	Kannan et al. (2013)
Chinese sweet leaf tea extract (GER)	HFD fed male SD rats	0.22g/kg BW, 12weeks	↓	↓	-↓ glucose, TG, and cholesterol levels in blood	Improvement of Obesity Phenotype	Koh et al. (2011)
Nanoparticle containing EA and coenzyme Q10	HFD fed male SD rats	10% (w/w of polymer), 2 weeks	-	-	-↓ glucose and hyperlipidemic conditions, -↑endothelial functioning	Ameliorates hyperlipidemia	Ratnam et al. (2009)
EA	HFD fed KKAY mice	0.1% of EA in diet, 68 days	-	-	-↓ serum resistin and -↓ hepatic steatosis and serum lipid profile, -↑ ApoA1, LDLr, CPT1, and PPAR $\gamma$ genes in the liver	Improves hepatic steatosis	Yoshimura et al. (2013)
Pomegranate fruit extract	Female ddY mice (ovariectomized)	30mg/kg BW, 12weeks	-	↓	-↓ serum TC levels	Degradation of intracellular resistin	Makino-Wakagi et al. (2012)
Pomegranate leaf extract (PLE)	HFD fed ICR mice	400 or 800mg/kg BW of PLE, 5 weeks	↓	↓	- improves lipid profiles	Anti-obesity	Let et al. (2007)

**Table I-2 (continued)**

Test material	Test model	Dose/Duration	Results			Physiological effects	References
			ΔBW	ΔFat	Cell responses		
EA	HFHC fed wistar rat	0.8 g/kg of BW, 16 weeks	↓	↓	-Improves cardiovascular remodeling, ventricular function, glucose tolerance, non-alcoholic fatty liver disease, -↑ Nrf2, and CPT1 in heart and liver	Attenuates high-carbohydrate, high-fat diet-induced metabolic syndrome	Panchal et al. (2013)
Muscadine grape phytochemicals (MGP)	HFD fed C57BL/6J mice	0.4% of MGP in diet, 15 weeks	-	↓	-Improves glucose, insulin FFA, TG, TC and CRP in plasma	anti-obesity and metabolic complications	Gourineni et al. (2012)
Hydro-alcoholic fruit extract of avocado (HFEA)	HFD fed SD rats	100 mg/kg BW of HFEA, 11 weeks	↓	↓	-↓ TG, TC, LDL and leptin in plasma, ↓ FASN, LPL, and leptin while ↑ FGF21 gene expressions in WAT	Hypolipidemic effect	Monika et al. (2015)

*Abbreviation:* EA, ellagic acid; wk, week; HFD, high fat diet; STZ, streptozotocin; TC, total cholesterol; LDL-C, low density lipoprotein-cholesterol; VLDL-C, very low density lipoprotein; FFA, free fatty acid; TG, triglyceride; HDL-C, high density lipoprotein-cholesterol; SD, Sprague Dawley; BW, body weight; ApoA1, Apolipoprotein A-I; LDLr, LDL receptor; CPT1, Carnitine palmitoyltransferase I; PPAR $\gamma$ , Peroxisome proliferator-activated receptor gamma; FI, food intake; WAT, white adipose tissue; Nrf2, nuclear factor erythroid 2-related factor 2; NF-kB, Nuclear factor kappa B; HFHC, high fat and high carbohydrate; CRP, C-Reactive Protein; BMI, Body Mass Index; FASN, Fatty acid synthetase; LPL, Lipoprotein lipase; FGF21, Fibroblast growth factor 21.

**Table I-3 Effect of ellagic acid (EA)-containing diet from different sources intake on improvement of lipid profiles in small animals <sup>1</sup>**

EA intake (mg/kg BW)	Source of EA	Treatment ave	n	Study, year	Weighted mean differences (95% of CI)
Unidentified	Pomegranate flower	-14.81	6	Wang 2012	-14.81 (-5.89, -23.73)
4.9	Muscadine grape	-41.30	8	Gourineni 2012	-41.30 (-37.69, -44.91)
6	Mango	-16.95	9	Lucas 2011	-16.95 (-10.69, -23.21)
72	Chinese sweet leaf	-47.02	10	Koh 2011	-47.02 (-37.89, -56.15)
88	Pomegranate leaf	-61.83	5	Zhang 2007	-61.83 (-40.65, -83.02)
10	Pure EA	-23.79	9	Yoshimura 2013	-23.79 (-17.10, -29.88)
34.14	Pure EA	-58.33	12	Panchal 2013	-58.33 (-51.66, -65.00)
40	Pure EA	-50.44	6	Ahad 2014	-50.44 (-45.82, -55.06)
100	Pure EA	-59.52	6	Yu 2005	-59.52 (-47.47, -71.57)
200	Pure EA	-13.01	8	Rani P. 2013	-13.01 (-11.07, -14.95)
-	-	-25.44	80	Combined	-25.44 (-24.02, -26.86)

Δ Plasma TG levels (Mean and 95% CI)

<sup>1</sup> Analysis was performed using meta-analysis calculator at

<http://www.healthstrategy.com/meta/meta.pl>

## **Mechanisms involved in anti-obesity effects of EA**

### ***Oxidative stress and inflammation***

Obesity is defined as chronic low-grade inflammation and increased oxidative stress [51]. In obese state, the inflamed adipose tissue is directly associated with activation of inflammatory signaling with abnormal production of pro-inflammatory adipokines [52]. The pro-inflammatory signaling pathways are closely related to oxidative stress via reactive oxygen species (ROS) including free radicals [53]. It has been reported that EA reduces tumor necrosis factor  $\alpha$  (TNF $\alpha$ ), interleukin-6 (IL-6) and chemokine C-C motif ligand-2 (CCL-2) secretion in lipopolysaccharides (LPS) stimulated macrophages and adipocytes, indicating that EA may directly reduce adipose inflammation *in vitro* [54]. Ahad et al. [50] demonstrated that EA inhibits NF- $\kappa$ B, the major transcription factor for proinflammatory responses, for ameliorating dyslipidemia and diabetic nephropathy in rats. The increasing dose of EA administration (20, 40, 80, 100 mg/kg BW, 14 days) significantly inhibits NF- $\kappa$ B-p65, transforming growth factor  $\beta$  (TGF- $\beta$ ) and fibronectin and proinflammatory cytokine release with the improvement of insulin resistance. Moreover, a recent study showed that EA (0.1 % in diet) [55] or EA-containing pomegranate fruits extract (30 mg/kg BW) [40] improve hepatic steatosis and dyslipidemia by reduction of resistin [47], which is closely associated with obesity and chronic inflammation. Reduction of resistin release was confirmed in 3T3-L1 cells with 20-70  $\mu$ M of EA treatment [40]. The direct anti-inflammatory effects of EA in white adipose tissue (e.g. alternative M2 macrophage polarization, changes in innate or adaptive immune responses) have not been identified. Despite EA shows no evidence of accumulating in adipose tissue, our recent study clearly demonstrated that EA decreases

proinflammatory cytokine secretion in adipose tissue extract as well as decreases macrophage infiltration against high fat high sugar diet (under review).

In addition to the attenuation of inflammation, EA supplementation is seemingly inhibit oxidative stress. High cholesterol/fat diet with EA supplementation (1% w/w diet) improved lipid profiles and decreased lipid peroxidation by reducing malondialdehyde (MDA) production, caspase-8, caspase-9, Fas ligand levels in aortic arches [56]. Consistently, EA supplementation for 14 weeks was able to protect oxidative stress-induced endothelial dysfunction and atherosclerosis through Nrf2 activation in HF diet-fed ApoE KO mice [57]. Intriguingly, EA supplementation (2 or 5 % of EA in diet) reversed STZ induced type 1 diabetic symptoms decreasing protein glycation levels and inflammatory action in male Balb/Ca mice [58]. These data clearly indicated that the anti-inflammatory and anti-oxidative characteristics are sufficient to attenuate or ameliorate metabolic dysfunction due to obesity.

### **Epigenetic regulation**

Accumulating evidence suggests that HF diet in early life can influence obesity phenotype via mechanisms associated with epigenetic modification [59]. Conversely, epidemiological studies show that fruits and vegetable consumption shows a reciprocal correlation with the incidence of obesity [12]. In respond to this new research initiatives, study to determine whether dietary components of fruits and vegetables participate in the epigenetic regulation of obesity are gradually increasing. Boque et al. reported that apple polyphenol consumption increases DNA methylation by attenuating adipocyte hypertrophy in a diet-induced obese rat model [60]. Moreover, Okla et al. also showed

that HF diet with MGP supplementation upregulates HDAC9 expression, which is known as a negative regulator of adipogenesis [34]. These data implied that dietary polyphenols may affect chromatin remodeling to regulate obesity outcome. Interestingly, Kang et al. found that EA is the responsible polyphenolic compound in MGP to increase HDAC9 expressions, and further identified that EA inhibits histone methyltransferase (CARM1), an enzyme necessary for adipogenesis, during the differentiation of *hASCs* [35]. Even though there is no direct evidence that EA metabolites alter epigenetic enzymes to regulate obesity-associated adipose expansion, UroC was reported to reduce TNF $\alpha$ -induced inflammation through inhibition of histone acetyltransferase (HAT) activity in the monocyte cell [61]. It implies the possibility that EA metabolites may resemble the action of EA to modulate chromatin remodeling during adipogenesis. Not only EA, but also several dietary phytochemicals including curcumin [62], genistein [63], and isoflavone [64] are reported to improve obesity-associated metabolic index (dyslipidemia, hyperglycemia, and hyperinsulinemia) by altering DNA methylation and/or histone acetylation. An increasing number of studies are revealing that FV consumption in pregnancy may result in metabolic benefits to the offspring [63]. It is unknown whether polyphenolic constituents found in FV (including EA) may positively affect chromatin reprogramming of fetus, which may exert lifelong metabolic benefits against obesity and its associated metabolic dysfunction. Further studies in this aspect would be important to provide novel insights into prevention for childhood obesity as well as for adults.

### **Potential role of gut microbiota**

The gut microbial community has been proposed as a crucial environmental factor to control obesity by altering host's energy homeostasis [65, 66]. The colonic microbiota is also responsible for the extensive breakdown of the polyphenolic structures into a series of phenolic metabolites that may be responsible for the human health effects. Thus, recently, many researchers have investigated to establish the relationship between polyphenols supplementation and changes in the microbiome. Neyrinck et al. reported that mice fed with HF diet with pomegranate peel extract reduces inflammation and hypercholesterolemia by promoting the growth of *Bifidobacterium* spp. in the ceca [42]. Anhê et al. also described that a consumption of polyphenol-rich cranberry extract protects from HFHS diet-induced obesity, insulin resistance through modulation of microbiota ecology (*Akkermansia* spp. Population) of mice [67]. These data suggested the potential implication of the gut microbiota by dietary polyphenols. There is growing evidence EA or EA-enriched food consumption may attenuate obesity and its metabolic complications through altering gut microflora-associated metabolism, or different Uro production by gut microbes. Tomas-Barberan et al. suggested that different Uro is produced in response to host's metabolic health and that each Uro may potentiate or nullify the health benefits of EA [68]. In other words, metabolically healthy subjects may possess microbiota that are able to generate mainly active Uro such as UroA (i.e. subjects belonging to the so-called 'metabotype A' [68]). In contrast, metabolically unhealthy humans may have bacterial communities producing UroA but also other less active urolithins such as iso-UroA and UroB (i.e., subjects with 'metabotype B' [68]). García-Villalba et al. reported that there were compositional differences in the gut microbiome

between human subjects who produce UroA (effective Uro) and who produce iso-UroA and B (less active Uro) [21]. Also, subjects who have a higher risk of chronic illness produce iso-UroA and UroB [68], the two inactive EA metabolites in our experimental setting (Fig. 2-4). Recently, *Gordonibacter urolithinfaciens* sp. nov. has been identified as a novel bacterial species responsible for converting EA into UroM5 and UroC [69]. This bacterium belongs to the family *Coriobacteriaceae* a family that is associated with benefits in obesity [70]. Since the bacterial phylum that specifically transform EA or its intermediate metabolites into UroA vs. iso-UroA/UroB have not yet been identified, it could be of interest for future studies.

## **Implications and Conclusion**

The excessive expansion of white adipose tissue during obesity triggers complex and multifactorial conditions of chronic inflammation and oxidative stress. In this review, we summarized that EA plays a critical role in attenuating the prevalence of obesity by decreasing both hyperplastic and hypertrophic adipocyte expansion *in vivo* and *in vitro*. In terms of mode of action by which EA attenuates obesity-mediated metabolic dysfunction, the anti-oxidative and anti-inflammatory characteristics of EA have been presented. In addition, we have been addressed the emerging role of EA in modifying histone remodeling by altering methylation and/or acetylation levels of histone and potential role of Uro in regulating gut microbial community. A better explanation to fill the gap between ‘low bioavailability’ and ‘evident benefits of EA in improving plasma lipid profiles’ should be identified in future studies.

Hitherto, human studies are concentrated on determining the bioavailability of EA by using various EA-containing whole foods such as pomegranate extracts, or intervention studies for cancer treatment. The investigation of metabolic benefits of EA in humans against obesity and its metabolic complication, should be the next-step challenge to validate the ‘proof of concept’ that we learned from obesity-prone experimental animals with EA supplementation. In conclusion, recommending an inclusion of EA-containing fruits and nuts in our daily diets potentially could be a simple strategy to lessen adiposity or improve obesity-mediated metabolic complication even without weight loss.

## REFERENCES

- [1] Ogden CL, Carroll MD, Curtin LR, McDowell MA, Tabak CJ, Flegal KM. Prevalence of overweight and obesity in the United States, 1999-2004. *JAMA* 2006;295:1549-55.
- [2] Flegal KM, Carroll MD, Kuczmarski RJ, Johnson CL. Overweight and obesity in the United States: prevalence and trends, 1960-1994. *Int J Obes Relat Metab Disord* 1998;22:39-47.
- [3] Ng M, Fleming T, Robinson M, Thomson B, Graetz N, Margono C, et al. Global, regional, and national prevalence of overweight and obesity in children and adults during 1980-2013: a systematic analysis for the Global Burden of Disease Study 2013. *Lancet* 2014;384:766-81.
- [4] Weinsier RL, Hunter GR, Heini AF, Goran MI, Sell SM. The etiology of obesity: relative contribution of metabolic factors, diet, and physical activity. *Am J Med* 1998;105:145-50.
- [5] Hill JO, Melanson EL, Wyatt HT. Dietary fat intake and regulation of energy balance: implications for obesity. *J Nutr* 2000;130:284s-8s.
- [6] Kershaw EE, Flier JS. Adipose tissue as an endocrine organ. *J Clin Endocrinol Metab* 2004;89:2548-56.
- [7] Corbett SW, Stern JS, Keeseey RE. Energy expenditure in rats with diet-induced obesity. *Am J Clin Nutr* 1986;44:173-80.
- [8] Wellen KE, Hotamisligil GS. Obesity-induced inflammatory changes in adipose tissue. *J Clin Invest* 2003;112:1785-8.
- [9] Duval C, Thissen U, Keshtkar S, Accart B, Stienstra R, Boekschoten MV, et al. Adipose tissue dysfunction signals progression of hepatic steatosis towards nonalcoholic steatohepatitis in C57BL/6 mice. *Diabetes* 2010;59:3181-91.
- [10] Xu H, Barnes GT, Yang Q, Tan G, Yang D, Chou CJ, et al. Chronic inflammation in fat plays a crucial role in the development of obesity-related insulin resistance. *J Clin Invest* 2003;112:1821-30.
- [11] He K, Hu FB, Colditz GA, Manson JE, Willett WC, Liu S. Changes in intake of fruits and vegetables in relation to risk of obesity and weight gain among middle-aged women. *Int J Obes Relat Metab Disord* 2004;28:1569-74.
- [12] Epstein LH, Gordy CC, Raynor HA, Beddome M, Kilanowski CK, Paluch R. Increasing fruit and vegetable intake and decreasing fat and sugar intake in families at risk for childhood obesity. *Obes Res* 2001;9:171-8.
- [13] Law DJ. Synthetic tannins: Their synthesis, industrial products and application. By Georg Grasser. Translated by F. G. A. Enna. Pp. vi+143. (London: Crosby Lockwood and Son. 1922.) Price 12s. net. *Journal of the Society of Chemical Industry* 1922;41:R141-R.
- [14] Rossi M, Erlebacher J, Zacharias DE, Carrell HL, Iannucci B. The crystal and molecular structure of ellagic acid dihydrate: a dietary anti-cancer agent. *Carcinogenesis* 1991;12:2227-32.
- [15] Clifford MN, Scalbert A. Ellagitannins – nature, occurrence and dietary burden. *Journal of the Science of Food and Agriculture* 2000;80:1118-25.

- [16] Anderson KJ, Teuber SS, Gobeille A, Cremin P, Waterhouse AL, Steinberg FM. Walnut polyphenolics inhibit in vitro human plasma and LDL oxidation. *J Nutr* 2001;131:2837-42.
- [17] Zafrilla P, Ferreres F, Tomas-Barberan FA. Effect of processing and storage on the antioxidant ellagic acid derivatives and flavonoids of red raspberry (*Rubus idaeus*) jams. *J Agric Food Chem* 2001;49:3651-5.
- [18] Gourineni V, Shay NF, Chung S, Sandhu AK, Gu L. Muscadine Grape (*Vitis rotundifolia*) and Wine Phytochemicals Prevented Obesity-Associated Metabolic Complications in C57BL/6J Mice. *J Agric Food Chem* 2012;60:7674-81.
- [19] Gil MI, Tomas-Barberan FA, Hess-Pierce B, Holcroft DM, Kader AA. Antioxidant activity of pomegranate juice and its relationship with phenolic composition and processing. *J Agric Food Chem* 2000;48:4581-9.
- [20] Lee JH, Johnson JV, Talcott ST. Identification of ellagic acid conjugates and other polyphenolics in muscadine grapes by HPLC-ESI-MS. *J Agric Food Chem* 2005;53:6003-10.
- [21] Garcia-Villalba R, Beltran D, Espin JC, Selma MV, Tomas-Barberan FA. Time course production of urolithins from ellagic acid by human gut microbiota. *J Agric Food Chem* 2013;61:8797-806.
- [22] Truchado P, Larrosa M, Garcia-Conesa MT, Cerda B, Vidal-Guevara ML, Tomas-Barberan FA, et al. Strawberry processing does not affect the production and urinary excretion of urolithins, ellagic acid metabolites, in humans. *J Agric Food Chem* 2012;60:5749-54.
- [23] Borges G, Roowi S, Rouanet JM, Duthie GG, Lean ME, Crozier A. The bioavailability of raspberry anthocyanins and ellagitannins in rats. *Mol Nutr Food Res* 2007;51:714-25.
- [24] Gonzalez-Barrio R, Truchado P, Ito H, Espin JC, Tomas-Barberan FA. UV and MS identification of Urolithins and Nasutins, the bioavailable metabolites of ellagitannins and ellagic acid in different mammals. *J Agric Food Chem* 2011;59:1152-62.
- [25] Seeram NP, Henning SM, Zhang Y, Suchard M, Li Z, Heber D. Pomegranate juice ellagitannin metabolites are present in human plasma and some persist in urine for up to 48 hours. *J Nutr* 2006;136:2481-5.
- [26] Seeram NP, Aronson WJ, Zhang Y, Henning SM, Moro A, Lee RP, et al. Pomegranate ellagitannin-derived metabolites inhibit prostate cancer growth and localize to the mouse prostate gland. *J Agric Food Chem* 2007;55:7732-7.
- [27] Espin JC, Gonzalez-Barrio R, Cerda B, Lopez-Bote C, Rey AI, Tomas-Barberan FA. Iberian pig as a model to clarify obscure points in the bioavailability and metabolism of ellagitannins in humans. *J Agric Food Chem* 2007;55:10476-85.
- [28] Gonzalez-Sarrías A, Gimenez-Bastida JA, Nunez-Sanchez MA, Larrosa M, Garcia-Conesa MT, Tomas-Barberan FA, et al. Phase-II metabolism limits the antiproliferative activity of urolithins in human colon cancer cells. *Eur J Nutr* 2014;53:853-64.
- [29] González-Sarrías A, García-Villalba R, Núñez-Sánchez MÁ, Tomé-Carneiro J, Zafrilla P, Mulero J, et al. Identifying the limits for ellagic acid bioavailability: A crossover pharmacokinetic study in healthy volunteers after consumption of pomegranate extracts. *Journal of Functional Foods* 2015;19, Part A:225-35.

- [30] Mejia-Meza EI, Yanez JA, Remsberg CM, Takemoto JK, Davies NM, Rasco B, et al. Effect of dehydration on raspberries: polyphenol and anthocyanin retention, antioxidant capacity, and antiadipogenic activity. *J Food Sci* 2010;75:H5-12.
- [31] Wang L, Li L, Ran X, Long M, Zhang M, Tao Y, et al. Ellagic Acid Reduces Adipogenesis through Inhibition of Differentiation-Prevention of the Induction of Rb Phosphorylation in 3T3-L1 Adipocytes. *Evid Based Complement Alternat Med* 2013;2013:287534.
- [32] Woo MS, Choi HS, Seo MJ, Jeon HJ, Lee BY. Ellagic acid suppresses lipid accumulation by suppressing early adipogenic events and cell cycle arrest. *Phytother Res* 2015;29:398-406.
- [33] Bunnell BA, Flaatt M, Gagliardi C, Patel B, Ripoll C. Adipose-derived stem cells: isolation, expansion and differentiation. *Methods* 2008;45:115-20.
- [34] Okla M, Kang I, Kim dM, Gourineni V, Shay N, Gu L, et al. Ellagic acid modulates lipid accumulation in primary human adipocytes and human hepatoma Huh7 cells via discrete mechanisms. *J Nutr Biochem* 2015;26:82-90.
- [35] Kang I, Okla M, Chung S. Ellagic acid inhibits adipocyte differentiation through coactivator-associated arginine methyltransferase 1-mediated chromatin modification. *J Nutr Biochem* 2014;25:946-53.
- [36] Hardie DG, Ross FA, Hawley SA. AMPK: a nutrient and energy sensor that maintains energy homeostasis. *Nat Rev Mol Cell Biol* 2012;13:251-62.
- [37] Kahn BB, Alquier T, Carling D, Hardie DG. AMP-activated protein kinase: ancient energy gauge provides clues to modern understanding of metabolism. *Cell Metab* 2005;1:15-25.
- [38] Poulouse N, Prasad C, Haridas P, Anilkumar G. Ellagic Acid Stimulates Glucose Transport in Adipocytes and Muscles through AMPK Mediated Pathway. *J Diabetes Metab* 2011;2.
- [39] Koh GY, McCutcheon K, Zhang F, Liu D, Cartwright CA, Martin R, et al. Improvement of obesity phenotype by Chinese sweet leaf tea (*Rubus suavissimus*) components in high-fat diet-induced obese rats. *J Agric Food Chem* 2011;59:98-104.
- [40] Makino-Wakagi Y, Yoshimura Y, Uzawa Y, Zaima N, Moriyama T, Kawamura Y. Ellagic acid in pomegranate suppresses resistin secretion by a novel regulatory mechanism involving the degradation of intracellular resistin protein in adipocytes. *Biochem Biophys Res Commun* 2012;417:880-5.
- [41] Park SH, Kim JL, Lee ES, Han SY, Gong JH, Kang MK, et al. Dietary ellagic acid attenuates oxidized LDL uptake and stimulates cholesterol efflux in murine macrophages. *J Nutr* 2011;141:1931-7.
- [42] Neyrinck AM, Van Hee VF, Bindels LB, De BF, Cani PD, Delzenne NM. Polyphenol-rich extract of pomegranate peel alleviates tissue inflammation and hypercholesterolaemia in high-fat diet-induced obese mice: potential implication of the gut microbiota. *Br J Nutr* 2012:1-8.
- [43] Song Y, Park HJ, Kang SN, Jang SH, Lee SJ, Ko YG, et al. Blueberry peel extracts inhibit adipogenesis in 3T3-L1 cells and reduce high-fat diet-induced obesity. *PLoS One* 2013;8:e69925.
- [44] Lucas EA, Li W, Peterson SK, Brown A, Kuvibidila S, Perkins-Veazie P, et al. Mango modulates body fat and plasma glucose and lipids in mice fed a high-fat diet. *Br J Nutr* 2011;106:1495-505.

- [45] Jung-Ran Noh Y-HKG-TGK-JYH-SLPHNW-KOK-SSC-HL. Chestnut (*Castanea crenata*) inner shell extract inhibits development of hepatic steatosis in C57BL/6 mice fed a high-fat diet. *Food chemistry* 2012;121:437-42.
- [46] Wang J, Rong X, Um IS, Yamahara J, Li Y. 55-week treatment of mice with the unani and ayurvedic medicine pomegranate flower ameliorates ageing-associated insulin resistance and skin abnormalities. *EvidBasedComplement AlternatMed* 2012;2012:350125.
- [47] Yoshimura Y, Nishii S, Zaima N, Moriyama T, Kawamura Y. Ellagic acid improves hepatic steatosis and serum lipid composition through reduction of serum resistin levels and transcriptional activation of hepatic ppara in obese, diabetic KK-A(y) mice. *Biochem Biophys Res Commun* 2013;434:486-91.
- [48] Panchal SK, Ward L, Brown L. Ellagic acid attenuates high-carbohydrate, high-fat diet-induced metabolic syndrome in rats. *Eur J Nutr* 2013;52:559-68.
- [49] Kannan MM, Quine SD. Ellagic acid inhibits cardiac arrhythmias, hypertrophy and hyperlipidaemia during myocardial infarction in rats. *Metabolism* 2013;62:52-61.
- [50] Ahad A, Ganai AA, Mujeeb M, Siddiqui WA. Ellagic acid, an NF-kappaB inhibitor, ameliorates renal function in experimental diabetic nephropathy. *Chem Biol Interact* 2014;219:64-75.
- [51] Ziccardi P, Nappo F, Giugliano G, Esposito K, Marfella R, Cioffi M, et al. Reduction of inflammatory cytokine concentrations and improvement of endothelial functions in obese women after weight loss over one year. *Circulation* 2002;105:804-9.
- [52] Fruhbeck G, Gomez-Ambrosi J, Muruzabal FJ, Burrell MA. The adipocyte: a model for integration of endocrine and metabolic signaling in energy metabolism regulation. *AmJPhysiol EndocrinolMetab* 2001;280:E827-E47.
- [53] Roberts CK, Sindhu KK. Oxidative stress and metabolic syndrome. *Life Sci* 2009;84:705-12.
- [54] Winand J, Schneider YJ. The anti-inflammatory effect of a pomegranate husk extract on inflamed adipocytes and macrophages cultivated independently, but not on the inflammatory vicious cycle between adipocytes and macrophages. *Food Funct* 2014;5:310-8.
- [55] Stepan CM, Bailey ST, Bhat S, Brown EJ, Banerjee RR, Wright CM, et al. The hormone resistin links obesity to diabetes. *Nature* 2001;409:307-12.
- [56] Yu YM, Chang WC, Wu CH, Chiang SY. Reduction of oxidative stress and apoptosis in hyperlipidemic rabbits by ellagic acid. *J Nutr Biochem* 2005;16:675-81.
- [57] Ding Y, Zhang B, Zhou K, Chen M, Wang M, Jia Y, et al. Dietary ellagic acid improves oxidant-induced endothelial dysfunction and atherosclerosis: role of Nrf2 activation. *Int J Cardiol* 2014;175:508-14.
- [58] Chao CY, Mong MC, Chan KC, Yin MC. Anti-glycative and anti-inflammatory effects of caffeic acid and ellagic acid in kidney of diabetic mice. *Mol Nutr Food Res* 2010;54:388-95.
- [59] Wu Q, Suzuki M. Parental obesity and overweight affect the body-fat accumulation in the offspring: the possible effect of a high-fat diet through epigenetic inheritance. *Obes Rev* 2006;7:201-8.
- [60] Boque N, de la Iglesia R, de la Garza AL, Milagro FI, Olivares M, Banales O, et al. Prevention of diet-induced obesity by apple polyphenols in Wistar rats through

- regulation of adipocyte gene expression and DNA methylation patterns. *Mol Nutr Food Res* 2013;57:1473-8.
- [61] Kiss AK, Granica S, Stolarczyk M, Melzig MF. Epigenetic modulation of mechanisms involved in inflammation: Influence of selected polyphenolic substances on histone acetylation state. *Food Chemistry* 2012;131:1015-20.
- [62] Yun JM, Jialal I, Devaraj S. Epigenetic regulation of high glucose-induced proinflammatory cytokine production in monocytes by curcumin. *J Nutr Biochem* 2011;22:450-8.
- [63] Dolinoy DC, Weidman JR, Waterland RA, Jirtle RL. Maternal genistein alters coat color and protects Avy mouse offspring from obesity by modifying the fetal epigenome. *Environ Health Perspect* 2006;114:567-72.
- [64] Howard TD, Ho SM, Zhang L, Chen J, Cui W, Slager R, et al. Epigenetic changes with dietary soy in cynomolgus monkeys. *PLoS One* 2011;6:e26791.
- [65] Backhed F, Ding H, Wang T, Hooper LV, Koh GY, Nagy A, et al. The gut microbiota as an environmental factor that regulates fat storage. *Proc Natl Acad Sci USA* 2004;101:15718-23.
- [66] Backhed F, Manchester JK, Semenkovich CF, Gordon JI. Mechanisms underlying the resistance to diet-induced obesity in germ-free mice. *Proc Natl Acad Sci U S A* 2007;104:979-84.
- [67] Anhe FF, Roy D, Pilon G, Dudonne S, Matamoros S, Varin TV, et al. A polyphenol-rich cranberry extract protects from diet-induced obesity, insulin resistance and intestinal inflammation in association with increased *Akkermansia* spp. population in the gut microbiota of mice. *Gut* 2015;64:872-83.
- [68] Tomas-Barberan FA, Garcia-Villalba R, Gonzalez-Sarrias A, Selma MV, Espin JC. Ellagic acid metabolism by human gut microbiota: consistent observation of three urolithin phenotypes in intervention trials, independent of food source, age, and health status. *J Agric Food Chem* 2014;62:6535-8.
- [69] Selma MV, Beltran D, Garcia-Villalba R, Espin JC, Tomas-Barberan FA. Description of urolithin production capacity from ellagic acid of two human intestinal *Gordonibacter* species. *Food Funct* 2014;5:1779-84.
- [70] Clavel T, Desmarchelier C, Haller D, Gérard P, Rohn S, Lepage P, et al. Intestinal microbiota in metabolic diseases. *Gut Microbes* 2014;5:544-51.

## **HYPOTHESIS AND SPECIFIC AIMS**

The central hypothesis for this dissertation research is that dietary ellagic acid (EA) attenuates obesity and obesity-mediated metabolic complications. To test this hypothesis, the following four specific aims were pursued using primary cultures of newly differentiated / mature human adipocytes as an *in vitro* model, and obesity-prone C57BL/6 mice as an *in vivo* model (**Figure I-5**).

Aim 1. Define that EA exerts the lipid-lowering effects both in adipose tissue and liver via distinct mechanisms (Chapter I).

Aim 2. Determine the mechanisms underlying EA's effects on modulating new fat cell formation by CARM1-mediated epigenetic regulation (Chapter II).

Aim 3. Ascertain the effects of EA on the obesity and obesity mediated oxidative stress/inflammation in a mice model (Chapter III).

Aim 4. Evaluate the effects of gut microbiota-driven EA metabolites, Uro, on regulating TG accumulation using primary-cultured human adipocytes (Chapter IV).

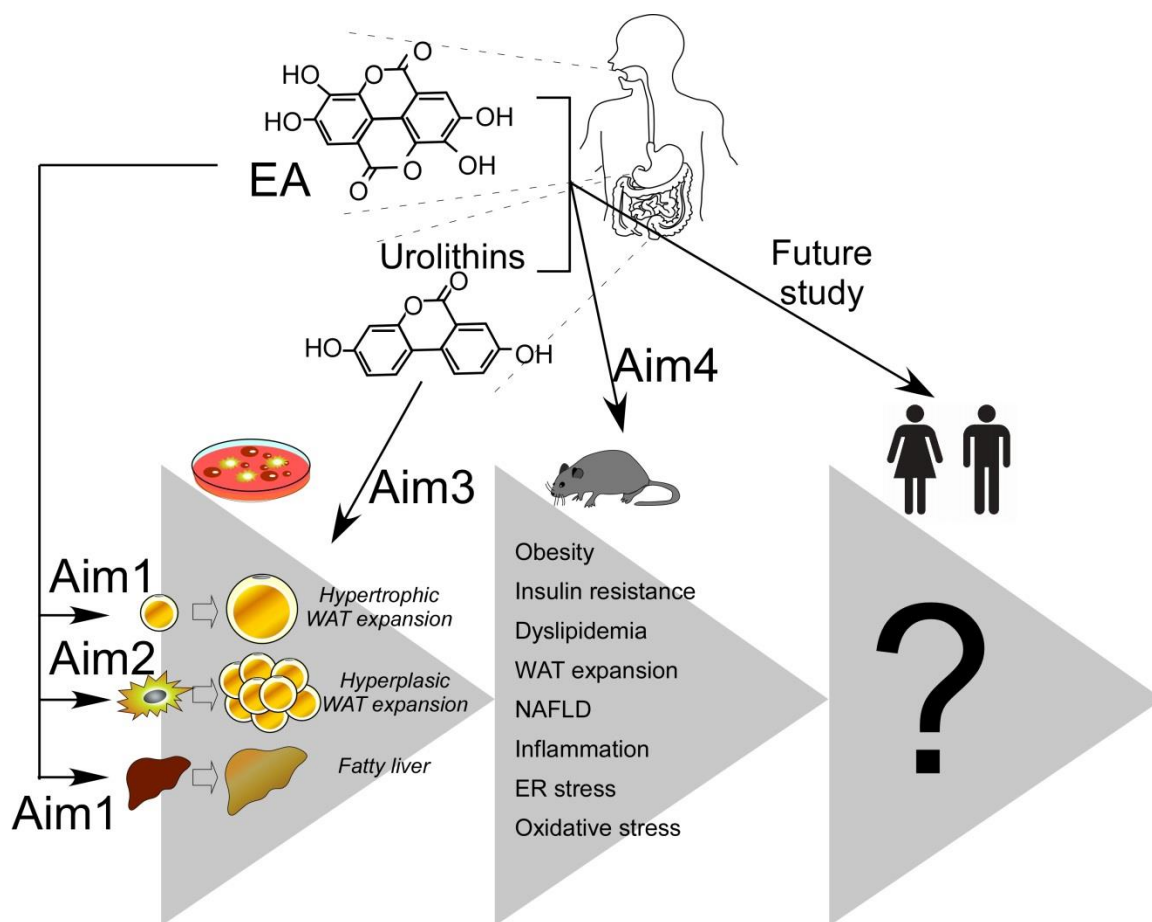


**Figure I-5 The central hypothesis and aims of this dissertation research.**

The central hypothesis of this research project is that dietary ellagic acid (EA) attenuates obesity and obesity-mediated metabolic complications. To test the hypothesis, in Aim #1, I focused on lipid-lowering effects of EA both in adipose tissue and liver via distinct mechanisms. In Aim #2, I focused on anti-adipogenic effects of EA via CARM1-mediated epigenetic regulation. In Aim #3, I ascertained the effects of EA on the prevention of obesity and its metabolic complications in a mouse model. Lastly, in Aim #4, I focused on whether EA-metabolites, Uro, resemble the health beneficial effects of EA in human adipocytes.

**II. CHAPTER I: Ellagic acid modulates lipid accumulation in primary human adipocytes and human hepatoma Huh7 cells via distinct mechanisms**

Inhae Kang<sup>a,b,\*</sup>, Meshail Okla<sup>a,b,\*</sup>, Da Mi Kim<sup>a</sup>, Vishinu Gourninei<sup>a</sup>, Neil Shay<sup>c</sup>, Liwei Gu<sup>a</sup>, Soonkyu Chung<sup>a,b,§</sup>

<sup>a</sup>Department of Food Science and Human Nutrition, University of Florida, Gainesville, FL and <sup>b</sup>Department of Nutrition and Health Sciences at the University of Nebraska, Lincoln, NE, <sup>c</sup>Department of Food Science and Technology at the Oregon State University, Corvallis, OR

\*Equal contribution

§To whom correspondence should be addressed: Soonkyu Chung, PhD, Department of Nutrition and Health Sciences, the University of Nebraska-Lincoln, 316G Ruth Leverton Hall P.O. Box 830806, Lincoln, NE, 68583, Fax: (402) 472-0806, E-mail: [schung4@unl.edu](mailto:schung4@unl.edu)

This work was supported by USDA-HATCH program

Key words: muscadine grape, ellagic acid; adipogenesis; obesity, liver lipid

## Abstract

Previously, we have reported that supplementation of muscadine grape phytochemical (MGP) decreased lipid accumulation against the high fat (HF)-diet. The aim of this study was to identify responsible polyphenolic constituents and to elucidate the underlying mechanisms. In mice, MGP supplementation significantly reduced visceral fat mass as well as adipocyte size. To determine whether MGP affects adipogenesis or hypertrophic lipid accumulation, we used human adipogenic stem cell (*hASCs*) model. Among the MGP, ellagic acid (10  $\mu\text{mol/L}$ ) was identified as a potent negative regulator in repressing adipogenesis of *hASCs*. In addition, ellagic acid substantially decreased the conversion of [ $^3\text{H}$ ]-acetyl CoA into fatty acid, suggesting that ellagic acid inhibits *de novo* synthesis of fatty acid in mature adipocytes. Similarly, MGP supplementation significantly decreased hepatic TG contents in liver. The TG-lowering effects of ellagic acid was confirmed in human hepatoma Huh7 cells. Ellagic acid reduced  $^3\text{H}$ -oleic acid esterification into [ $^3\text{H}$ ]-TG as well as *de novo* the synthesis of fatty acid from  $^3\text{H}$ -acetyl CoA in Huh7 cells. Intriguingly, ellagic acid also increased oxygen consumption rate and  $\beta$ -oxidation related gene expression. Taken together, ellagic acid attenuates new fat cell formation and fatty acid biosynthesis in adipose tissue, while it reduces the synthesis of triglyceride and fatty acid and increases fatty acid oxidation in liver. These results suggest that ellagic acid exerts unique lipid-lowering effects both in adipose tissue and liver via distinct mechanisms.

## 1. Introduction

Liver and adipose tissue are two major organs regulating the whole body lipid metabolism. Excessive lipid accumulation in fat and liver is a hallmark of obesity and metabolic syndrome. Obesity is characterized by abnormal expansion of white adipose tissue either by increasing number of adipocytes from mesenchymal progenitor cells (adipocyte hyperplasia) or by simply increasing its size (hypertrophy). The number of adipocytes is tightly controlled after puberty [1]. However, abnormal increase of adipocyte number is evident in childhood obesity and also frequently associated with extreme obesity in adults [2]. In contrast, enlargement of the adipocytes is the most common mechanism to accommodate surplus energy in the form of triglyceride in adults. It is well established that the adipocyte hypertrophy is concurred with adipose inflammation [3, 4]. Enlarged and inflamed adipocytes are key contributors to the pathogenesis of obesity by impairing endocrine function of adipocytes [5]. Although it is controversial that hyperplastic expansion of subcutaneous fat could be a defense mechanism to attenuate lipotoxicity, adipocyte hyperplasia also results in metabolically unfavorable ectopic adipogenesis and increases the risk for cardiovascular diseases (reviewed in [6]), suggesting that both hyperplastic and hypertrophic expansion of adipocytes are associated with adipocyte remodeling during the pathogenesis of metabolic syndrome [7].

The development of hepatic steatosis is intimately associated with the pathological conditions of adipocytes. Redistribution of fat in lipodystrophic conditions such as diabetes or uncontrolled lipolysis from the inflamed adipocytes increases the influx of FFA into the portal vein leading to hepatic steatosis [8]. Reversely, fatty liver is

a significant risk factor for hyperlipidemia, insulin resistance, and diabetes [9]. Supporting this notion, it has been reported that 76% of those with nonalcoholic fatty liver disease (NAFLD) are obese [10].

Attenuation of obesity by limiting adipocyte's capacity to expand (inhibition of either hypertrophic or hyperplastic expansion) is a general target of dietary supplementation, which may lead to detrimental consequences if the surplus FFA are re-directed into liver. Some food-borne dietary compounds that were claimed to be effective in attenuating adiposity (e.g., trans-10, cis-12 conjugated linoleic acid) had to be reevaluated its value due to an adverse side effect on hepatic steatosis [11, 12]. Recently, our group has reported that supplementation of muscadine grape phytochemicals (MGP) decreased visceral fat mass [13]. In addition, MGP supplementation was effective in reducing systemic and retinal inflammation, and glucose intolerance [13, 14]. However, the crosstalk of lipids between liver and adipose tissue by MGP has not been fully investigated yet. The aim of this study was 1) to identify the polyphenolic compounds posing the lipid-lowering effects of MGP and 2) to investigate the metabolic modification by MGP in adipocytes as well as in hepatocytes. Here we identified that ellagic acid inhibits adipogenesis and decreases lipid accumulation both in mature human adipocytes and hepatocytes via distinct mechanisms. Our results also suggest that ellagic acid may constitute consumer-friendly dietary strategy that may effective in reducing lipid accumulation both in adipose and liver.

## **2. Materials and Methods**

### *2.1 Chemicals*

Fetal bovine serum (FBS) was purchased from Cellgro. Rosiglitazone (BRL49653) was purchased from Cayman Chemical. All other chemicals and reagents were purchased from Sigma Chemical Co., unless otherwise stated.

## 2.2. *Animals*

The adipose tissue and liver samples were collected from our previous study [13]. Tissue was fixed in 10% buffered formaldehyde for paraffin embedding and hematoxylin and eosin (H&E) staining. All protocols and procedures were approved by the Institutional Animal Care and Use Committee (IACUC) at the University of Florida.

## 2.3. *Cell culture*

For isolation of human adipogenic stem cells (*hASCs*), abdominal adipose tissue was obtained from females with a body mass index (BMI) of ~30 during liposuction or abdominal plastic surgeries. Isolation of *hASCs* and differentiation of adipocytes was conducted as we described previously [15]. All protocols and procedures were approved by the Institutional Review Board (#693-2011) at the University of Florida and the University of Nebraska. Huh7 cells were a kind gift from Dr. Kim (the University of Florida). Huh7 cells were maintained in Dulbecco's modification of Eagle's medium (DMEM) containing 1% L-glutamine, 10% fetal bovine serum, 100 units/ml penicillin, 100 g/ml streptomycin in 5% CO<sub>2</sub> at 37°C. The medium was changed every 3 days.

## 2.4. *Adipocyte size measurement*

H&E stained-sections of epididymal adipose tissue were used for size determination by following the published protocol by Chen *et al.* [16]. Briefly, adipocyte size was examined by analyzing digital images of H&E stained paraffin sections (n=300

cells /mouse, total=1,500-2,000 adipocytes from 7-9 mice/diet group) by using Image J software.

### 1.5. *Lipid accumulation*

The colorimetric triglyceride quantification kit (BioVision, K622-100) was used to quantify the hepatic TG contents according to the manufacturer's protocol. To measure the lipid accumulation in human adipocytes and Huh7 cells, cells were fixed with isopropanol and stained with oil-red O. For determination of relative TG contents, bright field images were taken by eVOS XL microscope (AMG), or ORO dye was extracted for quantification (OD500 nm).

### 1.6. *Preparation of MGP and sub-fractionation*

Preparation of MGP has been described by Gourineni *et al.* [13]. The subfractionation of MGP into non-anthocyanin (NAcy) and anthocyanin (Acy) was completed as described previously [17]. To examine the effects of different phytochemicals on *hASCs* differentiation, ellagic acid (EA), quercetin (Quer), myricetin (My), and kaempferol (KMP) (Sigma) stocks were prepared in dimethyl sulfoxide (DMSO); aliquots of each stock were kept at -20 °C and freshly diluted at the time of addition to *hASCs*. The presence of intracellular lipid accumulation was visualized by oil red-O (ORO) staining.

### 2.7 *[<sup>3</sup>H]-oleic acid and [<sup>3</sup>H]-acetyl CoA incorporation into FFA and TG*

To measure fatty acid esterification rate into triglycerides, we followed the previously published methods by Chung *et al.* [18] in cultures of mature adipocytes or human hepatoma Huh7 cells were used. Briefly, cells incubated with serum-free low

glucose (1,000 mg/L d-glucose) overnight before experiment.  $^3\text{H}$ -oleic acid (Perkin Elmer, final concentration of 0.5  $\mu\text{Ci/mL}$ ) was complexed with fatty acid-free BSA, then added to cells for 3 hr (a time course study indicated a linear incorporation into cellular TG fraction over a 6 hr period; data not shown). After 3 hr incubation with  $^3\text{H}$ -oleic acid, medium containing unincorporated isotope was removed by washing PBS. The cellular lipids were extracted by Bligh and Dyer method. Then thin layer chromatography was performed to fractionate FFA and TG, and the [ $^3\text{H}$ ] radioactivity was measured by liquid scintillation counting (Beckman LS 6000; Beckman Instruments, Palo Alto, CA). Radioactivity was normalized by protein concentration quantified by bicinchoninic acid (BCA) colorimetric assay (Pierce, Rockford, IL). Similarly, for the measurement of *de novo* synthesis of fatty acid, [ $^3\text{H}$ ]-acetyl CoA (Perkin Elmer, final concentration of 0.5  $\mu\text{Ci/mL}$ ) were added to cells for 3 hr and unincorporated isotope was removed by washing PBS three times.

### 2.8. [ $^3\text{H}$ ] 2-deoxy-glucose uptake

To determine the basal, and insulin-stimulated glucose uptake, cultures of mature human adipocytes were incubated with or without 10 $\mu\text{mol/L}$  of EA for 3 days. The day before the experiment, cultures were incubated with 1ml serum free basal medium containing 1,000 mg/L d-glucose and 20 pmol/L human insulin (Thermo scientific, SH30021.01) in the presence of vehicle or treatment. After 24hrs serum starvation, culture media was removed and replaced with 1 ml of HBSS buffer containing 100 nmol/L human insulin for 10 min then add [ $^3\text{H}$ ]-2DOG (Perkin Elmer, final concentration was 0.5  $\mu\text{Ci/mL}$ ) and incubated at 37°C for 90 min. Glucose uptake was terminated by adding 1 ml of stop buffer (ice-cold Krebs-Ringers bicarbonate (KRBC) buffer

supplemented with 25mmol/L d-glucose. After washing cells with KRBC buffer three times to reduce background radioactivity, cells were lysed in 0.1% SDS. The total cellular lysates were subjected to determine glucose uptake by liquid scintillation counting [19] .

#### *2.10. Oxygen consumption rate (OCR)*

Huh7 cells were seeded into 96-well clear bottom black polystyrene sterile plate (Corning). Oxygen consumption rate (OCR) was determined by using the assay kit MitoXpress<sup>®</sup> (Cayman Chemical, 600800) according to the manufacturer's protocol. Briefly, an increase of phosphorescence signal from the oxygen-sensitive probe was measured over 5 hr with 3 minutes interval using Synergy H1 multi-mode microplate reader (BioTek).

#### *2.11. qPCR*

Gene-specific primers for qPCR were obtained from Integrated DNA Technologies (Chicago, IL). Total mRNA of *hASCs* was isolated using Trizol reagent (Invitrogen). To remove genomic DNA contamination, mRNA was treated with DNase (Mediatech); 2 µg of mRNA was converted into cDNA in a total volume of 20 µL (iScript cDNA synthesis kit, Bio-Rad). Gene expression was determined by real-time qPCR (CFX96, Bio-Rad), and relative gene expression was normalized by 36b4 (primer sequences will be available upon request).

#### *2.12. Western blot analysis*

To prepare tissue lysates, 0.1 g of snap-frozen tissue was homogenized in ice-cold RIPA buffer (Thermo Scientific) with protease inhibitors (Sigma) and phosphatase inhibitors (2 mmol/L Na<sub>3</sub>VO<sub>4</sub>, 20 mmol/L β-glycerophosphate and 10 mmol/L NaF).

Lysate of adipose tissue was incubated in ice for 10 minutes to remove the solidified fat cake. To prepare total cell lysates, monolayers of differentiated cultures of human adipocytes were harvested with RIPA buffer. Proteins were fractionated onto 4-15% pre-casted SDS-PAGE (Biorad), transferred to PVDF membranes with a semi-dry transfer unit (Hoefer TE77X) and incubated with the relevant antibodies. Chemiluminescence from ECL (Western Lightning) solution was detected with FluorChem E (Cell Biosciences) imaging system. Polyclonal or monoclonal antibodies targeting to FAS (3180),  $\beta$ -actin (4967), and H3K9Ac (AcH3, 9649) were purchased from Cell Signaling Technology. Antibodies targeting HDAC9 (ab 59718) and histone H3 (ab1791) were purchased from Abcam. The mouse monoclonal antibodies for PPAR $\gamma$  (sc-7273), FABP (aP2, sc-271529) were purchased from Santa Cruz Biotechnology.

### *2.13. Statistical analysis*

Results are presented as the mean  $\pm$  SEM. The data were statistically analyzed using Student's t-test or one-way ANOVA with Tukey's multiple comparison tests. For the analysis of adipocyte size, Gaussian curve fitting and linear regression were performed. To calculate oxygen consumption rate, linear regression (95% confidence,  $p < 0.05$  significant) was conducted. All analyses were performed with GraphPad Prism 6 (Version 6.02).

## **3. Results**

### *3.1 MGP supplementation attenuated adipocyte size in C57BL/6 mice*

Previously, we reported that the supplementation of MGP (*Vitis rotundifolia*) significantly reduced HF-diet induced epididymal fat mass [13]. However, mechanistic details by which MGP supplementation reduced adiposity is unknown. To determine whether MGP decreases adipocyte hypertrophy, we first examined epididymal adipocyte size by analyzing digital images of H&E stained paraffin sections. Consistent with the reduced epididymal fat mass (Fig. 1A), adipocyte size was significantly reduced with MGP supplementation compared to HF alone (Fig. 1B,  $86.8 \pm 2.8$ ,  $100.6 \pm 3.3$  and  $86.5 \pm 1.4$   $\mu\text{m}$  for LF, HF, and HF+MGP, respectively). Histograms of adipocyte size distribution also demonstrated a clear shift toward smaller sizes for the HF+MGP group, which is comparable to LF control (Fig. 1C, D).

### *3.2. EA in MGP is a potent negative regulator of adipogenesis*

To gain insights into whether MGP supplementation also decreases hyperplastic expansion of adipocytes (adipogenesis) as well as hypertrophic expansion of adipocytes (Fig 1), we examined protein expression that are known to influence adipogenesis. As we expected, PPAR $\gamma$  expression levels were higher in the HF group in comparison to LF or HF+MGP group. Interestingly, HDAC9 expression, a negative regulator of adipogenesis [20], was reduced in the HF group compared to LF or HF+MGP. Conversely, histone lysine 9 acetylation (H3K9Ac) levels, a positive epigenetic marks for adipocyte differentiation, were markedly increased in the HF group compared to LF or HF+MGP (Fig. 2A), providing a hint that adipocyte differentiation might be reduced by MGP supplementation. To pursue this possibility, we conducted in vitro studies using adipose-derived human stem cells (*hASCs*). First, we fractionated MGP into Acy and NAcy

fractions. The effect of each fraction on adipocyte development was examined. The anthocyanin fraction had significant but minor impact on adipogenesis. In contrast, the NAcy fraction dramatically suppressed lipid accumulation in a dose-dependent manner as assessed by oil red O (ORO) staining (Fig. 2B,C). Consistent with reduced TG accumulation, the NAcy fraction of MGP dramatically suppressed adipogenic gene expression including PPAR $\gamma$  and adipocyte protein 2 (aP2) (**Fig 2D**). Next, we performed HPLC analysis and found that the NAcy fraction composed of four major polyphenols, EA, My, Quer and KMP (Fig. 3A). When *h*ASCs were exposed to 10  $\mu$ M of these individual pure polyphenols, EA almost exclusively repressed the adipogenesis compared to the other polyphenols. In in vitro model of human adipocytes, EA decreased: 1) TG accumulation as assessed by ORO-staining (Fig. 3B); 2) adipogenic gene expression by qPCR including PPAR $\gamma$ , CCAAT/enhancer binding protein alpha (C/EBP $\alpha$ ), aP2, and fatty acid synthase (FAS) (Fig. 3C); and 3) adipogenic protein expression including PPAR $\gamma$ , aP2, and FAS (Fig. 3D).

### *3.3. EA attenuated lipid accumulation in mature adipocytes*

Next, we asked whether EA is the key polyphenolic component that antagonizing the adipocyte hypertrophy as we have observed in Fig.1, as well as suppressing adipogenesis. To answer this question, EA was treated to the fully-differentiated cultures of human adipocytes (d7). EA incubation was last for 3 or 7 days depends on experimental design in Fig 4A. Addition of 10 $\mu$ M EA for 7 days caused a significant reduction of triglyceride accumulation by oil red O staining (Fig. 4B). To test whether the decrease of triglyceride accumulation is due to an alteration of lipogenic pathways, [ $^3$ H]-

acetyl CoA and [<sup>3</sup>H]-oleic acid was added to the adipocytes and examined its conversion into triglyceride. The conversion of [<sup>3</sup>H]-acetyl CoA to radiolabeled FFA (Fig. 4C) and TG (Fig. 4D) was almost completely blunted by 3 days of EA treatment. However, exposure of EA exert no significant impact on conversion of <sup>3</sup>H-oleic acid into [<sup>3</sup>H]-TG at 3 days (Fig. 4E). In addition, the basal- and insulin-stimulated [<sup>3</sup>H]-2-deoxyglucose uptake was not affected by EA treatment (Fig. 4F). The extended treatment of EA for 7 days decreased adipocyte specific mRNA expression including PPAR $\gamma$ , C/EBP $\alpha$ , and fatty acid synthase (FAS) compared to vehicle control (no changes in adipogenic genes in EA treatment for 3 days, data not shown). There were no significant changes in fatty acid oxidation-related gene expression (PPAR $\alpha$  and CPT1), but lipolysis related genes expression (i.e., hormone sensitive lipase (HSL) and adipocyte triglyceride lipase (ATGL)) was substantially lower in EA treated adipocytes (Fig. 4G). Taken together, these data implicates that the inhibition of *de novo* synthesis of fatty acid is accompanied by transcriptional regulation of lipogenic gene expression in EA-treated human adipocytes.

#### 3.4. MGP decreased hepatic lipid accumulation in C57BL/6 mice

Attenuation of adipogenesis could cause hepatic steatosis if the liver mishandles fatty acid (FA) influx from adipose tissue [21]. To determine the effects of MGP on hepatic lipid metabolism, we also measured hepatic TG contents. H&E staining showed a reduction of hepatic lipid accumulation in HF+MGP group compared to HF only group, which was confirmed by ~50 % reduction of hepatic TG content in MGP-fed group compared to HF group (Fig. 5A,B). Interestingly, fatty acid oxidation-related genes including PPAR $\alpha$ , FGF21, ACOX1 and CPT1 were significantly higher in the MGP

group (Fig. 5C), suggesting that MGP decreased hepatic TG accumulation, at least in part, by augmenting hepatic fatty acid oxidation as well as attenuating adipocyte expansion.

### 3.5. EA attenuated lipid accumulation in Huh7 cells

To determine whether EA is the primary polyphenolic compound in reducing hepatic triglyceride accumulation, we further examined effects of EA on fatty acid esterification, *de novo* synthesis, and FA oxidation in human hepatocarcinoma Huh7 cells. Pretreatment with EA for 24 hr significantly attenuated lipid accumulation in a dose-dependent manner in Huh7 cells (Fig. 6A). In parallel to MGP-fed mice this, mRNA expression of fatty acid  $\beta$ -oxidation relative genes such as PPAR $\alpha$  and carnitine palmitoyltransferase 1 (CPT1) was up-regulated, but not ACOX1, in EA treated samples. In contrast, genes involved in lipogenesis, i.e., FAS and diacylglycerol acyltransferase 2 (DGAT2), were significantly reduced by EA treatment without affecting stearoyl-CoA desaturase 1(SCD1) gene expression (Fig. 6B). Accordingly, the oxygen consumption rate, measured by oxygen-sensitive phosphorescence probe, was higher in Huh7 cells treated with EA than vehicle control (Fig. 6C) demonstrating an up-regulation of fatty acid oxidation by ellagic acid in hepatocytes. Interestingly, the uptake of [ $^3$ H]-oleic acid (OA) into the cells was similar between groups (Fig. 6D), while incorporation of [ $^3$ H]-oleic into TG was significantly lower in Huh7 cells treated with EA (Fig. 6E). Similar to adipocytes, incorporation of  $^3$ H-acetyl CoA into FFA and TG was markedly decreased with EA treatment (Fig. 6F,G). Collectively, our data clearly showed that MGP and its active polyphenolic constituent ellagic acid decrease hepatic lipid accumulation by targeting multiple mechanisms including FFA synthesis, TG esterification, and FFA oxidation.

#### 4. Discussion

Obesity and hepatic steatosis are the two manifest phenotypes of metabolic syndrome and are inextricably linked together. The simultaneous reduction of lipid accumulation both in adipose tissue and liver would be the ultimate goal for the dietary intervention strategies. The present study was designed to determine the TG-lowering effect of MGP supplementation on adipose and liver, and to identify the metabolic alterations by ellagic acid by using the human model of adipocyte and hepatocytes in parallel. We demonstrated that the supplementation of MGP attenuated hypertrophic obesity (Fig. 1) and hepatic steatosis (Fig. 5) in HF-fed mice. Ellagic acid has been identified as the active polyphenolic compound that suppressed the hyperplastic expansion of adipocytes (Fig. 2, 3). Besides, ellagic acid exerted the distinctive lipid-lowering properties by decreasing biosynthesis of fatty acid in both adipocytes and hepatocytes but by augmenting fatty acid oxidation only in hepatocytes (Fig. 4, 6). Our data provide the first evidence that ellagic acid plays separate roles in manipulating excess lipid in adipocytes versus hepatocytes, resulting in a concerted attenuation of obesity and hepatic steatosis. Collectively, our results suggest that ellagic acid-containing foods may constitute a novel and effective dietary strategy to prevent and/or treat obesity and metabolic syndrome.

Muscadine grape (*V. rotundifolia*) contains an array of health-promoting bioactive phytochemicals [22-24]. Our previous study has provided the implication that unique lipid-lowering property of MGP may attribute to the high content of ellagic acid [13]. In the present study, we proved that ellagic acid exhibits broad action spectrum by targeting to multiple mechanisms, i.e., adipocyte differentiation, *de novo* synthesis of fatty acid,

FA esterification, and FA oxidation, probably through different mechanisms in liver and adipose tissue. Numerous reports implicated that ellagic acid-containing fruits, vegetables, and nuts are effective dietary sources to attenuate obesity. However, direct evidence of the underlying mechanism of how ellagic acid displays an anti-obesity effect, has not been addressed yet. To better understand the relationship between the ellagic acid intake and adiposity, we have reviewed and combined the results from published, peer-reviewed literature, mainly in rodents [13, 25-31] (Supplement Table 1). Despite the variations related to the differences in sources and contents of ellagic acid, daily intake of ellagic acid in the range of 5-88 mg/kg BW was strongly correlated with >25% decrease of fat mass (with minor impact on lean body mass), and improvement of glucose metabolism. The conclusion deduced from these summary (Supplement Table 1) correlates with our present data that EA-enriched MGP is associated with a reduction of fat mass, adipocyte hypertrophy, and hepatic lipid accumulation. Interestingly, the muscadine wine extract that has almost identical phytochemical composition except for markedly reduced ellagic acid content due to filtration [32], was lack of lipid-lowering effects. It provides us with additional rationale to draw the conclusion that ellagic acid is a key ingredient of MGP to reduce fat mass.

It has been well documented that ellagic acid possesses anti-proliferative and anti-inflammatory characteristics in various cancerous cell lines [25, 33]. Also, ellagic acid has shown to be effective in reducing atherosclerotic lesions [34] and increasing cholesterol efflux in macrophages [35]. In this study, we add the previously unappreciated value of ellagic acid as a lipid-lowering dietary compound both in adipose and liver. The reduction of adiposity attribute to a reduction of both hyperplastic and

hypertrophic expansion of adipocytes. The inhibitory effects of MGP (or ellagic acid) on adipogenesis seem to be associated with, at least partly, epigenetic modification (Fig. 2, 3). Recently, ellagic acid was identified as a negative regulator of histone 3 arginine 17 methylation (H3R17me) by inhibiting CARM1 (coactivator-associated arginine methyltransferase 1) in cancerous cells [36]. Given to the fact that CARM1 activity is required for adipogenesis [37], we investigated the epigenetic regulation of adipogenesis by ellagic acid in a separate study using the same primary human adipocytes. In that study, we demonstrated that ellagic acid alters epigenetic marks of adipocyte differentiation by altering histone deacetylase (HDAC) activity, acetylation, and methylation levels. It may align well with the study by Wang et al. showing that ellagic acid inhibits differentiation of 3T3L1 preadipocyte into adipocytes by inhibiting mitotic clonal expansion [38], although primary adipogenic progenitor cells do not enter mitotic clonal expansion and the involvement of CARM1 need to be verified in 3T3L1 cells.

The attenuation of the hypertrophic expansion (increase in size by excessive TG accumulation) was clearly detectable both in epididymal fat of MGP-fed mice (Fig. 1) as well as in the ellagic acid-treated mature adipocyte cultures (Fig. 4). A reduction of FA biosynthesis in mature adipocytes (Fig. 4C) was an earlier event than transcriptional down-regulation of adipogenic gene expression (Fig. 4G). Conversely, FA esterification into TG, glucose uptake (both basal- and insulin-stimulated), and fatty acid oxidation were not altered by ellagic acid at the same window of time when fatty acid biosynthesis is markedly reduced by ellagic acid. It is unlikely that the inhibition of fatty acid synthesis is due to diminished CARM1 activity, as we do not examine the differences in H3R17me levels in mature adipocytes before and after ellagic acid treatment (data not

shown). Based on our results, there is a likelihood that ellagic acid may directly affect fatty acid synthase (FAS). We are currently under investigation whether ellagic acid alters global lipid metabolism using the different mutant strains of yeast (*Saccharomyces cerevisiae*) carrying deletion of critical genes related to lipid metabolism.

The impact of MGP and ellagic acids on lipid metabolism in the liver was more phenomenal than in adipose tissue. MGP supplementation decreased hepatic TG content by ~50% compared to HF alone, probably through the augmented fatty acid oxidation (Fig. 5). In agreement with our findings, Yoshimura et al. reported that supplementation of 0.1% of ellagic acid for 68 days was effective in decreasing hepatic steatosis by increasing mRNA expression of PPAR $\alpha$  and CPT1 $\alpha$  genes in KK-A<sup>y</sup> mice, a model of obesity type 2 diabetes [39]. Consistently, we were able to reproduce that ellagic acid lowered TG accumulation (Fig. 6A), increased of fatty acid oxidation-related gene expression (Fig. 6B) and, more importantly, oxygen consumption rate (Fig. 6C) in human hepatoma cells. Moreover, despite that it was less evident in MGP-fed mice, ellagic acid decreased FA uptake, *de novo* synthesis, and its esterification into TG (Fig6. D-G). These TG-lowering effects are also supported by ellagic acid supplementation in rats [31], and our pilot study with pure ellagic-fed mice supplementation (unpublished data). The exact mechanistic nature by which ellagic acid targets to multiple metabolic pathways in liver is uncertain. Some potential mechanism that ellagic acid represses *de novo* synthesis of FA could be found. Sarikaya et al. showed that ellagic acid is an inhibitor of carbonyl anhydrilase (CA) activity [40], and a reduction of CA activity has been associated with lowering hepatic *de novo* lipid synthesis in primary rat hepatocytes [41]. We are currently investigating the two possibilities that 1) ellagic acid may change epigenetic

marks such as H3R17me2 by CARM1 [36], leading to transcriptional inhibition of lipogenic gene expression in hepatocytes, and 2) ellagic acid directly inhibits lipogenic enzyme activities including fatty acid synthase (FAS) and acetyl CoA carboxylase activity (ACC).

Free ellagic acid can be found in plasma up to  $\sim 1 \mu\text{mol/L}$  concentration after oral administration [42], but it rapidly metabolizes into urolithins by gut microbes [43]. Our current study design has the obvious limitations to translate into humans, as we used the  $10 \mu\text{mol/L}$  ellagic acid in 0.1 % DMSO, and metabolite information was not taken into consideration in cellular studies. Intriguingly, treatment of physiologically achievable concentration of ellagic acid ( $< 1 \mu\text{mol/L}$ ), took the longer period of time to detect the measurable reduction of TG levels in hepatocytes and adipocytes (unpublished data), implicating that reduction of lipid accumulation could be attainable via chronic supplementation of ellagic acid-containing diet. Actually, pure ellagic acid (0.08 %) supplementation for 8 wks was effective in reducing fat pad size and liver weight against HF diet in rats [31]. Our pilot study with 0.1 % of ellagic acid supplementation for 12 wks reduced the liver lipid contents (data not shown). We are under investigation to determine whether urolithin A, the major metabolite of ellagic acid, could reiterate multiple lipid-lowering effects of ellagic acid with greater biological potency than ellagic acid.

In summary, here we identified ellagic acid as the primary polyphenolic component to lower triglycerides among MGP, and delineated the metabolic pathways that affected by ellagic acid in adipocyte and hepatocytes. There are unanswered questions regarding physiological levels of ellagic acid and generation of microbial

metabolites, but we believe, nonetheless, our works provide mechanistic insights into lipid-lowering effects of ellagic acid. It is the first report that separately investigated the lipid-lowering effects of ellagic acid in adipose and liver. More research will be implemented for better understanding of multiple metabolic benefits of ellagic acid-containing foods.

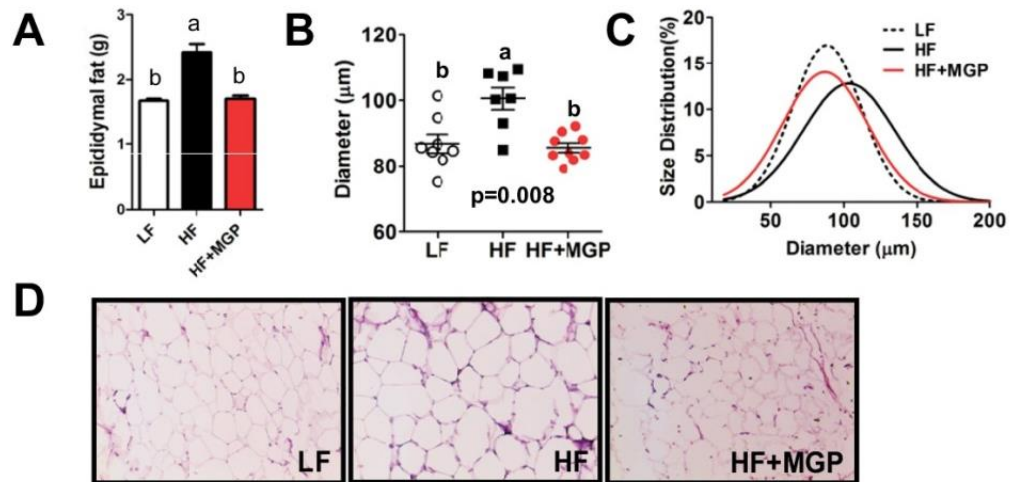
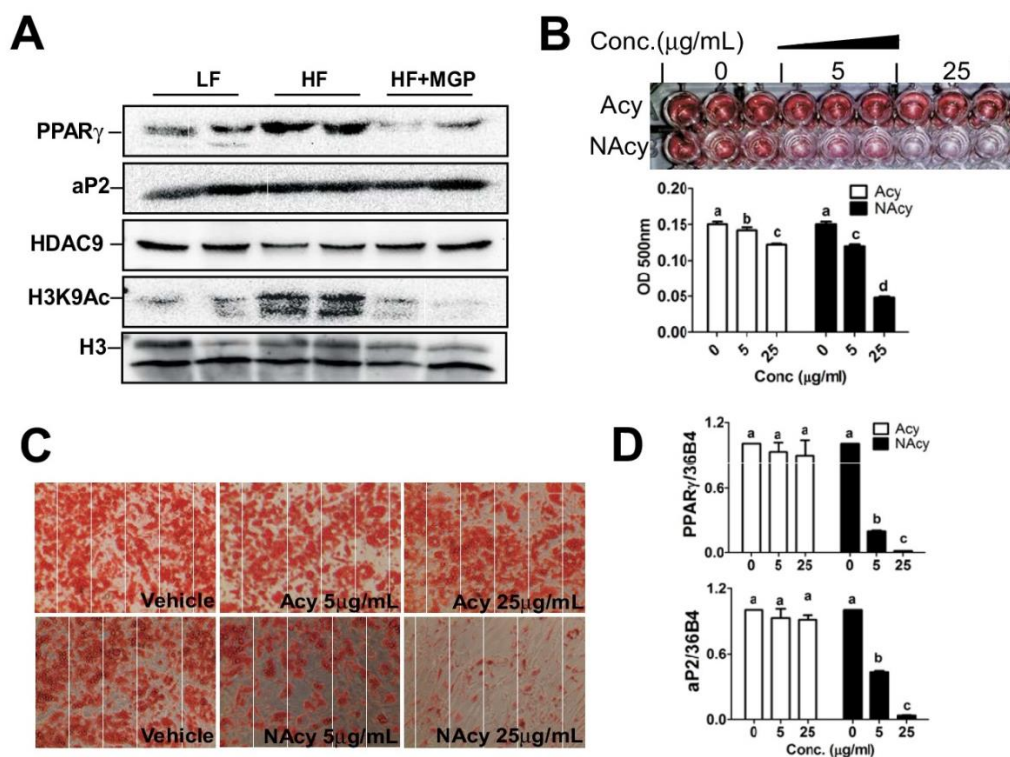
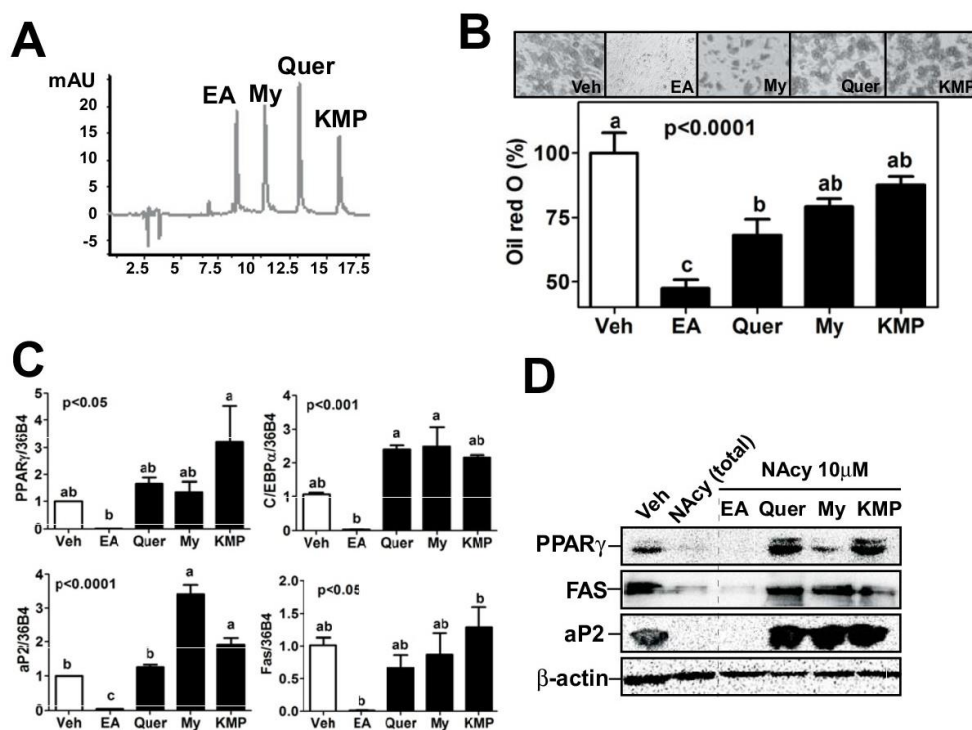


Figure II-1 MGP supplementation attenuated fat mass and adipocyte size.



**Figure II -2 NAcy constituents of MGP were associated with a decrease of adipocyte differentiation.**

A, Protein expression of PPAR $\gamma$ , aP2, HDAC9, H3K9Ac, and H3 by western blot analysis from the mice fed with either low fat (LF), high fat (HF), or HF+0.4% MGP for 15 wks. Cultures of *h*ASCs were differentiated and incubated with either Acy or NAcy fractions for seven days. **B**, Triglyceride Lipid accumulation in 96 well culture plates was visualized by ORO-staining (upper). Extracted ORO-staining was quantified (OD500 nm) (lower). **C**, Bright field images with ORO-staining for cultures differentiated with different doses of NAcy and Acy. **D**, Adipogenic gene expression of PPAR $\gamma$  and aP2 by qPCR analysis. All values are presented as the mean  $\pm$ SEM. Means not sharing a common superscript differ,  $p < 0.05$ .



**Figure II -3 EA suppressed adipogenesis of *hASCs*.**

Cultures of *hASCs* were induced to differentiation in the presence of either vehicle (Veh) or 10  $\mu\text{mol/L}$  of NAcY components of EA, My, Quer, and KMP. **A**, HPLC chromatogram showing major phenolic constituents of NAcY fraction in MGP. **B**, Effects of individual polyphenols on TG accumulation measured by ORO-staining. **C**, Adipogenic gene expressions of PPAR $\gamma$ , aP2, C/EBP $\alpha$  and FAS by qPCR analysis. **D**, Adipogenic protein expression of PPAR $\gamma$ , Fas, and aP2 by western blot analysis. All values are presented as the mean  $\pm$ SEM. Means not sharing a common superscript differ,  $p < 0.05$ .

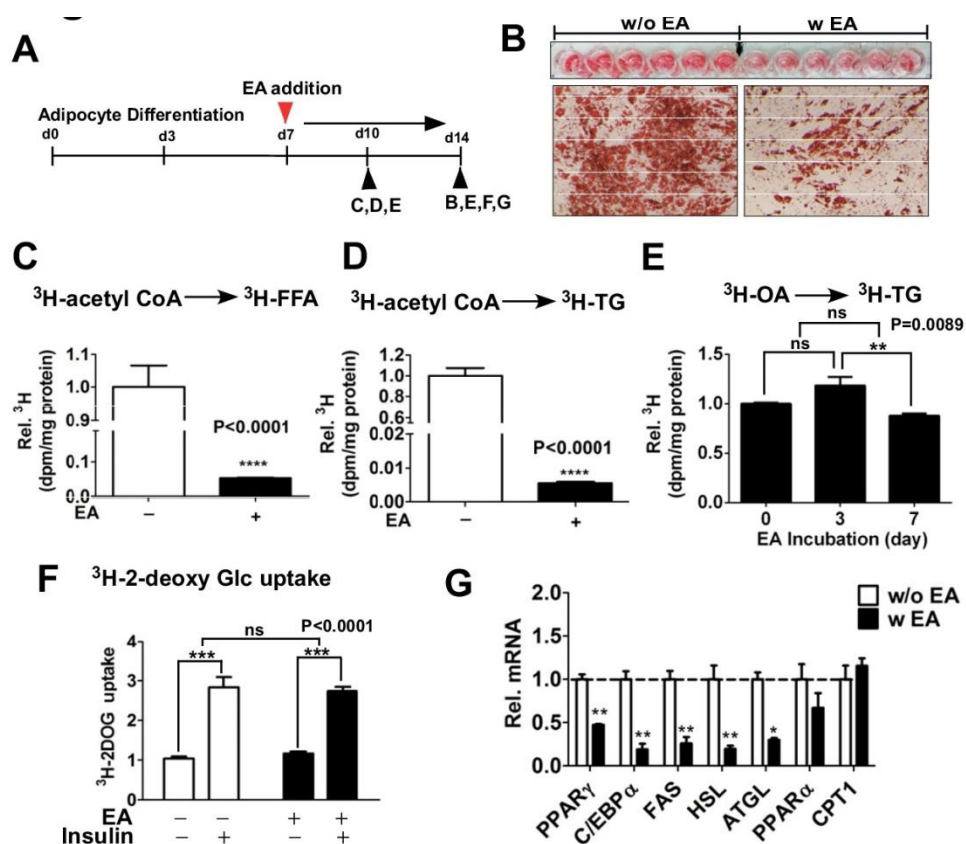


**Figure II -4 EA decreased triglyceride accumulation in mature human adipocytes. A. Experimental scheme.**

EA (10 $\mu\text{M}$ ) was added to the newly differentiated human adipocytes (at day 7) and incubated for 3-7 day. Experiments were conducted at the given time (arrows). **B**, Lipid accumulation was visualized by ORO-staining. **C**, Conversion of [ $^3\text{H}$ ]-acetyl coA into [ $^3\text{H}$ ]-fatty acid. **D**, Conversion of [ $^3\text{H}$ ]-acetyl CoA into [ $^3\text{H}$ ]-triglyceride. **E**, Conversion of [ $^3\text{H}$ ]-oleic acid into  $^3\text{H}$ -TG. **F**, Basal and insulin-stimulated [ $^3\text{H}$ ]-2-deoxyglucose uptake. **G**, Gene expression levels of PPAR $\gamma$ , C/EBP $\alpha$ , FAS, PPAR $\alpha$ , and CPT1 by qPCR. In C-F, data were normalized by protein concentration. All values are presented as the mean  $\pm$ SEM, \* p < 0.05, \*\*p < 0.01, and \*\*\*\* P < 0.0001 by student t-tests.

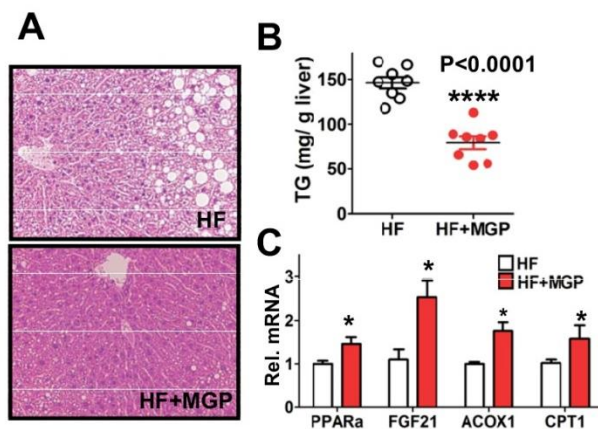


**Figure II -5 MGP supplementation decreased hepatic lipid accumulation.**

C57BL/6 mice were fed with either high fat (HF) or HF + 0.4% MGP for 15 wks. **A**, H&E staining for liver tissues. **B**, TG content in liver. **C**, mRNA levels of PPAR $\alpha$ , FGF21, ACOX1 and CPT1 in liver by qPCR. All values are presented as the mean  $\pm$ SEM, \*\*\*\* P < 0.0001, \* P < 0.05.

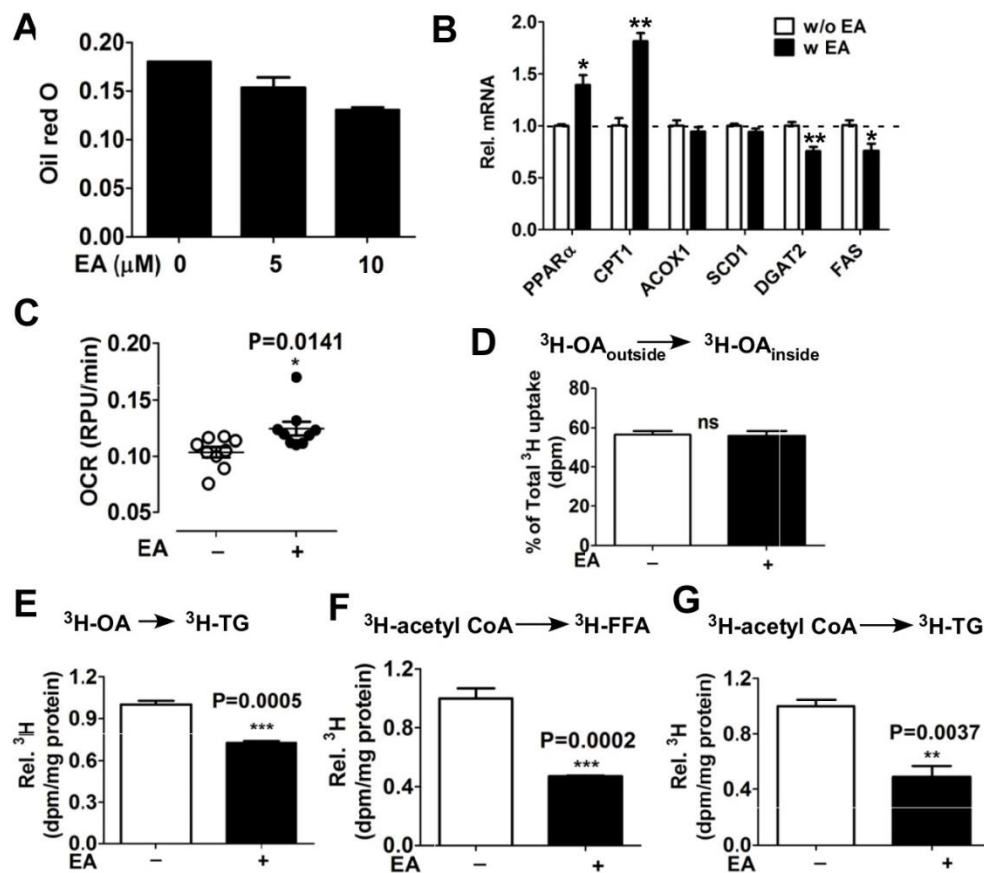
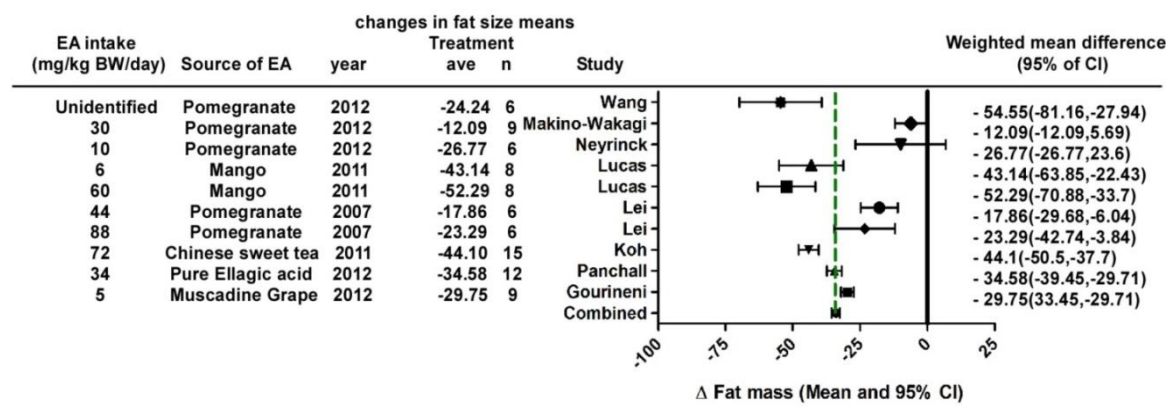


**Figure II -6 EA decreased triglyceride accumulation in human hepatoma Huh7 cells.** Huh7 cells were preincubated overnight with or without (w/o) ellagic acid (EA). **A**, Lipid accumulation quantified by oil red O staining in Huh7 cells that received 5 or 10  $\mu\text{mol/L}$  of EA. **B**, mRNA expression levels involved in FA  $\beta$ -oxidation and lipogenesis by qPCR. **C**, Oxygen consumption rate (OCR) in the presence or absence of EA. **D**, Uptake of  $^3\text{H}$ -oleic acid (OA) into cells. **E**, Conversion of  $^3\text{H}$ -OA into  $^3\text{H}$ -triglyceride (TG). **F**, Conversion of  $^3\text{H}$ -acetyl CoA into  $^3\text{H}$ -FFA. **G**, Conversion of  $^3\text{H}$ -acetyl CoA into  $^3\text{H}$ -TG.

Supplement Table 1. Effect of ellagic acid (EA)-containing diet on adiposity from different sources<sup>1</sup>



<sup>1</sup> Analysis was performed using meta-analysis calculator at <http://www.healthstrategy.com/meta/meta.pl>

## References

- [1] Spalding KL, Arner E, Westermark PO, Bernard S, Buchholz BA, Bergmann O, Blomqvist L, Hoffstedt J, Naslund E, Britton T, Concha H, Hassan M, Ryden M, Frisen J, Arner P. Dynamics of fat cell turnover in humans. *Nature* 2008;453:783-7.
- [2] Drolet R, Richard C, Sniderman AD, Mailloux J, Fortier M, Huot C, Rheaume C, Tchernof A. Hypertrophy and hyperplasia of abdominal adipose tissues in women. *Int J Obes (Lond)* 2008;32:283-91.
- [3] Weisberg SP, McCann D, Desai M, Rosenbaum M, Leibel RL, Ferrante AW, Jr. Obesity is associated with macrophage accumulation in adipose tissue. *J Clin Invest* 2003;112:1796-808.
- [4] Winkler G, Kiss S, Keszthelyi L, Sapi Z, Ory I, Salamon F, Kovacs M, Vargha P, Szekeres O, Speer G, Karadi I, Sikter M, Kaszas E, Dworak O, Gero G, Cseh K. Expression of tumor necrosis factor (TNF)-alpha protein in the subcutaneous and visceral adipose tissue in correlation with adipocyte cell volume, serum TNF-alpha, soluble serum TNF-receptor-2 concentrations and C-peptide level. *Eur J Endocrinol* 2003;149:129-35.
- [5] Skurk T, Alberti-Huber C, Herder C, Hauner H. Relationship between adipocyte size and adipokine expression and secretion. *J Clin Endocrinol Metab* 2007;92:1023-33.
- [6] Britton KA, Fox CS. Ectopic fat depots and cardiovascular disease. *Circulation* 2011;124:e837-e841.
- [7] Sun K, Kusminski CM, Scherer PE. Adipose tissue remodeling and obesity. *J Clin Invest* 2011;121:2094-101.
- [8] Youssef W, McCullough AJ. Diabetes mellitus, obesity, and hepatic steatosis. *Semin Gastrointest Dis* 2002;13:17-30.
- [9] Savage DB, Semple RK. Recent insights into fatty liver, metabolic dyslipidaemia and their links to insulin resistance. *Curr Opin Lipidol* 2010;21:329-36.
- [10] Farrell GC, Larter CZ. Nonalcoholic fatty liver disease: from steatosis to cirrhosis. *Hepatology* 2006;43:S99-S112.
- [11] Poirier H, Shapiro JS, Kim RJ, Lazar MA. Nutritional supplementation with trans-10, cis-12-conjugated linoleic acid induces inflammation of white adipose tissue. *Diabetes* 2006;55:1634-41.
- [12] Clement L, Poirier H, Niot I, Bocher V, Guerre-Millo M, Krief S, Staels B, Besnard P. Dietary trans-10,cis-12 conjugated linoleic acid induces hyperinsulinemia and fatty liver in the mouse. *J Lipid Res* 2002;43:1400-9.
- [13] Gourineni V, Shay NF, Chung S, Sandhu AK, Gu L. Muscadine Grape ( *Vitis rotundifolia* ) and Wine Phytochemicals Prevented Obesity-Associated Metabolic Complications in C57BL/6J Mice. *J Agric Food Chem* 2012;60:7674-81.
- [14] Jung-Heun Ha, Pollob Kumar Shil, Ping Zhu, Liwei Gu, Qihong Li, Soonkyu Chung. Ocular Inflammation and Endoplasmic Reticulum Stress Are Attenuated by Supplementation with Grape Polyphenols in Human Retinal Pigmented Epithelium Cells and in C57BL/6 Mice. *J Nutr* 2014;144:1-14.
- [15] Zhao L, Ha JH, Okla M, Chung S. Activation of autophagy and AMPK by gamma-tocotrienol suppresses the adipogenesis in human adipose derived stem cells. *Mol Nutr Food Res* 2014;58:569-79.

- [16] Chen HC, Farese RV, Jr. Determination of adipocyte size by computer image analysis. *J Lipid Res* 2002;43:986-9.
- [17] Sandhu AK, Gu L. Antioxidant capacity, phenolic content, and profiling of phenolic compounds in the seeds, skin, and pulp of *Vitis rotundifolia* (Muscadine Grapes) As determined by HPLC-DAD-ESI-MS(n). *J Agric Food Chem* 2010;58:4681-92.
- [18] Chung S, Gebre AK, Seo J, Shelness GS, Parks JS. A novel role for ABCA1-generated large pre-beta migrating nascent HDL in the regulation of hepatic VLDL triglyceride secretion. *J Lipid Res* 2010;51:729-42.
- [19] Chung S, LaPoint K, Martinez K, Kennedy A, Boysen SM, McIntosh MK. Preadipocytes mediate lipopolysaccharide-induced inflammation and insulin resistance in primary cultures of newly differentiated human adipocytes. *Endocrinology* 2006;147:5340-51.
- [20] Chatterjee TK, Idelman G, Blanco V, Blomkalns AL, Piegore MG, Jr., Weintraub DS, Kumar S, Rajsheker S, Manka D, Rudich SM, Tang Y, Hui DY, Bassel-Duby R, Olson EN, Lingrel JB, Ho SM, Weintraub NL. Histone deacetylase 9 is a negative regulator of adipogenic differentiation. *J Biol Chem* 2011;286:27836-47.
- [21] He W, Barak Y, Hevener A, Olson P, Liao D, Le J, Nelson M, Ong E, Olefsky JM, Evans RM. Adipose-specific peroxisome proliferator-activated receptor gamma knockout causes insulin resistance in fat and liver but not in muscle. *Proc Natl Acad Sci U S A* 2003;100:15712-7.
- [22] Banini AE, Boyd LC, Allen JC, Allen HG, Sauls DL. Muscadine grape products intake, diet and blood constituents of non-diabetic and type 2 diabetic subjects. *Nutrition* 2006;22:1137-45.
- [23] Pastrana-Bonilla E, Akoh CC, Sellappan S, Krewer G. Phenolic content and antioxidant capacity of muscadine grapes. *J Agric Food Chem* 2003;51:5497-503.
- [24] Yi W, Fischer J, Akoh CC. Study of anticancer activities of muscadine grape phenolics in vitro. *J Agric Food Chem* 2005;53:8804-12.
- [25] Adams LS, Zhang Y, Seeram NP, Heber D, Chen S. Pomegranate ellagitannin-derived compounds exhibit antiproliferative and antiaromatase activity in breast cancer cells in vitro. *Cancer Prev Res (Phila)* 2010;3:108-13.
- [26] Koh GY, McCutcheon K, Zhang F, Liu D, Cartwright CA, Martin R, Yang P, Liu Z. Improvement of obesity phenotype by Chinese sweet leaf tea (*Rubus suavissimus*) components in high-fat diet-induced obese rats. *J Agric Food Chem* 2011;59:98-104.
- [27] Lee JH, Johnson JV, Talcott ST. Identification of ellagic acid conjugates and other polyphenolics in muscadine grapes by HPLC-ESI-MS. *J Agric Food Chem* 2005;53:6003-10.
- [28] Lei F, Zhang XN, Wang W, Xing DM, Xie WD, Su H, Du LJ. Evidence of anti-obesity effects of the pomegranate leaf extract in high-fat diet induced obese mice. *Int J Obes (Lond)* 2007;31:1023-9.
- [29] Lucas EA, Li W, Peterson SK, Brown A, Kuvibidila S, Perkins-Veazie P, Clarke SL, Smith BJ. Mango modulates body fat and plasma glucose and lipids in mice fed a high-fat diet. *Br J Nutr* 2011;106:1495-505.
- [30] Makino-Wakagi Y, Yoshimura Y, Uzawa Y, Zaima N, Moriyama T, Kawamura Y. Ellagic acid in pomegranate suppresses resistin secretion by a novel regulatory

- mechanism involving the degradation of intracellular resistin protein in adipocytes. *Biochem Biophys Res Commun* 2012;417:880-5.
- [31] Panchal SK, Ward L, Brown L. Ellagic acid attenuates high-carbohydrate, high-fat diet-induced metabolic syndrome in rats. *Eur J Nutr* 2013;52:559-68.
- [32] Neyrinck AM, Van Hee VF, Bindels LB, De Backer F, Cani PD, Delzenne NM. Polyphenol-rich extract of pomegranate peel alleviates tissue inflammation and hypercholesterolaemia in high-fat diet-induced obese mice: potential implication of the gut microbiota. *British journal of nutrition* 2012;7:1-8.
- [33] Losso JN, Bansode RR, Trappey A, Bawadi HA, Truax R. In vitro anti-proliferative activities of ellagic acid. *J Nutr Biochem* 2004;15:672-8.
- [34] Rani UP, Kesavan R, Ganugula R, Avaneesh T, Kumar UP, Reddy GB, Dixit M. Ellagic acid inhibits PDGF-BB-induced vascular smooth muscle cell proliferation and prevents atheroma formation in streptozotocin-induced diabetic rats. *J Nutr Biochem* 2013;24:1830-9.
- [35] Park SH, Kim JL, Lee ES, Han SY, Gong JH, Kang MK, Kang YH. Dietary ellagic acid attenuates oxidized LDL uptake and stimulates cholesterol efflux in murine macrophages. *J Nutr* 2011;141:1931-7.
- [36] Selvi BR, Batta K, Kishore AH, Mantelingu K, Varier RA, Balasubramanyam K, Pradhan SK, Dasgupta D, Sriram S, Agrawal S, Kundu TK. Identification of a novel inhibitor of coactivator-associated arginine methyltransferase 1 (CARM1)-mediated methylation of histone H3 Arg-17. *J Biol Chem* 2010;285:7143-52.
- [37] Yadav N, Cheng D, Richard S, Morel M, Iyer VR, Aldaz CM, Bedford MT. CARM1 promotes adipocyte differentiation by coactivating PPARgamma. *EMBO Rep* 2008;9:193-8.
- [38] Wang L, Li L, Ran X, Long M, Zhang M, Tao Y, Luo X, Wang Y, Ma X, Halmurati U, Mao X, Ren J. Ellagic Acid Reduces Adipogenesis through Inhibition of Differentiation-Prevention of the Induction of Rb Phosphorylation in 3T3-L1 Adipocytes. *Evid Based Complement Alternat Med* 2013;2013:287534.
- [39] Yoshimura Y, Nishii S, Zaima N, Moriyama T, Kawamura Y. Ellagic acid improves hepatic steatosis and serum lipid composition through reduction of serum resistin levels and transcriptional activation of hepatic ppara in obese, diabetic KK-A(y) mice. *Biochem Biophys Res Commun* 2013;434:486-91.
- [40] Sarikaya SB, Gulcin I, Supuran CT. Carbonic anhydrase inhibitors: Inhibition of human erythrocyte isozymes I and II with a series of phenolic acids. *Chem Biol Drug Des* 2010;75:515-20.
- [41] Lynch CJ, Fox H, Hazen SA, Stanley BA, Dodgson S, Lanoue KF. Role of hepatic carbonic anhydrase in de novo lipogenesis. *Biochem J* 1995;310 ( Pt 1):197-202.
- [42] Seeram NP, Lee R, Heber D. Bioavailability of ellagic acid in human plasma after consumption of ellagitannins from pomegranate (*Punica granatum L.*) juice. *Clin Chim Acta* 2004;348:63-8.
- [43] Garcia-Villalba R, Beltran D, Espin JC, Selma MV, Tomas-Barberan FA. Time course production of urolithins from ellagic acid by human gut microbiota. *J Agric Food Chem* 2013;61:8797-806.

**III. CHAPTER II: Ellagic acid inhibits adipocyte differentiation  
through coactivator associated arginine methyltransferase 1-mediated  
chromatin modification**

Inhae Kang<sup>a,b</sup>, Meshail Okla<sup>a,b</sup>, and Soonkyu Chung<sup>a,b,\*</sup>

From the <sup>a</sup> Department of Food Science and Human Nutrition, University of Florida,  
Gainesville, FL, 32611, <sup>b</sup> Department of Nutrition and Health Sciences, University of  
Nebraska-Lincoln, Lincoln, NE, 68583

Running Title: Epigenetic modification of adipogenesis by ellagic acid

\*To whom correspondence should be addressed: Soonkyu Chung, PhD, Department of  
Nutrition and Health Sciences, University of Nebraska-Lincoln, 316G Ruth Leverton  
Hall P.O. Box 830806, Lincoln, NE, 68583, Fax: (402) 472-0806, E-mail:  
[schung4@unl.edu](mailto:schung4@unl.edu)

This work was supported by USDA-HATCH program (University of Florida)

*Key words:* Ellagic acid; adipogenesis; chromatin histone modification; CARM1,  
HDAC9

## ABSTRACT

Chromatin remodeling is a key mechanism in adipocyte differentiation. However, it is unknown whether dietary polyphenols are epigenetic effectors for adiposity control. Recently, we have identified that ellagic acid (EA), a naturally occurring polyphenol in numerous fruits and vegetables, represses adipogenic conversion of human adipose-derived stem cells (*hASCs*). In the present study, we sought to determine whether EA inhibits adipogenesis by modifying chromatin remodeling in *hASCs*. qPCR microarray of chromatin modification enzymes revealed that 10  $\mu\text{mol/L}$  of EA significantly inhibits histone deacetylase (HDAC) 9 down-regulation. In addition, EA was associated with an up-regulation of HDAC activity and a marked reduction of histone acetylation (HAc) levels. However, chemical inhibition of HDAC activity or depletion of HDAC9 by *siRNA* were not sufficient to reverse the anti-adipogenic effects of EA. Intriguingly, EA treatment was also associated with reduced histone 3 arginine 17 methylation levels (H3R17me<sub>2</sub>), implying the inhibitory role of EA in coactivator-associated arginine methyltransferase 1 (CARM) 1 activity during adipogenesis. Boosting CARM1 activity by delivering cell-penetrating peptides of CARM1 (CPP-CARM1) not only recovered H3R17me<sub>2</sub>, but also restored adipogenesis evidenced by H3K9Ac, HDAC9 downregulation, PPAR $\gamma$  expression, and triglyceride accumulation. Taken together, our data suggest that reduced CARM1 activity by EA results in a decrease of H3R17me<sub>2</sub> levels, which may interrupt consecutive histone remodeling steps for adipocyte differentiation including histone acetylation and HDAC9 dissociation from chromatin. Our work provides the mechanistic insights into how EA, a polyphenol ubiquitously

found in fruits and vegetables, attenuates human adipocyte differentiation by altering chromatin remodeling.

## **1. Introduction**

Epigenetic modification refers to the inheritable changes of gene expression in the absence of a change in the DNA sequence itself. Epigenetic modification comprises DNA methylation in CpG islands, covalent modification of histone tails, and noncoding microRNA-mediated gene silencing [1-6]. In particular, histone modification is a key mechanism in the switching on and off of genes for differentiation; N-terminal tails of H3 and H4 interact with the negatively charged DNA backbone in unmodified states. Histone modifying enzymes target specific amino acids of histones, producing changes in acetylation, methylation, phosphorylation or ubiquitination status. Modifications of these histone codes alter chromatin conformation, which subsequently induce dissociation of transcriptional (co)repressors as well as recruitment of transcriptional (co)activators [7-10]. In general, histone acetylation on lysine residues decreases chromatin compactness, increases accessibility to genes, and thereby induces transcriptional activation. Several transcriptional co-activators possess histone acetyltransferase (HAT) activity to transfer acetyl groups to lysine residues in histones, promoting conformational change in euchromatin structure [11-14]. In contrast, transcriptional co-repressors often possess HDAC activity to remove acetyl moieties from histone tails, leading to a less accessible heterochromatin conformation [15, 16]. Regulation of transcription by histone methylation is more complex than by histone acetylation. Histone methylation can be correlated with either gene activation or repression depending on histone residues (lysine

or arginine), specific genetic loci, or distinctive methylation pattern (e.g., asymmetric or symmetric) [17-21].

A growing body of literature has revealed that epigenetic regulation is a key mechanism for adipocyte differentiation. Although considered controversial, an increase in global histone acetylation is preceded by adipocyte differentiation as the consequence of decreased HDAC activity [22]. More specifically, H3 acetylation at lysine 9 (H3K9Ac), and H3 methylation at lysine 4 (H3K4Me2) have been implicated for positive regulation of adipocyte differentiation [23]. The obligatory suppression of Wnt signaling is also regulated by chromatin modification via H3 lysine 27 (H3K27Ac vs. H3K27me3) [24]. Several histone modification enzymes, e.g., protein arginine methyltransferase 4 (PRMT4 also known as coactivator-associated arginine methyltransferase 1 (CARM1)) [25], PRMT5 [26], histone methyltransferase G9a [27], and HDAC9 [28], have been identified as either positive or negative regulators for adipocyte differentiation. Moreover, recent advances in chromatin immunoprecipitation (ChIP) methodology has revealed that activation of transcriptional cascade networks during early adipogenesis coincides with the regulation of histone modification of key transcription factors such as peroxisome proliferator-activated receptor gamma (PPAR $\gamma$ ) [25]. These studies have clearly demonstrated that chromatin remodeling dictates adipocyte differentiation.

However, less information is available whether environmental effectors are able to reprogram epigenetic codes for adipocyte differentiation. Interestingly, accumulating evidence suggests that our daily diet is an important epigenetic determinant regulating obesity. Exposure to a HF-diet early in life can alter chromatin structure, leading to an increased risk of obesity in adulthood [29-31]. Conversely, consumption of fruits and

vegetables (FV) is inversely associated with obesity [32]. It is largely unknown whether epigenetic regulation could be a viable mechanism to explain reduced adiposity by FV consumption. By displacing energy-dense foods, FV consumption increases satiety, decreases food intake, and therefore induces weight loss [33]. Besides this satiety effect, it is plausible to hypothesize that FV contain principle phytochemicals that can modulate the activity of chromatin-modifying enzymes, thereby reducing adiposity. Recently, our group has reported that supplementation of muscadine grape phytochemicals (MGP) decreased visceral obesity and obesity-mediated metabolic complications without altering food intake [34]. Among the polyphenolic compounds of MGP, EA has identified as the most potent polyphenol in inhibiting adipogenic conversion (under review). These studies led us to raise the question of whether EA regulates epigenetic regulatory factors in adiposity. Here, we present evidence that EA, a polyphenol commonly found in many FV, attenuates adipocyte differentiation by modulating histone arginine methylation and subsequent histone acetylation levels.

## **2. Materials and Methods**

### *2.1. Materials*

All cell culture dishes were purchased from Fisher Scientific. Fetal bovine serum (FBS) was purchased from Cellgro. Rosiglitazone (BRL49653) was purchased from Cayman Chemical. All other chemicals and reagents were purchased from Sigma Chemical Co., unless otherwise stated.

### *2.2. Preparation of human adipogenic stem cells (hASCs) and adipogenic differentiation*

Abdominal adipose tissue was obtained from females with a body mass index (BMI) of ~30 during liposuction or abdominal plastic surgeries. Isolation of *hASCs* and differentiation of adipocytes were conducted as described by Skurk *et al.* [35]. All protocols and procedures were approved by the Institutional Review Board (#693-2011) at the University of Florida. After removing initial monocytic cells (selective adherence to plastic), the released stromal vascular fractions were passaged down no more than three times. These adipogenic stem cell rich stromal vascular (SV) fractions are regarded as human adipogenic stem cells (*hASCs*) without further purification procedures [36]. A pool of *hASCs* from three or four different human subjects was used for each experiment to avoid individual variation. Conditions for *hASCs* proliferation and differentiation were described previously [37, 38]. Ellagic acid (E2250, Sigma) stock was prepared in dimethyl sulfoxide (DMSO); aliquots of stock (10 mmol/L) were kept at -20°C and freshly diluted at the time of addition to *hASCs*. For induction to adipogenic differentiation, cells were seeded ( $5 \times 10^5/\text{cm}^2$ ) in 35mm plates and allowed to attach for 24 hours in proliferation medium. After attachment, cultures were grown for the next 3 days in differentiation medium containing 0.25 mmol/L isobutylmethylxanthine, 1  $\mu\text{mol/L}$  rosiglitazone, and 500 nmol/L human insulin in commercially available human adipocyte medium (AM-1, ZenBio). Adipocyte medium (AM-1) was replenished every 3 days. Under these conditions, cultures of *hASCs* were induced to differentiation in the presence of 10  $\mu\text{M}$  EA or DMSO (vehicle) for seven days. The presence of intracellular lipid accumulation was visualized by oil red-O (ORO) staining.

### 2.3. *qPCR and microarray analysis*

Gene-specific primers for qPCR were obtained from Integrated DNA Technologies (Chicago, IL). Total mRNA of *hASCs* was isolated using Trizol reagent (Invitrogen). To remove genomic DNA contamination, mRNA was treated with DNase (Mediatech); 2  $\mu$ g of mRNA was converted into cDNA in a total volume of 20  $\mu$ l (iScript cDNA synthesis kit, Bio-Rad). Gene expression was determined by real-time qPCR (CFX96, Bio-Rad), and relative gene expression was normalized by the average of two reference genes, 36B4 and/or GAPDH (primer sequences will be available upon request). The complete gene lists can be found in **Supplemental Table 1**. For PCR microarray analysis, RT<sup>2</sup> profiler PCR array for Human epigenetic chromatin modification enzymes (QIAGEN, PAHS-085Z) was used according to the manufacture's protocol. For each group, pools of equal amounts of total mRNA provided from four different human subjects were used. The results were analyzed using software provided by QIAGEN ([http://www.sabiosciences.com/pcrarray\\_data\\_analysis.php#Excel](http://www.sabiosciences.com/pcrarray_data_analysis.php#Excel)).

#### 2.4. Western blot analysis

To prepare total cell lysates, monolayers of differentiated cultures of human adipocytes were harvested with ice cold RIPA buffer (Thermo Scientific) with protease and phosphatase inhibitors (Sigma). For nuclear extract preparation, NE-PER nuclear and cytoplasmic extraction kit (Thermo Scientific) was used according to the manufacturer's protocol. Proteins were fractionated onto 4-15% pre-casted SDS-PAGE (Biorad), transferred to PVDF membranes with a semi-dry transfer unit (Hoefer TE77X), and incubated with the relevant antibodies. Chemiluminescence from ECL solution (Western Lightning) was detected with FluorChem E (Cell Biosciences) imaging system.

Polyclonal or monoclonal antibodies targeting to  $\beta$ -actin (4967), H3K9Ac (AcH3, 9649), HDAC1 (5356), HDAC2 (5113), HDAC3 (3949), HDAC4 (7628), HDAC5 (2082), HDAC6 (7558), AcH4 (2594), H3K27Ac (4353), H4 (2935), lamin A/C (4777), CARM1 (3379) were purchased from Cell Signaling Technology. Antibodies to HDAC9 (ab 59718), and histone H3 (ab1791) were purchased from Abcam. PPAR $\gamma$  (sc-7273) and FABP (aP2, sc-271529) were purchased from Santa Cruz Biotechnology. The polyclonal antibody for detecting histone 3 asymmetric-dimethyl Arginine 17 (H3R17me2, NB21-1132) was purchased from Novus Biotechnology.

### 2.5. HDAC enzyme activity assays

Total cellular histone deacetylase enzymatic activity was measured using a commercial HDAC assay kit (Upstate Biotechnology) according to the manufacturer's protocol. Briefly, 30  $\mu$ g of nuclear lysate were incubated with fluorescent substrate in HDAC assay buffer for 45 minutes at 30°C. An activator solution was added to release the fluorophore from the deacetylated substrates, and fluorescence was measured in a multichannel fluorometer (Synergy H1, Biotech).

### 2.6. Depletion of HDAC9 using siRNA

For silencing HDAC9, *hASCs* were seeded at confluent density and allowed to attach for 24 hours in a proliferation medium. Culture of *hASCs* were transfected with either 200 nmol/L of human HDAC9 ON-TARGET plus SMART pool siRNA (Thermo Scientific) or 200 nmol/L non-targeting control siRNA (Thermo Scientific) at 48 hours prior to adipogenic stimulation using DharmaFECT1 transfection reagent according to the manufacturer's protocol. The transfection efficiency was determined by Cy3-tagged

siGLO (Thermo Scientific). After 48 hours of transfection, *hASCs* were stimulated for differentiation in the presence and absence of EA during 72 hours (**Fig. 3. A**).

### 2.7. Immunocytochemistry of H3R17me2 and HDAC9

*hASCs* were cultured onto coverslips and immunostained for immunofluorescence microscopy as described previously [37]. Briefly, cells were fixed with 3.7 % paraformaldehyde for 20 minutes. After quenching paraformaldehyde with glycine, coverslips were permeabilized with ice cold Triton X-100 (0.1 %) and blocked with 1.25 mg/ml normal goat serum for 1 hour. The coverslips were incubated overnight with 1:100 dilution of the antibodies of H3R17me2 (ab8284) and HDAC9 (ab18970) antibody (Abcam) at 4°C, followed by incubation for 1 hour with a 1:300 dilution of rhodamine red-conjugated goat anti-rabbit IgG (Jackson ImmunoResearch). Fluorescent images were captured using a digital inverted fluorescence EVOS microscope (AMG Inc.). DAPI staining was used for counter-staining of the nucleus.

### 2.8. Cell permeable peptide-CARM1 (CPP-CARM1)

Purified CPP-CARM1 was a generous gift from Dr. Dong Ryul Lee at the CHA University in South Korea [39]. CPP-CARM1 (2 µg/mL) was delivered to *hASCs* 24 hours prior to adipogenic stimulation with or without EA. This allows sufficient time for CPP-CARM1 to translocate into the nucleus before *hASCs* are exposed to EA. Every two days, fresh CPP-CARM1 was added during routine media changes.

### 2.9. Statistics

All data are presented as the mean  $\pm$  SEM. The data were statistically analyzed using a Student's t-test or one-way ANOVA with Tukey's multiple comparison tests. All analyses were performed with GraphPad Prism 5 (Version 5.04).

### 3. Results

#### *3.1. EA alters HDAC9 expression and HDAC activity during adipocyte differentiation*

Recently, we have identified that EA is most potent polyphenols that exerts the anti-adipogenic property (under review). To gain an insight into whether EA regulates epigenetic factors of adipogenesis, we performed qPCR microarrays for chromatin modification enzymes. Among the 84 genes that regulate chromatin accessibility to genomic DNA or histones (by altering the status of acetylation, methylation, phosphorylation or ubiquitination), 10 genes were upregulated ( $> 2$  fold) by EA treatment without any specific genes being significantly downregulated ( $< 2$  fold) (**Fig 1A**, also see **Supplemental Table 2**). In particular, HDAC9 gene expression levels were  $\sim 20$  fold higher than that of vehicle control. To validate the array results, HDAC gene expression was measured using individual gene-specific primers. As we expected, no difference was found in Class I (HDAC 1, 2, 3, 4, and 8) or Class III HDAC genes between EA-treated vs. control human adipocyte samples. In parallel to results from the qPCR array, HDAC9 gene expression was specifically higher in EA-treated adipocytes compared to vehicle controls among the Class II DAC genes (HDAC 5, 7, 9, 10). Interestingly, for HDAC11, a class IV HDAC enzyme, mRNA levels were also significantly higher than control (**Fig 1B**). HDAC9 protein levels were higher in EA-treated nuclear fraction, while other HDAC protein levels were similar between the two groups (**Fig 1C**).

Next, we examined whether EA also alter HDAC activity and histone acetylation levels. There was a  $< 50\%$  reduction of global HDAC activity during the early differentiation period (4 days after exposure to differentiation stimuli), which was almost completely dampened in cultures grown with EA (**Fig 2A**). In the presence of 100 nM

trichostatin A (TSA), a pan-HDAC inhibitor, there was an additional decrease of HDAC activity in the nuclear extract of differentiated cultures; only ~10% of HDAC activity remained in comparison to undifferentiated *hASCs* (**Fig 2B**, the second bar). In contrast, EA-treated nuclear extracts still possessed 50% of HDAC activity in the presence of TSA (**Fig 2B**, the last bar). Consistent with the literature [22, 24], differentiation of *hASCs* significantly increased acetylation levels of H3K9Ac, H3K27Ac as well as AcH4 (**Fig 2C, left panel**). Intriguingly, differentiation of *hASCs* with EA remarkably decreased histone acetylation levels (**Fig 2C, right panel**). To answer the question of whether the inhibition of HDAC activity is able to reverse the inhibitory effects of EA on adipogenesis, TSA was added to the *hASCs* along with EA. Consistent with results from Chatterjee *et al.* [28], the addition of TSA during the adipocyte differentiation procedures did not inhibit adipogenesis (**Fig 2D, upper panel**). Similarly, addition of TSA to EA-treated cultures during adipocyte differentiation failed to restore both adipocyte morphology (**Fig 2D**) and PPAR $\gamma$  expression (**Fig 2E**). Notably, HDAC9 gene expression was even higher with TSA treatment, suggesting that HDAC9 expression is not regulated by TSA-sensitive HDAC activity (**Fig 2E**). These results collectively demonstrate that: 1) EA inhibits downregulation of HDAC activity, presumably the TSA-insensitive portion; and 2) chemical inhibition of HDAC activity by TSA was unable to reverse EA-mediated HDAC9 expression as well as inhibition of adipogenesis.

### ***3.2. Silencing of HDAC9 is not sufficient to reverse the reduction of adipocyte differentiation by EA***

It has been shown that HDAC9 is a transcriptional co-repressor of adipogenesis by preventing the activation of C/EBP $\alpha$  [28]. Our next question was whether the knockdown

of HDAC9 could reverse the anti-adipogenic effects of EA. To address this question, we used *siRNA* to deplete HDAC9. Transfection efficiency of *hASCs* was > 90 % estimated by Cy3-tagged non-targeting *siGLO* (data not shown). To knockdown HDAC9, 200 nmol/L of *siCont* (non-targeting) or *siHDAC9* were transfected with *hASCs* for 48 hours followed by adipogenic differentiation for 72 hours (**Fig 3A**). Transfection of *siHDAC9* attenuated HDAC9 gene expression approximately ~70% compared to *siCont* (**Fig 3B**), which remained constant throughout the experiment (data not shown). Reduction of HDAC9 protein levels in nucleus by *siHDAC9* was comparable to *siCont* transfected cells without EA control (**Fig 3C**). Surprisingly, a substantial decrease of HDAC9 by *siHDAC9* had minimal impact on EA-mediated suppression of adipogenic gene expression, C/EBP $\alpha$  and PPAR $\gamma$  or on H3K9 acetylation (**Fig 3B, C**). These data showed that reduction of HDAC9 was unable to reverse inhibition of adipogenesis by EA. Additionally, this implicates that additional regulatory factor(s) might be involved in the suppression of adipocyte differentiation by EA other than HDAC9 regulation *per se*.

### **3.3. Inhibition of CARM1 by EA plays a key role in suppressing adipogenesis**

Recently, EA has been identified as a novel inhibitor for CARM1 [40], whose activity is required for asymmetric transfer of two methyl groups to the H3R17me2 (**Fig 4A**). Consistently, immunostaining of differentiated human adipocyte cultures (heterogeneous culture containing ~50 % adipocytes) with an H3R17me2 antibody showed that CARM1 activity is restricted to lipid-laden adipocytes, but not in undifferentiated *hASCs* (**Fig 4B**). To further determine whether inhibition of CARM1 activity by EA would be a key mechanism to block *hASCs* differentiation, we examined the H3R17me2 levels during differentiation with or without EA incubation. Supporting the important role of CARM1

activity in adipocyte differentiation, EA treatment significantly reduced H3R17me2 levels compared to vehicle control from the nuclear extract fraction used in Fig 1C (**Fig 4C**). However, there was no significant difference in mRNA or protein levels of CARM1 (**Fig 4C, D**), suggesting that EA inhibits enzyme activity of CARM1 rather than by transcriptional or translational modification of CARM1.

If the inhibition of CARM1 activity by EA is the major mechanism to block adipogenesis, the replenishment of CARM1 activity can rescue adipocyte differentiation. To test this concept, 2  $\mu\text{g/mL}$  of recombinant cell penetrating peptide CARM1 (CPP-CARM1) [39] were added to *hASCs* throughout the adipogenic differentiation with 10  $\mu\text{mol/L}$  EA. Although adipocyte morphology was not completely restored, addition of CPP-CARM1 substantially increased TG accumulation compared to EA only treatment assessed by ORO-staining (**Fig 5A**). Accordingly, co-stimulation of CPP-CARM1 with EA significantly increased PPAR $\gamma$  gene and protein level compared to EA treatment alone (**Fig 5B, C**). The restoration of CARM1 activity by addition of CPP-CARM1 also increased H3R17me2 and H3K9 acetylation levels (**Fig 5C**). Moreover, immunostaining of HDAC9 revealed that addition of CPP-CARM1 reduced EA-mediated retention of HDAC9 in nucleus (**Fig 5D**). Taken together, these data strongly suggest that inhibition of H3R17me2 by EA is the key step to repress the subsequent H3K9 acetylation, HDAC9 dissociation from chromatin, and PPAR $\gamma$  activation.

#### **4. Discussion**

White adipose tissue (WAT) is not only a storage organ for surplus energy, but is also active endocrine tissue critical in energy and glucose homeostasis [41-43]. The metabolic

and endocrine function of adipocytes correlate to the dynamics of adipocytes, i.e., adipocyte size and numbers [44]. Plasticity of the adipocytes seems to be dictated by chromatin remodeling and transcriptional networks in response to environmental effectors such as diet [45, 46]. Currently, little is known about the regulatory role of dietary polyphenols on epigenetic remodeling in adipocyte. The goal of this study was to identify potential links between dietary EA and epigenetic regulation of adipogenesis. We demonstrated that EA, a ubiquitous polyphenol in fruits and vegetables, inhibits adipocyte differentiation through CARM1-mediated epigenetic modification. Based upon our results, we propose the following working model (**Fig 6**): uncommitted *hASCs* are associated with high levels of HDAC9 that repress transcriptional activation of adipogenic genes [28]. Upon adipogenic stimuli, CARM1 enzyme facilitates the transfer of two methyl moieties to H3R17, which is accompanied by a subsequent H3K9 acetylation and HDAC9 dissociation. In the presence of EA, inhibition of CARM1 activity by EA results in suppression of H3R17 methylation, which in turn abolishes H3K9 acetylation and HDAC9 dissociation, and ultimately represses adipogenesis.

Extensive research from several groups has identified that histone modifying enzymes play pivotal roles in adipocyte development: 1) Deletion of histone methyl-transferase enhancer of zeste homolog (*Ezh2*) abolished trimethylation on H3K27 of Wnt promoter region, resulting in constitutive activation of Wnt signaling and transcriptional inhibition of adipogenesis [24]; 2) Silencing of PRMT5 repressed adipogenic gene expression, which was reversed by PRMT5 overexpression [26]; 3) Histone methyltransferase G9a seemed to play dual roles for turning on or off adipogenic signaling based on its methylation sites by serving as either a co-activator or co-repressor [47]; 4) Class II

HDACs have been reported to control PPAR $\gamma$  signaling [48]. Among the Class II HDACs, HDAC9 has been identified as a unique transcriptional co-repressor on C/EBP $\alpha$  promoter [28]; and 5) Mice born with the deletion of CARM1 lacked in fat pad development [49, 50], identifying the adipose specific role of CARM1 as a coactivator for PPAR $\gamma$  [25].

Despite accumulating evidence demonstrating the critical roles of individual histone modifying enzymes in adipogenesis, few studies have identified specific effectors that directly alter histone reprogramming by modulating histone modifying enzymes. In this study, we have identified that EA alters at least three distinctive epigenetic factors during adipogenesis of *hASCs*.

The first modification that we immediately noticed was the abnormally high expression of HDAC9 via qPCR microarray of histone modifying enzymes (**Fig 1**). However, an increase of HDAC9 levels did not seem to be the major cause for EA-mediated inhibitory effects on adipogenesis due to the following: 1) depletion of HDAC9 upto ~70% had minimal effects on adipogenesis (**Fig 3**), suggesting the existence of anti-adipogenic regulatory factor(s) occur ahead of the inhibition of HDAC9 downregulation; and 2) the possibility that EA increases HDAC9 activity does not seem to contribute anti-adipogenic effects of EA. If HDAC9-mediated HDAC activity is the key mechanism to inhibit adipogenesis, inhibition of HDAC9 activity by TSA (it has been shown that HDAC9 activity is inhibited by TSA treatment [22]) should restore adipogenic potential, which was not the case in our experiment (**Fig 2D, E**). These results are consistent with conclusion from Chatterjee *et al* [28] demonstrating that HDAC9 represses the adipogenic transcription factor in a deacetylase-independent mechanism. Based on our

observations, EA seems to cause an earlier modification before the HDAC9 dissociation step, which is necessary but not sufficient to initiate adipogenesis.

The second modification that we noticed was decreased histone acetylation levels and increased HDAC activity by EA (**Fig 2A, C**). The role of histone acetylation on adipogenesis seems to be inconsistent; inhibition of HDAC activity by TSA inhibits adipogenesis in 3T3-L1 cells [22], while it fails to inhibit adipogenesis in primary adipogenic precursor cells in mice and humans [28]. One thing we confirmed is that TSA-sensitive HDAC activity is not required for adipogenesis at least in *hASCs* ([28], our data **Fig 2**). Thus, downregulation of the TSA-insensitive portion of HDAC activity might be critical to initiate adipogenic differentiation. This is based upon our data showing that EA treatment during adipogenesis almost completely blocked the adipogenic cocktail-mediated HDAC activity; also that a significant amount of HDAC activity remained even with TSA treatment without promoting adipogenesis (**Fig 2**). Conversely, it indicates that downregulation of TSA-insensitive HDAC activity may be required for adipogenesis. Intriguingly, we did not find any evidence that EA directly alters HDAC or HAT activity (data not shown). This is also consistent with the report from Selvi *et al.* [40]. Although the mechanistic link between EA treatment and ‘HDAC activity and histone acetylation status’ is uncertain, our results suggest that EA may inhibit earlier signals that could lead to global histone acetylation for facilitation of adipogenesis.

The third and the most fundamental epigenetic modification that we have identified is the attenuation of H3R17me2 levels by EA, due to reduced CARM1 activity (**Fig 4**). Yadav *et al.* have established the role of CARM1 as a PPAR $\gamma$  coactivator in adipose

tissue [25], and Selvi *et al.* have reported the general effects of EA on CARM1 enzyme [40]. However, our work is the first to report that EA inhibits asymmetric dimethylation of H3R17 during adipogenic differentiation in *hASCs* by linking CARM1 activity to anti-adipogenic effects of EA. It was unexpected to find that HDAC9 depletion could not restore H3R17me2 in the presence of EA in *hASCs* (**Fig 3**). This implies that the modification of CARM1 activity may precede the dissociation of transcriptional repressor HDAC9. It was important to note that regaining CARM1 activity by adding CPP-CARM1 recovered HDAC9 dissociation from the nucleus, histone acetylation, as well as adipogenic gene expression and TG accumulation (**Fig 4**). These data clearly demonstrate that the modulation of CARM1 by EA is the key mechanism to inhibit successive epigenetic modification for adipocyte differentiation, i.e., releasing transcriptional (co)repressors. The exact mechanistic regulations collaboratively control methylation on H3R17, releasing HDAC9 from chromatin (probably from PPRE; PPAR response elements), and acetylation of histone are currently unknown. A recent work by Wu *et al.* demonstrated that arginine methylation on H3R17 and H3R26 by CARM1 is associated with discharging the transcriptional co-repressor NuRD, a nucleosome remodeling and the deacetylase complex, by facilitating histone acetylation in MEF cells [51]. This study supports our proposed model (**Fig 6**) in terms of connecting CARM1-mediated histone arginine methylation to the dissociation of HDAC activity-possessing transcriptional repressors and augmentation of histone acetylation.

Although our proposed model has built upon the data obtained from human adipogenic progenitor cells (*hASCs*), it still contains limitation to apply to humans: 1) we used the 10  $\mu\text{mol/L}$  of EA, which is difficult to be achieved in regular diets. Our unpublished data

showed that EA could be effective in inhibiting adipogenesis and altering histone acetylation with the concentration as little as 2.5  $\mu\text{mol/L}$  in *hASCs*. More information about optimal EA concentration to exhibit physiological effectiveness *in vivo* is required; 2) current study does not include the information about EA metabolites. There is emerging evidence that EA-derived gut microbial metabolite urolithin A exerts various health benefits [52, 53]. Therefore, it needs to be determined whether urolithin A is also proficient in modulating epigenetic factors that are proposed in this study. To investigate nutritional significance of EA *in vivo*, we are currently conducting animal studies by feeding HF diet with or without EA supplementation. In addition, to further establish the adipose tissue-specific role of CARM1 on metabolic syndrome, we are under preparation to generate adipocyte specific knockout mice of CARM1.

In conclusion, our present study provides mechanism-based evidence that EA attenuates adipogenesis and offers novel insights into targeting epigenetic modification for adipogenesis control using a dietary EA.

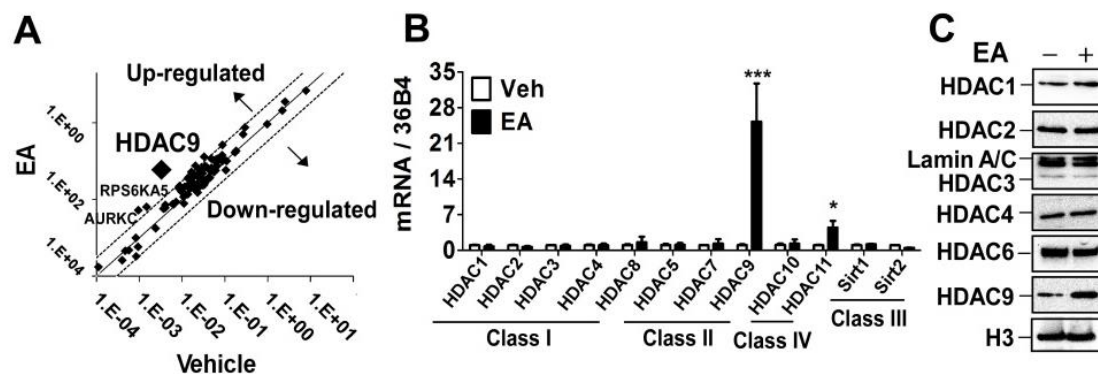


**Figure III-1 EA alters HDAC9 expression during adipocyte differentiation.**

Cultures of *hASCs* were induced to differentiation in the presence of 10  $\mu\text{mol/L}$  EA or DMSO (vehicle) for seven days. (A) Microarray analysis of human chromatin modification genes (84 genes) by qPCR from the *hASCs* treated with either 10  $\mu\text{M}$  EA or vehicle for seven days during differentiation. Pooled mRNA from four different human subjects was used for analysis. Broken lines indicate 2-fold expression of differences between treatments. (B) Gene expression levels of Class I, II, IV of HDAC and sirt1 and 2 (Class III) by qPCR. (C) Protein expression levels of HDAC 1, 2, 3, 4, 6 and 9 in nuclear extract. H3 and lamin A/C were used for loading control. \*  $P < 0.05$ , \*\*\*  $P < 0.001$  by student's t-test.

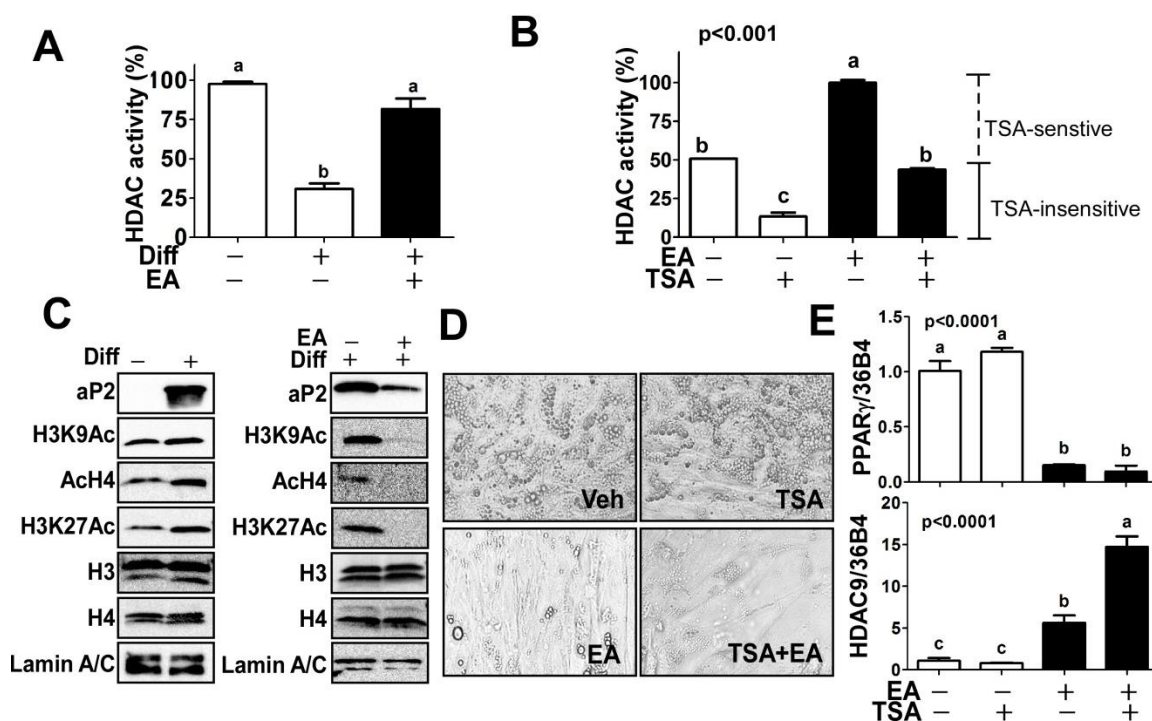


**Figure III -2 EA alters HDAC activity during adipocyte differentiation.**

(A) Nuclear HDAC enzyme activity in undifferentiated (Diff -) and differentiated (Diff +) adipocytes in the presence or absence of EA for four days. (B) HDAC activity with or without pan-HDAC inhibitor TSA (100 nmol/L). (C) Western blot analysis for detecting H3K9Ac and H3K27Ac and AcH4. H3, H4, lamin A/C were used for loading control and aP2 used as an adipocyte marker. (D) Phase contrast images of *h*ASCs differentiated with either EA or TSA only, or co-treatment of TSA+EA for seven days. (E) PPAR $\gamma$  and HDAC9 gene expression grown in the presence or absence of TSA and EA. Data are expressed as the mean  $\pm$  SEM from  $n = 4$  samples of two separate experiments. Means are not sharing a common superscript differ by one-way ANOVA with Turkey's multiple comparison ( $p < 0.05$ ).

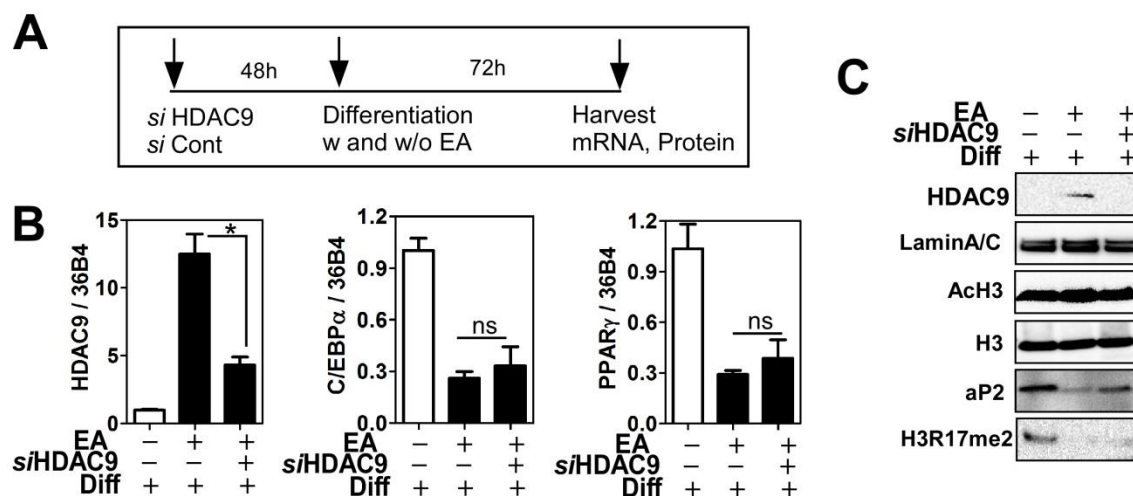


**Figure III -3 Depletion of HDAC9 in *h*ASCs has minimal impact on EA-mediated inhibition of adipogenesis.**

(A) Experimental scheme for depletion of HDAC9 before adipogenic differentiation with or without EA. *h*ASCs were transfected with *si*Cont or *si*HDAC9 at 48 hours before differentiation. Differentiated cultures were kept for 3 days before harvest of mRNA and protein after differentiation. (B) Relative gene expression of HDAC9, C/EBP $\alpha$  and PPAR $\gamma$  by qPCR analysis. (C) Protein levels of HDAC9, AcH3, H3R17me2, aP2, lamin A/C, and total H3 in *si*Cont or *si*HDAC9 transfected cells. All values are presented as the mean  $\pm$ SEM. \* P < 0.05 by one-way ANOVA.

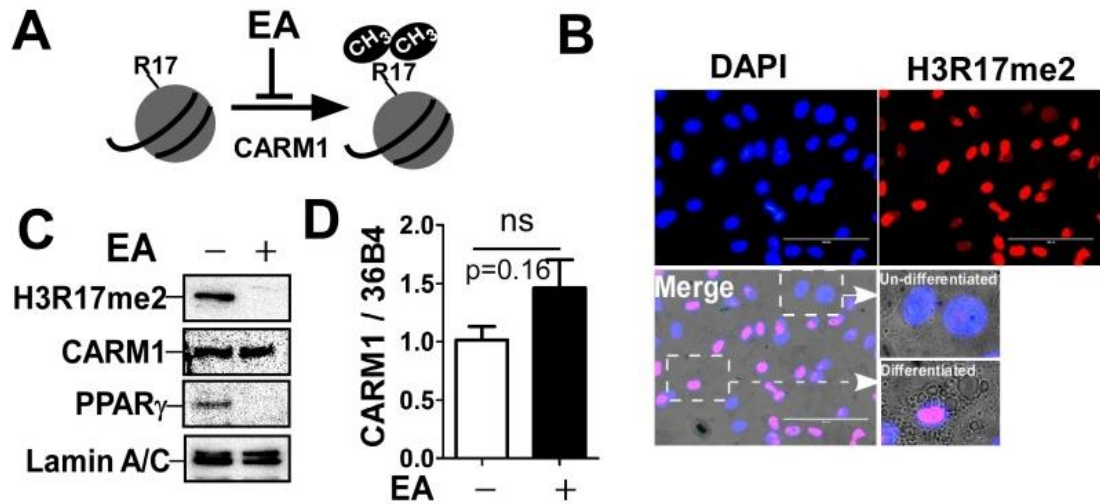


**Figure III -4 EA inhibits H3R17me2 without affecting CARM1 expression levels.**

(A) EA inhibits CARM1-mediated methylation of H3 arginine 17 in adipocytes. (B) Immunolocalization of H3R17me2 (red) and DAPI (blue). Differentiated *hASCs* were immunostained with H3R17me2 antibody and the nuclei were counterstained by DAPI. Phase contrast image (40X) was overlapped to distinguish lipid loaded adipocytes vs. undifferentiated cells. (C) Inhibition of H3R17me2 by EA without changes of CARM1 protein levels. Lamin A/C were used for loading control and PPAR $\gamma$  used as an adipocyte marker. (D) CARM1 gene expression measured by qPCR. Data are presented as the mean  $\pm$ SEM. ns= not significant by student's t-test.

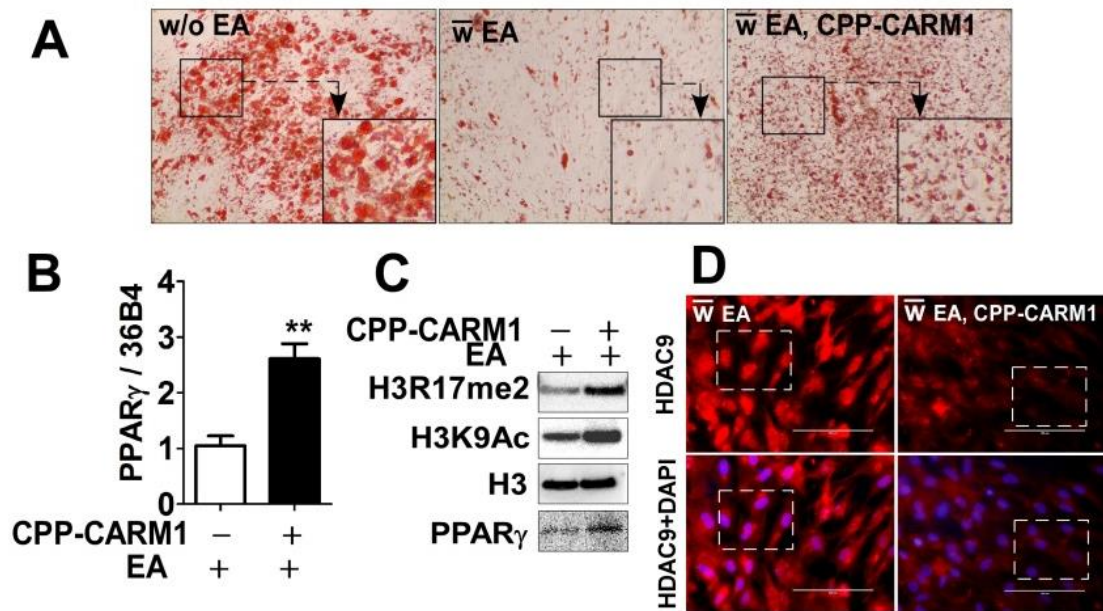


**Figure III -5 Rescue of CARM1 activity by delivering CPP- CARM1 partially reverses EA-mediated adipogenesis of *hASCs*.**

CPP-CARM1 was delivered to *hASCs* at 24 hours prior to adipogenic differentiation then differentiation was induced in the presence or absence of EA for seven days. (A) TG accumulation was visualized by ORO-staining. Black boxes show magnified images. (B) PPAR $\gamma$  gene expression determined by qPCR. (C) Protein levels of H3R17me2, H3K9Ac, H3, and PPAR $\gamma$  by western blot analysis. (D) Immunostaining of HDAC9 was merged with DAPI staining to show decreased HDAC9 levels in CPP-CARM1 added cultures. Data are presented as the mean  $\pm$ SEM., \*\* P < 0.001 by student's t-test.

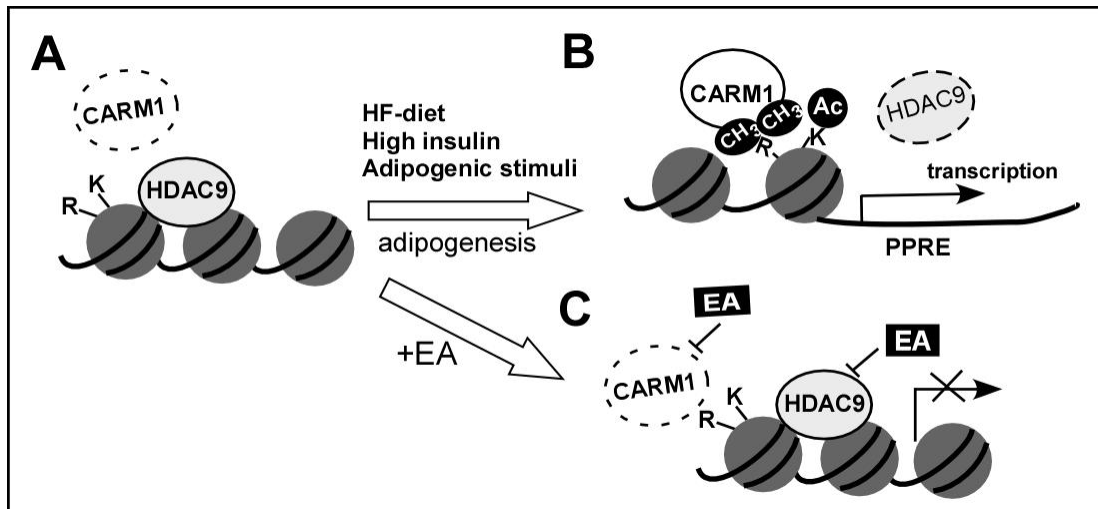


**Figure III -6 Epigenetic modification of adipogenesis by EA through the mechanism involved in CARM1 inhibition in *hASCs***

A working model illustrating the mechanism by which EA inhibits adipogenesis in *hASCs*. (A) Uncommitted *hASCs* are associated with high levels of HDAC9, a transcriptional corepressor of adipogenic genes. (B) Upon adipogenic stimuli (including HF diet and high insulin), CARM1 enzyme facilitates the transfer of two methyl moieties to H3 arginine 17 sites (H3R17m<sub>2</sub>), which subsequently increases histone acetylation and HDAC9 dissociation from chromatin. (C) In the presence of EA, EA inhibits CARM1 activity, which blocks subsequent epigenetic modification, resulting in transcription inactivation of adipogenic genes.

## References

- [1] Campos EI, Reinberg D. Histones: annotating chromatin. *Annu Rev Genet* 2009;43:559-99.
- [2] Handy DE, Castro R, Loscalzo J. Epigenetic modifications: basic mechanisms and role in cardiovascular disease. *Circulation* 2011;123:2145-56.
- [3] Fedorova E, Zink D. Nuclear architecture and gene regulation. *Biochim Biophys Acta* 2008;1783:2174-84.
- [4] Nomura J, Hisatsune A, Miyata T, Isohama Y. The role of CpG methylation in cell type-specific expression of the aquaporin-5 gene. *Biochem Biophys Res Commun* 2007;353:1017-22.
- [5] Hendrich B, Bird A. Identification and characterization of a family of mammalian methyl-CpG binding proteins. *Mol Cell Biol* 1998;18:6538-47.
- [6] Nan X, Ng HH, Johnson CA, Laherty CD, Turner BM, Eisenman RN, Bird A. Transcriptional repression by the methyl-CpG-binding protein MeCP2 involves a histone deacetylase complex. *Nature* 1998;393:386-9.
- [7] Taverna SD, Li H, Ruthenburg AJ, Allis CD, Patel DJ. How chromatin-binding modules interpret histone modifications: lessons from professional pocket pickers. *Nat Struct Mol Biol* 2007;14:1025-40.
- [8] Lee YH, Stallcup MR. Minireview: protein arginine methylation of nonhistone proteins in transcriptional regulation. *Mol Endocrinol* 2009;23:425-33.
- [9] Lee DY, Teyssier C, Strahl BD, Stallcup MR. Role of protein methylation in regulation of transcription. *Endocr Rev* 2005;26:147-70.
- [10] Martin C, Zhang Y. The diverse functions of histone lysine methylation. *Nat Rev Mol Cell Biol* 2005;6:838-49.
- [11] Marmorstein R. Structure and function of histone acetyltransferases. *Cell Mol Life Sci* 2001;58:693-703.
- [12] Kawasaki H, Schiltz L, Chiu R, Itakura K, Taira K, Nakatani Y, Yokoyama KK. ATF-2 has intrinsic histone acetyltransferase activity which is modulated by phosphorylation. *Nature* 2000;405:195-200.
- [13] Dhalluin C, Carlson JE, Zeng L, He C, Aggarwal AK, Zhou MM. Structure and ligand of a histone acetyltransferase bromodomain. *Nature* 1999;399:491-6.
- [14] Jacobson RH, Ladurner AG, King DS, Tjian R. Structure and function of a human TAFII250 double bromodomain module. *Science* 2000;288:1422-5.
- [15] Kuo MH, Allis CD. Roles of histone acetyltransferases and deacetylases in gene regulation. *Bioessays* 1998;20:615-26.
- [16] Maison C, Bailly D, Peters AH, Quivy JP, Roche D, Taddei A, Lachner M, Jenuwein T, Almouzni G. Higher-order structure in pericentric heterochromatin

- involves a distinct pattern of histone modification and an RNA component. *Nat Genet* 2002;30:329-34.
- [17] Bernstein BE, Humphrey EL, Erlich RL, Schneider R, Bouman P, Liu JS, Kouzarides T, Schreiber SL. Methylation of histone H3 Lys 4 in coding regions of active genes. *Proc Natl Acad Sci U S A* 2002;99:8695-700.
- [18] Feng Y, Wang J, Asher S, Hoang L, Guardiani C, Ivanov I, Zheng YG. Histone H4 acetylation differentially modulates arginine methylation by an in Cis mechanism. *J Biol Chem* 2011;286:20323-34.
- [19] Kouzarides T. Chromatin modifications and their function. *Cell* 2007;128:693-705.
- [20] Lachner M, O'Carroll D, Rea S, Mechtler K, Jenuwein T. Methylation of histone H3 lysine 9 creates a binding site for HP1 proteins. *Nature* 2001;410:116-20.
- [21] Santos-Rosa H, Schneider R, Bannister AJ, Sherriff J, Bernstein BE, Emre NC, Schreiber SL, Mellor J, Kouzarides T. Active genes are tri-methylated at K4 of histone H3. *Nature* 2002;419:407-11.
- [22] Yoo EJ, Chung JJ, Choe SS, Kim KH, Kim JB. Down-regulation of histone deacetylases stimulates adipocyte differentiation. *J Biol Chem* 2006;281:6608-15.
- [23] Yan C, Boyd DD. Histone H3 acetylation and H3 K4 methylation define distinct chromatin regions permissive for transgene expression. *Mol Cell Biol* 2006;26:6357-71.
- [24] Wang L, Jin Q, Lee JE, Su IH, Ge K. Histone H3K27 methyltransferase Ezh2 represses Wnt genes to facilitate adipogenesis. *Proc Natl Acad Sci U S A* 2010;107:7317-22.
- [25] Yadav N, Cheng D, Richard S, Morel M, Iyer VR, Aldaz CM, Bedford MT. CARM1 promotes adipocyte differentiation by coactivating PPARgamma. *EMBO Rep* 2008;9:193-8.
- [26] LeBlanc SE, Konda S, Wu Q, Hu YJ, Oslowski CM, Sif S, Imbalzano AN. Protein arginine methyltransferase 5 (Prmt5) promotes gene expression of peroxisome proliferator-activated receptor gamma2 (PPARgamma2) and its target genes during adipogenesis. *Mol Endocrinol* 2012;26:583-97.
- [27] Wang L, Xu S, Lee JE, Baldrige A, Grullon S, Peng W, Ge K. Histone H3K9 methyltransferase G9a represses PPARgamma expression and adipogenesis. *EMBO J* 2013;32:45-59.
- [28] Chatterjee TK, Idelman G, Blanco V, Blomkalns AL, Piegore MG, Jr., Weintraub DS, Kumar S, Rajsheker S, Manka D, Rudich SM, Tang Y, Hui DY, Bassel-Duby R, Olson EN, Lingrel JB, Ho SM, Weintraub NL. Histone deacetylase 9 is a negative regulator of adipogenic differentiation. *J Biol Chem* 2011;286:27836-47.
- [29] Sun B, Purcell RH, Terrillion CE, Yan J, Moran TH, Tamashiro KL. Maternal high-fat diet during gestation or suckling differentially affects offspring leptin sensitivity and obesity. *Diabetes* 2012;61:2833-41.

- [30] Murphy MM, Barraj LM, Herman D, Bi X, Cheatham R, Randolph RK. Phytonutrient intake by adults in the United States in relation to fruit and vegetable consumption. *J Acad Nutr Diet* 2012;112:222-9.
- [31] Miller P, Moore RH, Kral TV. Children's daily fruit and vegetable intake: associations with maternal intake and child weight status. *J Nutr Educ Behav* 2011;43:396-400.
- [32] Ledoux TA, Hingle MD, Baranowski T. Relationship of fruit and vegetable intake with adiposity: a systematic review. *Obes Rev* 2011;12:e143-e150.
- [33] Duncan KH, Bacon JA, Weinsier RL. The effects of high and low energy density diets on satiety, energy intake, and eating time of obese and nonobese subjects. *Am J Clin Nutr* 1983;37:763-7.
- [34] Gourineni V, Shay NF, Chung S, Sandhu AK, Gu L. Muscadine Grape ( *Vitis rotundifolia* ) and Wine Phytochemicals Prevented Obesity-Associated Metabolic Complications in C57BL/6J Mice. *J Agric Food Chem* 2012;60:7674-81.
- [35] Skurk T, Hauner H. Primary culture of human adipocyte precursor cells: expansion and differentiation. *Methods Mol Biol* 2012;806:215-26.
- [36] Cawthorn WP, Scheller EL, MacDougald OA. Adipose tissue stem cells meet preadipocyte commitment: going back to the future. *J Lipid Res* 2012;53:227-46.
- [37] Chung S, Brown JM, Provo JN, Hopkins R, McIntosh MK. Conjugated linoleic acid promotes human adipocyte insulin resistance through NFkappaB-dependent cytokine production. *J Biol Chem* 2005;280:38445-56.
- [38] Chung S, LaPoint K, Martinez K, Kennedy A, Boysen SM, McIntosh MK. Preadipocytes mediate lipopolysaccharide-induced inflammation and insulin resistance in primary cultures of newly differentiated human adipocytes. *Endocrinology* 2006;147:5340-51.
- [39] Jo J, Song H, Park SG, Lee SH, Ko JJ, Park JH, Jeong J, Cheon YP, Lee DR. Regulation of differentiation potential of human mesenchymal stem cells by intracytoplasmic delivery of coactivator-associated arginine methyltransferase 1 protein using cell-penetrating peptide. *Stem Cells* 2012;30:1703-13.
- [40] Selvi BR, Batta K, Kishore AH, Mantelingu K, Varier RA, Balasubramanyam K, Pradhan SK, Dasgupta D, Sriram S, Agrawal S, Kundu TK. Identification of a novel inhibitor of coactivator-associated arginine methyltransferase 1 (CARM1)-mediated methylation of histone H3 Arg-17. *J Biol Chem* 2010;285:7143-52.
- [41] Ronti T, Lupattelli G, Mannarino E. The endocrine function of adipose tissue: an update. *Clin Endocrinol (Oxf)* 2006;64:355-65.
- [42] Silvestri C, Ligresti A, Di M, V. Peripheral effects of the endocannabinoid system in energy homeostasis: adipose tissue, liver and skeletal muscle. *Rev Endocr Metab Disord* 2011;12:153-62.
- [43] Galic S, Oakhill JS, Steinberg GR. Adipose tissue as an endocrine organ. *Mol Cell Endocrinol* 2010;316:129-39.

- [44] Fruhbeck G, Gomez-Ambrosi J, Muruzabal FJ, Burrell MA. The adipocyte: a model for integration of endocrine and metabolic signaling in energy metabolism regulation. *Am J Physiol Endocrinol Metab* 2001;280:E827-E847.
- [45] Aagaard-Tillery KM, Grove K, Bishop J, Ke X, Fu Q, McKnight R, Lane RH. Developmental origins of disease and determinants of chromatin structure: maternal diet modifies the primate fetal epigenome. *J Mol Endocrinol* 2008;41:91-102.
- [46] Suter MA, Chen A, Burdine MS, Choudhury M, Harris RA, Lane RH, Friedman JE, Grove KL, Tackett AJ, Aagaard KM. A maternal high-fat diet modulates fetal SIRT1 histone and protein deacetylase activity in nonhuman primates. *FASEB J* 2012;26:5106-14.
- [47] Lee DY, Northrop JP, Kuo MH, Stallcup MR. Histone H3 lysine 9 methyltransferase G9a is a transcriptional coactivator for nuclear receptors. *J Biol Chem* 2006;281:8476-85.
- [48] Nebbioso A, Dell'Aversana C, Bugge A, Sarno R, Valente S, Rotili D, Manzo F, Teti D, Mandrup S, Ciana P, Maggi A, Mai A, Gronemeyer H, Altucci L. HDACs class II-selective inhibition alters nuclear receptor-dependent differentiation. *J Mol Endocrinol* 2010;45:219-28.
- [49] Kim J, Lee J, Yadav N, Wu Q, Carter C, Richard S, Richie E, Bedford MT. Loss of CARM1 results in hypomethylation of thymocyte cyclic AMP-regulated phosphoprotein and deregulated early T cell development. *J Biol Chem* 2004;279:25339-44.
- [50] Yadav N, Lee J, Kim J, Shen J, Hu MC, Aldaz CM, Bedford MT. Specific protein methylation defects and gene expression perturbations in coactivator-associated arginine methyltransferase 1-deficient mice. *Proc Natl Acad Sci U S A* 2003;100:6464-8.
- [51] Wu J, Cui N, Wang R, Li J, Wong J. A role for CARM1-mediated histone H3 arginine methylation in protecting histone acetylation by releasing corepressors from chromatin. *PLoS One* 2012;7:e34692.
- [52] Bialonska D, Kasimsetty SG, Khan SI, Ferreira D. Urolithins, intestinal microbial metabolites of Pomegranate ellagitannins, exhibit potent antioxidant activity in a cell-based assay. *J Agric Food Chem* 2009;57:10181-6.
- [53] Larrosa M, Gonzalez-Sarrias A, Yanez-Gascon MJ, Selma MV, Azorin-Ortuno M, Toti S, Tomas-Barberan F, Dolara P, Espin JC. Anti-inflammatory properties of a pomegranate extract and its metabolite urolithin-A in a colitis rat model and the effect of colon inflammation on phenolic metabolism. *J Nutr Biochem* 2010;21:717-25.

#### **IV. CHAPTER III: Raspberry seed flour attenuates high sucrose diet-mediated hepatic stress and adipose tissue inflammation**

Inhae Kang<sup>a</sup>, Juan Carlos Espín<sup>b</sup>, Timothy P. Carr<sup>a</sup>, Francisco A. Tomás-Barberán<sup>b</sup>, and Soonkyu Chung<sup>a,§</sup>

<sup>a</sup>Department of Nutrition and Health Sciences at the University of Nebraska-Lincoln, Lincoln, NE, USA and <sup>b</sup>Department of Food Science and Technology, CEBAS-CSIC, Murcia, Spain.

<sup>§</sup>To whom correspondence should be addressed: Soonkyu Chung, PhD, Department of Nutrition and Health Sciences, the University of Nebraska-Lincoln, 316G Ruth Leverton Hall, P.O. Box 830806, Lincoln, NE, 68583, Fax: (402) 472-1587, E-mail: [schung4@unl.edu](mailto:schung4@unl.edu)

Running title: Ellagic acid and sugar toxicity

Key words: ellagic acid; raspberry seed flour; obesity; hepatic stress; adipose inflammation.

## **Abstract**

Chronic intake of high sucrose (HS) diet exacerbates high fat (HF) diet-induced obesity and its associated metabolic complications. Previously, we have demonstrated that ellagic acid (EA), an abundant polyphenol found in some fruits and nuts, exerts distinct lipid-lowering characteristics in hepatocytes and adipocytes. In this study, we hypothesized that EA supplementation inhibits HS diet-mediated hepatic toxicity and its accompanied metabolic dysregulation. To test this hypothesis, C57BL/6 male mice were randomly assigned to three isocaloric HF diets (41 % calories from fat) containing either no-sucrose (HF), high-sucrose (HFHS), or high-sucrose plus EA (HFHS-R) from raspberry seed flour (RSF, equivalent to 0.03 % of EA), and fed for 12 weeks. The inclusion of EA from RSF significantly improved HFHS diet-mediated dyslipidemia and restored glucose homeostasis levels similar to the HF diet-fed mice. Despite marginal difference in hepatic triglyceride content, the addition of EA substantially reversed the activation of endoplasmic reticulum (ER) stress and oxidative damage triggered by HFHS diet in the liver. These effects of EA were further confirmed in human hepatoma cells by reducing ER stress and reactive oxygen species (ROS) production. Moreover, HFHS-R diet significantly decreased visceral adipocyte hypertrophy and adipose tissue inflammation evidenced by reduced pro-inflammatory gene expression and macrophage infiltration. In summary, EA supplementation from RSF was effective in reducing HFHS diet-mediated metabolic complication by attenuating hepatic ER and oxidative stresses as well as adipocyte inflammation. Our results suggest that the inclusion of EA in diets may normalize metabolic insults triggered by HS consumption.

## 1. Introduction

Obesity is defined as a chronic low-grade inflammatory condition, which causes major health problems in the United States and many parts of the world [1]. The obesity epidemic appears to have emerged largely from the imbalance between energy intake and energy expenditure. The critical role of HF diets on the pathogenesis of obesity has been well-established over the past fifteen years [2, 3]. In addition to the positive correlation between obesity and HF diets, accumulating evidence pinpoints that consumption of high contents of sucrose (or fructose) is an independent metabolic risk factor to exacerbate obesity and its accompanied health complications [4, 5].

Although it is controversial, the overall consumption of total sugar and sweeteners has increased in the United States over the past few decades [6, 7]. The surge of fructose into portal vein perturbs hepatic glucose and lipid metabolisms. High sugar intake is associated with reduced glucose uptake, elevated gluconeogenesis and hepatic glucose output, enhanced de novo TG synthesis, and promoted ER stress and hepatic inflammation [8]. These metabolic modifications appear to underlie the induction of insulin resistance commonly observed with HS feeding in both humans and rodent models of obesity. Moreover, epidemiological studies have revealed that sugar consumption is positively correlated with weight gain [7]. Given the deleterious contribution of HS intake to metabolic syndrome, there is an immense need for developing new strategies to counteract the HS diet-mediated metabolic insults.

EA is a dietary polyphenol abundantly found in many fruits such as pomegranate, berries, muscadine grapes and mangos, as well as nuts [9, 10]. EA exhibits anti-

proliferative, chemo-preventive, and anti-atherogenic properties in various cell types [11-14]. The major mechanism of action of EA includes 1) inhibition of redox stress responses [15] and 2) attenuating inflammatory damage through the regulation of NF- $\kappa$ B [16]. In addition, our group has identified that EA exerts lipid-lowering characteristics by inhibiting hyperplastic and hypertrophic expansion of adipocytes [17, 18], and by attenuating hepatic lipid accumulation [17]. Based on these unique properties, EA may downregulate the signaling modification triggered by HS diets, attenuating the attendant metabolic dysregulation. However, this possibility has not been investigated yet.

The objective of this study is to explore the role of EA-containing RSF on HS diet-mediated hepatic toxicity and its metabolic consequences. To achieve this goal, we prepared three isocaloric HF diets containing no sucrose (HF), high sucrose (HFHS) and HS plus EA (HFHS-R) from RSF as a source of EA. Here, we report that inclusion of EA in HFHS diets was effective in reversing HS-mediated 1) ER and oxidative stress responses in liver and 2) adipocyte hypertrophy and pro-inflammatory responses in adipose tissue.

## **2. Materials and Methods**

### *2.1. Chemical reagents*

All cell culture dishes were purchased from Fisher Scientific. Fetal bovine serum (FBS) was purchased from GIBCO. Pure EA (from tree bark) was purchased from Sigma Chemical Co. (#E2250). EA stock at 10 mM was prepared in dimethyl sulfoxide (DMSO) as described previously [17, 18]. Small aliquots of EA stocks were kept at -20 oC and

freshly diluted to 10  $\mu$ M with DMSO at the time of treatment in Huh7 cells. All other chemicals and reagents were purchased from Sigma Chemical Co., unless otherwise stated.

## *2.2. Analysis of phenolic compounds in RSF*

Raspberry seed flour was purchased from Millennium©Health (Meeker Red Raspberry seed flour). For the analysis of phenolic compounds of RSF, 10 mg of RSF was extracted with 1 mL of methanol:DMSO:water (40:40:20) acidified with 0.1% HCl. The mixture was vortexed, subjected to ultrasonic bath for 10 minutes, and centrifuged at 14,000g for 5 min in a Sigma 1-13 microcentrifuge (Braun Biotech. International, Germany). The supernatant was filtered through a 0.45  $\mu$ m polyvinylidene difluoride (PVDF) filter. The sample was analyzed in an Agilent 1200 high-performance liquid chromatography (HPLC) system equipped with a ultraviolet-visible diode array detector (UV-Vis-DAD) (Agilent Technologies, Waldbronn, Germany) and an Esquire 1100 ion trap mass spectrometer (IT) with an electrospray interface (ESI) (Agilent). Chromatographic separation was carried out on a reverse phase Pursuit XR<sub>s</sub> C18 column (Agilent) (250x4 mm, 5  $\mu$ m particle size) using water:formic acid (99:1, v/v) (A) and acetonitrile (B) as mobile phases. The gradient profile was: 0–20 min, 5–30% B; 20–30 min, 30–55% B; 30–38 min, 55–90% B. This percentage was maintained for 2 min and then the column was equilibrated with the initial conditions for 8 min. A volume of 8  $\mu$ L of sample was injected onto the column operating at room temperature and a flow rate of 0.8 mL/min. The separated compounds were monitored in sequence with DAD (280 and 360 nm) and with a mass spectrometry (MS) detector. Nitrogen was used as drying gas and nebulizing gas in the mass spectrometry detector with the following conditions:

nebulizer pressure 65 psi, dry gas flow 11 L/min, and dry gas temperature 350 °C. Mass scan (MS) and daughter (MS-MS) spectra were measured in the  $m/z$  range of 100-1800 in the negative ionization mode. Phenolics were identified according to their UV and MS spectra, as well as MS/MS fragments. The extracts were chemically hydrolyzed as previously reported [19].

### *2.3. Animal study*

Male C57BL/6 mice at six weeks of age were purchased from Jackson Laboratory (Bar Harbor, ME) and housed in a specific-pathogen free facility at the University of Nebraska-Lincoln. All animal experimental procedures were approved by the Institutional Animal Care and Use Committee at the University of Nebraska-Lincoln. At eight weeks of age, mice were randomly assigned to one of three experimental groups fed with different diets: isocaloric HF diets (41% calories from fat) containing either no-sucrose (HF group), HS (HFHS group, 37% calories from sucrose), or HS plus EA (HFHS-R group) from RSF (equivalent to 0.03% of EA based on RSF analysis) and fed for 12 weeks. Diet preparation was adapted from the AIN-93G diets. For HFHS-R diet, cellulose was substituted for RSF (mainly dietary fibers), and thus the total dietary fibers among the diets were not different (Supplemental Table 1). Mice were given fresh ration every other day and fed ad libitum. The daily food consumption per mouse was measured for 3 days at the last week of feeding before sacrifice. Changes in body weight (BW) of all mice were monitored weekly throughout the study (Supplemental Fig. 1).

### *2.4. Cell culture and EA treatment*

Huh7 cells were maintained in Dulbecco's modification of Eagle's medium (DMEM) /Ham's F12 containing 1 mM glucose, 1% L-glutamine, 10% fetal bovine

serum, 100 units/mL penicillin, and 100 g/mL streptomycin in 5% CO<sub>2</sub> at 37 °C. Huh7 cells were seeded into 6-well plates (0.25×10<sup>6</sup>) and pre-incubated with 10 μM of EA for 48 hours. To mimic the postprandial conditions of HFHS diet, Huh7 cells were challenged with mixtures of glucose (25 mM), fructose (50 mM) and palmitate-BSA complex (800 μM) (Glc/ Fr/ PA).

### *2.5. Measurement of blood biochemical parameters*

Enzymatic colorimetric assay kits were used to determine plasma levels of TG (Wako Diagnostics), total cholesterol (Roche Applied Sciences), and high-density lipoprotein (HDL) cholesterol (BioAssay Systems). Plasma low-density lipoprotein (LDL) cholesterol (mg/dL) was calculated from the Friedwald Equation [20]. Fasting blood glucose levels (mg/dL) were measured using a glucometer (Bayer, Contour). Commercial ELISA kit was used to determine plasma levels of insulin (Crystal Chem).

### *2.6. Glucose and insulin tolerance tests*

A glucose tolerance test (GTT) was performed on overnight fasted C57BL/6 mice by intraperitoneal (i.p.) injection of 10% D-glucose solution (0.5 g/kg BW). Blood glucose levels (mg/dL) were measured at 0, 15, 30, 60 and 120 min after injection using a glucometer (Bayer, Contour). For insulin tolerance test (ITT), overnight fasted C57BL/6 mice were administered 0.75 U/kg BW of insulin (Novolin R). Blood glucose levels were measured at 0, 10, 20, 30, 60 and 120 min after injection. The HOMA-IR (homeostasis model assessment of insulin resistance) index was calculated as [fasting plasma glucose × fasting plasma insulin/22.5] to assess insulin resistance.

### *2.7. H&E staining, adipocyte size measurement and F4/80 staining.*

Upon necropsy, liver and adipose tissues were dissected from the mice and immediately fixed in 10% buffered formalin. Tissues were embedded in paraffin, cut to 5-7 micrometer sections, and processed for hematoxylin and eosin (H&E) staining as described previously [17]. H&E stained-sections of epididymal adipose tissue were used for size determination by following the published protocol by Chen et al. [21]. Briefly, adipocyte size was examined by analyzing digital images of H&E stained paraffin sections by using Image J software. For fluorescent immunohistochemistry (IHC)-F4/80 staining, paraffin embedded adipose tissue sections were stained with a primary F4/80 antibody (dilution 1:50, Abcam), followed by incubation with Alexa Fluor® 488 (Cell Signaling). Images were taken by using an EVOS microscope (AMG Inc.)

### *2.8. Hepatic lipid accumulation*

The colorimetric triglyceride quantification kit (BioVision, K622-100) was used to quantify the hepatic TG contents according to the manufacturer's protocol.

### *2.9. Quantitative Real-Time PCR*

Gene expression analysis was performed as described previously [17]. Relative gene expression was determined based on the  $2^{-\Delta\Delta CT}$  method with normalization of the raw data to 36B4 (primer sequences in Supplemental Table 1).

### *2.10. Western blotting analysis*

Snap frozen adipose and liver samples were homogenized with a polytron homogenizer (Elkhart, IN). Huh7 cell cultures were scraped in ice-cold radioimmune precipitation assay (RIPA) buffer (Thermo Scientific) with protease inhibitors and phosphatase inhibitor as described previously [22]. Proteins were separated using 8 or 10%

SDS-PAGE gels, transferred to PVDF membranes, and incubated with the relevant antibodies. Chemiluminescence was detected with ECL solution (PerkinElmer) using a FluorChem E system (Protein Simple). Polyclonal or monoclonal antibodies targeting phospho-JNK (4668), phospho-p38 (4511), phospho-eukaryotic translation initiation factor 2 $\alpha$  (eIF2 $\alpha$ ) (9721), phospho-Akt (Ser473, 4060), total Akt (9272) and  $\beta$ -actin (4967) were purchased from Cell Signaling Technology (Danvers, MA). Phospho-insulin receptor substrate 2 (IRS2) (Ser388, 07-15171) or total-IRS2 (MABS15) were purchased from Invitrogen.

### *2.11. Measurement of hepatic oxidative stress*

For the determination of hepatic oxidative stress, liver tissue (50-100 mg) was homogenized. Amplex® Red Hydrogen Peroxide/Peroxidase Assay Kit (Invitrogen) were used to determine hepatic H<sub>2</sub>O<sub>2</sub> content according to the provider's instruction. To measure the intracellular accumulation of ROS in Huh7 cells, commercial kit of 2,7-dichloro-dihydro-fluorescein diacetate (DCFDA) cellular ROS detection assay was used (Abcam). Briefly, Huh7 cells were pre-incubated with either DMSO or EA (0-40  $\mu$ M) in a dose-dependent manner for 2 days. Then, Huh7 cells were treated with Glc (25 mM), Fr (50 mM), and PA (800  $\mu$ M) with or without EA. After 12 hours later, Huh7 cells were washed with hanks' balanced salt solution (HBSS), and loaded with 20  $\mu$ M DCFDA for 1 hour at 37 °C. After 1 hour incubation, unincorporated dye was removed by washing with HBSS. Then 250  $\mu$ M of H<sub>2</sub>O<sub>2</sub> (t-butyl hydroperoxide (Sigma Aldrich)) was spiked to Huh7 cell with experimental conditioned media in the presence or absence of EA. Fluorescence intensity was measured by Synergy H1 (Biotech). Oxidation of DCFDA to

the highly fluorescent 2,7-dichloro-fluorescein (DCF) was proportionate to ROS generation.

### 2.12. *Inflammatory cytokine assay*

Homogenized epididymal adipose tissue and plasma were prepared for testing the levels of multiple inflammatory cytokines by using the Mouse Inflammation Array C1 (Ray Biotech, Norcross, GA) according to the manufacturer's protocol. The complete blots were imaged by a FluorChem E System (Proteinsimple, Santa Clara, CA).

### 2.13. *Statistical analysis*

The data were statistically analyzed using one-way ANOVA analysis of variance with Tukey's multiple comparison tests or Student's t-test. All analyses were performed with GraphPad Prism 5 (Version 5.04). Results are presented as mean  $\pm$  SEM.

## 3. **Results**

### 3.1. *Raspberry seed flour (RSF) is a natural source of free EA and its precursors*

To investigate the potential role of dietary EA in normalizing the HS intake-mediated metabolic complications, we prepared HFHS diet with or without EA from natural sources. We selected RSF as the source of EA as it has been reported to contain high levels of EA, ellagitannins (ETs), and its derivatives [23]. Our analysis shows that there were a negligible amount of anthocyanins or flavonols in RSF (Table 1). RSF mainly contained different proanthocyanidins (condensed tannins) and ETs (hydrolysable tannins), confirming that RSF was prepared from achenes of raspberries. Free EA content in the RSF was 1.1 mg/g whereas gallic acid was found only in trace amounts. To release the EA from tannins, RSF was hydrolyzed and neutralized for further analysis. After

hydrolysis, the amount of free EA increased up to 7 mg/g and gallic acid up to 0.39 mg/g (Fig. 1). In addition, valoneic acid dilactone (2 mg/g), another hydrolysis product of ETs, was also found upon hydrolysis. Based on this analysis, the maximally attainable EA contents by the ingestion of RSF (sum of parental compounds, EA and potential other metabolites) would be approximately 10 mg/g (1% in RSF). As we added 3 % of RSF to HFHS diet (Supplementary Table 1), we assume that total EA and its responsible derivatives in HFHS-R preparation would be equivalent to 0.03 % of EA. Furthermore, as the complete hydrolysis of ETs may not be achievable in vivo, we regarded HSHS-R as a source of EA no more than 0.03 % for the rest of the study.

### *3.2. RSF supplementation attenuated HFHS diet-induced metabolic parameters and dyslipidemia in C57BL/6 mice*

We first investigated whether RSF supplementation alters HFHS diet-induced obesity. As seen in Table 2, there was no difference in food intake between the groups. After 12 weeks of the diet, mice fed with HFHS diet significantly promoted BW gain compared to mice fed with HF alone, which was partially normalized in mice fed with HFHS-R. Similarly, the extent to which HFHS diet promoted liver and visceral fat (epididymal and mesenteric) mass gain compared to HF diet, was partly attenuated by HFHS-R diet. However, liver/BW ratio did not reach statistical significance among groups despite the trend of stepwise decline in mice fed with HFHS>HFHS-R>HF. Next, we investigated whether the inclusion of RSF in HFHS diet improves plasma lipid profiles. As we expected both plasma TG and total cholesterol levels were higher in HFHS group than HF control. The elevated levels of TG and total cholesterol by HFHS

diet were almost completely dampened in HFHS-R group comparable to HF control. Consistently, decreased HDL cholesterol and elevated LDL cholesterol levels were restored in HFHS-R group close to the HF-fed control mice (Table 2). These data demonstrated that EA-containing RSF supplementation confers a resistance to HS-mediated exacerbation of obesity and dyslipidemia.

### *3.3. RSF supplementation normalized HS diet-mediated abnormal glucose metabolism*

Next, we asked whether RSF modulates HS-mediated abnormal glucose metabolism. As expected, HFHS fed mice exhibited higher fasting glucose and insulin levels than HF fed mice. Consistent with the improved plasma lipid profile by RSF (Table 2), inclusion of RSF decreased HS-mediated abnormal increase of blood glucose and insulin concentration to the levels of HF only group (Fig. 2A, B). The HOMA-IR index, an indicator of insulin resistance, revealed the HFHS-R fed group was approximately 3-fold more sensitive to insulin than HFHS group; sensitivities between HFHS-R fed group and HF fed group were similar (Fig. 2C). To confirm this, glucose (GTT) and insulin tolerance tests (ITT) were conducted. During GTT, glucose disposal was significantly slower in HFHS fed mice than HF fed mice. HFHS diet-mediated glucose tolerance was improved by RSF supplementation, which was confirmed by quantification of GTT area under curve (AUC) (Fig. 2D). In parallel, HFHS fed mice maintained higher glucose levels than HF fed mice during ITT. In contrast, glucose disposal rate between mice fed HFHS-R and HF alone was almost identical, showing no

difference in AUC (Fig. 2E). These data suggested that EA-containing RSF supplementation normalized the HS-induced glucose and insulin resistance in mice.

#### *3.4. RSF supplementation attenuated HS-mediated hepatic ER stress.*

HS intake has known to alter hepatic lipid metabolism and cause hepatic ER stress [24]. Given the significant improvement in plasma lipid profile by RSF (Table. 2), we hypothesized that RSF supplementation attenuates HS diet-induced hepatic steatosis and ER stress. The gross images of liver fed HFHS-R showed darker brownish color than HFHS fed liver, implicating that TG accumulation might be decreased. H&E staining of liver section revealed that TG accumulation appeared to be lower in HFHS-R fed group than HFHS fed mice (Fig. 3A). There was a decrease in TG content in HFHS-R fed group from HFHS, but it was not significant (Fig. 3B). It may reflect that HFHS-R diet showed a tendency to decrease liver mass compared to HFHS, but it was not significant (Table 2). Despite the marginal difference in liver mass, lipogenic related gene expression of stearoyl CoA desaturase-1 (SCD-1), lipoprotein lipase (LPL) and diacylglycerol acyltransferases 2 (DGAT2) were markedly decreased in mice fed with HFHS-R compared to HFHS. However, hepatic gene expression levels of carbohydrate response element-binding protein (ChREBP) and sterol regulatory element-binding protein 1c (SREBP1c) did not differ between HFHS and HFHS-R fed mice (Fig. 3C). Intriguingly, the two genes promoting gluconeogenesis, glucose 6-phosphase (G6Pase) and phosphoenolpyruvate carboxyl kinase (PEPCK) were also significantly down-regulated, suggesting that HS-mediated hepatic glucose output may be decreased by EA-containing RSF supplementation (Fig. 3D).

HS-mediated hepatic ER stress is associated with hepatic steatosis and upregulation of gluconeogenesis [25]. Thus, we determined the expression of ER stress markers in mice fed with HFHS vs. HFHS-R diet. RSF supplementation attenuated phosphorylation of JNK (p-JNK), p38 mitogen-activated protein kinase (p-p38 MAPK), and eukaryotic translation initiation factor 2A (p-eIF2 $\alpha$ ) compared to HFHS feeding (Fig. 3E). To validate these results in vitro system, we simulated ER stress condition in human hepatoma Huh7 cells by insulting cells with the combination glucose (Glc), fructose (Fr) and palmitate (PA). Pre-incubation of EA abolished the HFHS-triggered activation of p-JNK and p-p38 in a dose-dependent manner (Fig. 3F). To determine whether EA attenuates HFHS-mediated inhibition of hepatic insulin signaling, basal and insulin-stimulated phosphorylation of IRS-2 and Akt were measured in huh 7 cells (Fig. 3G). Huh 7 cells pre-treated with or without EA were simulated for ER stress by adding a high concentration of Glc, Fr and PA. Even in basal conditions, phosphorylation levels of IRS-2 and Akt appear to be increased slightly in the presence of 10  $\mu$ M EA (Fig 3G, lane 1 vs. 2). Insulin-stimulated p-IRS-2 and p-Akt were markedly higher in EA treated Huh7 cells (Fig 3G, lane 3 vs. 4), indicating that EA protects insulin signaling pathways against HSHS-mediated ER stress.

### *3.5. RSF supplementation attenuated hepatic oxidative stress.*

Prolonged ER stress leads to ROS production and causes oxidative stress [26]. We hypothesized that RSF supplementation reduces HFHS-mediated hepatic oxidative stress. To address this, we first determined the hepatic H<sub>2</sub>O<sub>2</sub> levels ( $\mu$ mol/ mg protein), an indicator of ROS production in liver, was significantly higher in mice fed with HFHS

diet compared to mice fed with HSHF-R and mice fed with HF diet alone, which showed similar values (Fig. 4A). To confirm the effects of EA on ROS production in vitro, we measured ROS production in the presence or absence of EA by measuring DCFDA fluorescence levels in Huh7 cells. The ROS production rate (DCFDA fluorescence) increased drastically upon stimuli with high concentration of Glc, Fr and PA cocktail, which was significantly decreased in EA pretreated cells (Fig. 4B, also see Supplemental Fig. 2 for kinetic production of ROS). Collectively these data suggest that EA in RSF may contribute to a reduction in HSHS-mediated hepatic ROS production.

### *3.6. RSF supplementation attenuated the HS-mediated adipose tissue inflammation*

To determine whether inclusion of RSF alters HFHS diet-induced adipose tissue remodeling, we first examined morphological changes of epididymal fat. H&E staining of adipose tissue clearly revealed that HFHS diet promotes adipocyte hypertrophy and macrophage infiltration compared to isocaloric HF diet. Despite the marginal difference in visceral fat mass (Table 2), HFHS-R diet significantly decreased adipocyte size and immune cell infiltration compared to HFHS diet (Fig. 5A). The analysis of adipocyte size and distribution confirmed these morphological changes. HFHS-R diet normalized HFHS-mediated adipocyte size expansion ( $111.53 \pm 1.09$  vs.  $95.37 \pm 0.86$ , HFHS vs. HFHS-R) (Fig. 5B) nearer to the HF control. Similarly, adipocyte size distribution from HFHS-R fed mice was shifted toward smaller sizes similar to HF diet feeding (Fig. 5C). Reflecting the smaller and more insulin-sensitized adipocytes, plasma levels of adiponectin levels (Fig. 5D) as well as adiponectin gene expression (Fig. 5E) were

significantly higher with HFHS-R diet than HFHS diet. The proinflammatory gene expressions including IL-6, IL-8, F4/80 (a marker for monocytic cells), tumor necrosis factor  $\alpha$  (TNF $\alpha$ ) and monocyte chemoattractant protein 1 (MCP-1) were significantly reduced in HFHS-R-fed adipose tissue compared to HFHS-fed adipose tissue (Fig. 5E). The decrease of macrophage infiltration by HFHS-R was also confirmed by immunostaining of F4/80 (Fig. 5F). Inflammatory protein profiles were also determined using the membrane-based inflammatory cytokine array in adipose tissue and plasma. HFHS diet decreased proinflammatory adipokine production from epididymal adipose tissue including leptin, C-X-C motif chemokine 5 (CXCL5), chemokine (C motif) ligand (XCL1), MCP-1, macrophage colony-stimulating factor (M-CSF), soluble tumour necrosis factor receptor 1 (sTNFR1), and sTNFR2 (Fig. 5G, upper) and decreased plasma levels of proinflammatory cytokines XCL1, MCP-1, M-CSF, sTNFR1, and sTNFR2 (Fig. 5G, below). Collectively, these data demonstrated that EA-containing RSF supplementation attenuated HS diet-mediated adipose inflammation and as well as systemic levels of inflammation.

#### **4 Discussion**

Western diet, high in saturated fat and sugar, but low in fresh fruits and vegetables, is the primary culprit to increase the risk of obesity and its associated metabolic dysfunction. This study was specifically designed to test the hypothesis whether the inclusion of EA in HFHS diet reverses the HS-induced metabolic complications. Here, we demonstrated that addition of EA-containing RSF significantly normalizes HFHS-

induced dyslipidemia (Table 2), enhances hepatic and systemic insulin sensitivity (Fig. 2, 3), reduces hepatic ER and oxidative stress (Fig. 3, 4), and inhibits proinflammatory adipose tissue remodeling and adipose dysfunction (Fig. 5) in C57BL/6 mice. To our knowledge, this is the first study to report the previously unrecognized function of EA in attenuating high sugar intake-inducible metabolic dysfunction by alleviating hepatic stress and adipose tissue inflammation.

Despite the numerous health beneficial effects of EA, low bioavailability is the biggest caveat for the practical use of EA [27]. However, a recent study has suggested that plasma concentrations of free EA in peripheral human plasma could be higher than previously expected (80 nM vs. 10 nM), and the concentrations of EA in liver tissues could also be relevant [28]. Furthermore, EA is extensively metabolized by gut microbes producing urolithins. Although there are several studies showing that urolithins may resemble metabolic characteristics of EA [29, 30], it is difficult to estimate the exact physiological contribution of urolithins to metabolism. Moreover, urolithin production is highly compounding with the individual variability of microbiome [31]. Prior to this study, we had conducted a pilot study by feeding HF diet with 0.1 % of pure EA from tree bark (unpublished data). To our disappointment, we were not able to observe physiological benefits that we proposed in our cellular studies [17, 18]. We speculated that free EA consumption may dilute the EA's health benefits due to its insolubility or prompt microbial conversion into urolithins. In this study, our criteria for selecting EA source were, 1) to use natural dietary source (ET form) rather than synthetic EA or isolated EA from tree bark, 2) to avoid complete conversion into urolithins before absorption, and 3) to minimize the other bioactive polyphenolic contamination to isolate

the role of EA. RSF appeared to fit our experimental requirements because 1) raspberry is an affordable fruit with easy access, 2) RSF contains very few other polyphenolic compounds (Table 1), and 3) the ratio of free EA to EA precursors (mostly ETs) was roughly 1:6 (based on before and after hydrolysis of RSF), which may allow sufficient time to be released from tannin and absorbed in the gut, delaying microbial action. Supporting our rationales, Kosmala et al. has recently analyzed the chemical composition of raspberry vs. strawberry seeds; the main component of raspberry seed was fiber and the major polyphenols were polymerized ETs (dimer or trimer), while strawberry seed mainly composed of monomers of ET [23]. Proanthocyanidins (condensed tannin), the other polyphenolic compounds found in RSF, were relatively low compared to ET-containing compounds [23]. Furthermore, the concentrations to exert bioactivity (lipid lowering and anti-inflammation) of depolymerized proanthocyanidins were in range of 50-100  $\mu\text{g/mL}$  in vitro (our unpublished data), whereas EA is in 10  $\mu\text{M}$  (2.7  $\mu\text{g/mL}$ ) [17, 18]. Therefore, RSF effects are likely due to combinatory of EA, ET, and its metabolites rather than other phytochemicals. In accordance with our results, raspberry ETs was more effective in lowering plasma TG levels than that of strawberry seed, suggesting that degree of conjugation with tannin (dimer/trimer>monomer> free EA) might regulate bioavailability of EA [23].

A growing body of evidence suggests that there is a substantial link between HS consumption and metabolic dysfunction including non-alcoholic fatty liver diseases (NAFLD), obesity, dyslipidemia, and insulin resistance (sugar toxicity) [8, 32]. To test the central hypothesis that EA inhibits sugar toxicity, we prepared HFHS diets with and without RSF and compared their metabolic markers with isocaloric HF diet with no

sucrose. The inclusion of RSF in HFHS diet was associated with at least three metabolic outcomes attenuating 1) obesity and dyslipidemia, 2) hepatic ER/oxidative stress and 3) adipose inflammation.

The first systemic metabolic benefit that we immediately noticed after RSF supplementation was the improvement of dyslipidemia and insulin sensitivity against HFHS diet (Table 1 and Fig. 1). Numerous studies in experimental animals and humans (both epidemiological and clinical intervention studies) have established that consumption of high-fructose promotes obesity, dyslipidemia (increased in plasma TG, LDL cholesterol, but decreased in HDL cholesterol) and insulin resistance [8, 33]. In agreement with this notion, switching carbohydrate source from dextrin (HF) to sugar (HFHS) without altering total calories, effectively promoted weight gain, dyslipidemia, and insulin resistance. These sugar toxicity-mediated metabolic abnormalities were ameliorated in the presence of RSF (Table 1). As RSF contains few other bioactive phytochemicals, the improvement of lipid profile and insulin sensitivity must be originated from EA and its derivatives in RSF. It is supported by growing evidence that consumption of EA-containing fruits protects high fructose-mediated metabolic abnormal modifications [34, 35]. The most noticeable benefits by RSF was a normalization of HS-mediated elevation of total and LDL cholesterol (Table 2). It implicates that RSF may promote LDL catabolism. In fact, HFHS diet reduced hepatic LDL receptor (LDLr) resulting in an accumulation of LDL particles while inclusion of EA in HFHS diet upregulated LDLr and apoA-I (Supplemental Fig. 3). In agreement with our results, Yoshimura et al. showed that EA effectively upregulates LDLr gene expression in diabetic KK-Ay mice [36]. Several papers reported that either free EA or EA (or ET)-

containing berries improve glucose and insulin tolerance against diet-induced obesity [35, 37]. As an underlying mechanism, it has been suggested EA and gallic acid selectively inhibit  $\alpha$ -glycosidase, suppressing entry of monosaccharides from the lumen to intestinal epithelium [38]. If the inhibition of  $\alpha$ -glycosidase enzyme activity by RSF was the key mechanism to reduce plasma glucose level, HFHS-R-fed mice may exhibit lower blood glucose than HF-fed mice, because HF diet contains the same amount of  $\alpha$ -glycosidase bondages with HFHS-R. However, it does seem to be the case since RSF supplementation improved the only HS-mediated metabolic abnormality (comparable with HF only group). However, at this point, we do not entirely exclude the possibility that inhibition of  $\alpha$ -glycosidase by RSF contributes to the improvement of insulin tolerance against sugar toxicity. Unexpectedly, the apparent improvement in dyslipidemia and insulin sensitivity with 0.03% of EA supplementation was not directly correlated with the decrease in BW or adipose tissue weight; HS-mediated weight gain was significantly ( $p < 0.05$ ) reversed by RSF but to a lesser magnitude. We assume that modulation of adiposity may require a higher concentration of EA than controlling insulin sensitivity or plasma lipids. Taken together, the inclusion of no more than 0.03 % of EA in HFHS diet (roughly 30 mg EA /kg BW/day or ~1.8 g/60 kg BW) substantially reversed sugar-mediated insulin resistance and dyslipidemia. We believe that RSF-mediated normalization of glucose tolerance would be the consequences of alleviated metabolic stress primarily from liver.

Subsequently, we examined the potential benefit of RSF against sugar toxicity in the liver, the primary metabolic target organ for sugar toxicity. There is convincing literature demonstrating that HS intake promotes hepatic lipogenesis. It is due to unique

properties of fructose metabolism that 1) fructose is mostly metabolized in liver (about 80% in contrast to only 20% for glucose) [39], 2) entry of fructose into hepatic glycolysis bypasses the regulatory control of phosphofructokinase (PFK) producing unregulated lipogenic and proinflammatory precursors [39], and thus 3) fructose activates lipogenic transcription factors of SREBP1c, and ChREBP [25] leading to ER stress and insulin resistance. Furthermore, high fructose intake also impedes fatty acid oxidation and augments very-low-density lipoprotein (VLDL) secretion expediting hepatic lipid accumulation and systemic obesity [40]. Complying with metabolic modification by HS intake, our results showed that HFHS diet was associated with a 2-fold increase of hepatic TG deposition and significant upregulation of both lipogenic transcription factors (SREBP1c and ChREBP) and their target genes compared to isocaloric HF diet. Unexpectedly, hepatic TG contents were not apparently different between mice fed with HFHS and HFHS-R. These results are conflicting with our previous *in vitro* study showing that EA attenuated hepatic TG accumulation by decreasing both *de novo* synthesis FA and its esterification [17]. However, it is notable that hepatic lipogenic gene expressions of SCD-1, LPL and DGAT2 were downregulated in mice fed with HFHS-R compared to HFHS (Fig. 3C), despite insignificant differences in transcription factor levels of SREBP1c and ChREBP. More importantly, two critical regulators of gluconeogenesis and hepatic glucose output, G6Pase and PEPCK, were significantly lower in HFHS-R mice (Fig. 3D). This supports our finding that HSHF-R-fed mice were more glucose tolerant than HFHS-fed mice (Fig. 2). Augmented insulin sensitivity may be attributed to the decreased hepatic ER stress and ROS production (Fig. 3, 4). In agreement with our results, a few studies supported the notion that EA is capable of

scavenging free radicals and decreasing ROS production [41]. It is unclear why EA is more sensitive in repressing oxidative stress signaling than the transcriptional repression of lipogenic genes. It could be attributed to limited accessibility of EA to the nucleus or higher concentration of EA may be required for optimal regulation of gene regulation. Further studies should be conducted to validate these possibilities. Taken together, herein we report that EA supplementation by RSF could effectively suppress HS-induced hepatic ER stress, ROS production, and hepatic glucose output in the absence of an obvious reduction in hepatic TG content.

Lastly, we assessed the impact of RSF on obesity and adipose tissue inflammation. The rank order of visceral adiposity among the mice fed with 12 weeks of isocaloric diet was, HFHS>HFHS-R>>HF, paralleling changes in body and liver weight. More importantly, there was a distinct improvement of adipose tissue remodeling by decreasing adipocyte size, immune cell infiltration and pro-inflammatory gene and protein expression (Fig. 5). Supporting our finding, the recent study by Winand et al. demonstrated that EA decreased TNF $\alpha$ , IL-6 and chemokine (C-C motif) ligand-2 (CCL-2) secretion in lipopolysaccharides (LPS) induced macrophage and adipocyte [42]. Notably, minor changes in adiposity by HFHS-R, promoted almost complete reversal of adipose tissue inflammation. At this point, it is unknown whether the reversal of HS-mediated adipose tissue inflammation reflects role of EA in adipose tissue *in situ*, or indirect influence primarily from metabolic adaptation in liver (e.g., reduced VLDL secretion). We have previously reported that EA may impose direct lipid-lowering effects in human adipocytes. Several other studies have demonstrated that EA can impede adipocyte differentiation *in vitro* [43, 44]. Also, our preliminary work in human

adipocytes showed that urolithins are able to regulate adipogenesis or lipogenesis in vitro (unpublished). Future studies that analyze tissue levels of EA and its urolithin metabolites are necessary to identify whether EA or its metabolites urolithins directly target adipose tissue metabolism.

In summary, here we tested an innovative idea whether inclusion of EA in HF diet could inhibit high sugar intake-mediated metabolic dysfunction. We identified that RSF, as a source of EA, effectively antagonized the effects of sugar toxicity including dyslipidemia, hepatic ER stress and ROS, and pro-inflammatory adipose tissue remodeling. Whether these initial findings in rodents will be confirmed in humans must await future studies. Nevertheless, we believe that our study shed new insight into EA-containing foods consumption for the prevention of sugar toxicity.

**Table IV-0-1 Main phenolic compounds identified in RSF.**

<b>Compound</b>	<b>Retention time</b>	<b><i>m/z</i></b>	<b>MS/MS</b>
<b>Flavan-3-ol and proanthocyanidins</b>			
Proanthocyanidin dimers (epi)catechin-(epi)catechin	10.82; 12.33;14.82	577	451, 425, 407, 289
(Epi)catechin (monomer)	11.76	289	271, 245, 161, 125
Proanthocyanidin trimer 3 (epi)catechin	12.90	865	289
Proanthocyanidin dimers (epi)afzelechin-(epi)catechin	13.19; 14.26; 15.25;17.06	561	543, 435, 407, 289
proanthocyanidin trimer 2 (epi)catechin-(epi)afzelechin	15.04	849	
Proanthocyanidin dimer (epi)afzelechin-(epi)afzelechin	16.05	545	549,419,273,164
Proanthocyanidin trimer 2 (epi)afzelechin-(epi)catechin	16.41	833	
<b>Ellagic acid derivatives and ellagitannins</b>			
*HHDP-hexoside	3.28	481	301
bis-HHDP-hexoside (pedunculagin isomers)	7.47; 9.52	783	481,301
Castalagin/vescalagin isomers	8.52; 15.69, 16.70	466 (double charged)	865, 781, 631, 481, 451, 301
Galloyl-HHDP-glucose (corilagin isomers)	8.91;9.69;11.42	633	481, 463, 301
Valoneic acid dilactone isomers	8.98;11.54;14.20	469	425
Digalloyl hexoside	10.60	483	331, 313, 271, 169
Ellagitannin (unidentified)	13.50	631 (double charged)	938, 783, 695, 451, 301
Galloyl bis HHDP-glucoside isomers	14.97;15.69;16.70, 17.35	467(double charged)	751, 633, 451, 391, 301
Di-galloyl HHDP glucoside	15.25	785	633, 483, 301
Ellagitannin (unidentified)	15.54	551(double charged)	765, 631, 448, 301
Ellagic acid pentoside isomers	16.84;17.35	433	301
Ellagic acid	18.28	301	257
<b>Phenolic acid derivatives</b>			
Caffeoyl hexoside	2.51	341	179, 161

**Table IV-0-2 Food intake, metabolic parameters and blood lipid profiles \***

<b>Group</b>	<b>HF</b>	<b>HFHS</b>	<b>HFHS-R</b>	<b>p-value</b>
<b>Food intake</b>				
(g/mouse/day)	3.43 ± 0.13	3.45 ± 0.13	3.27 ± 0.04	0.840
<b>Phenotypes</b>				
BW (g)	36.67 ± 0.74 <sup>b</sup>	45.00 ± 0.59 <sup>a</sup>	40.50 ± 0.73 <sup>ab</sup>	0.011
Δ BW (g)	10.00 ± 0.46 <sup>b</sup>	18.5 ± 0.27 <sup>a</sup>	14.50 ± 0.77 <sup>ab</sup>	0.002
Liver (g)	1.57 ± 0.04 <sup>b</sup>	2.97 ± 0.18 <sup>a</sup>	1.97 ± 0.07 <sup>ab</sup>	0.046
Liver/BW (%)	4.27 ± 0.10	5.93 ± 0.49	4.86 ± 0.18	0.223
Epididymal fat (g)	1.82 ± 0.07 <sup>b</sup>	2.51 ± 0.048 <sup>a</sup>	2.14 ± 0.08 <sup>ab</sup>	0.040
Mesenteric fat (g)	0.60 ± 0.07 <sup>b</sup>	1.08 ± 0.07 <sup>a</sup>	0.88 ± 0.07 <sup>ab</sup>	0.015
<b>Blood Chemistry</b>				
Triglyceride (mg/dL)	25.59 ± 0.77 <sup>ab</sup>	38.93 ± 2.41 <sup>a</sup>	21.67 ± 2.07 <sup>b</sup>	0.056
Total Cholesterol				
(mg/dL)	110.33 ± 4.12 <sup>b</sup>	184.50 ± 2.36 <sup>a</sup>	122.83 ± 1.83 <sup>b</sup>	0.001
HDL (mg/dL)	71.28 ± 0.48 <sup>a</sup>	60.82 ± 0.22 <sup>b</sup>	72.13 ± 0.40 <sup>a</sup>	< 0.0001
LDL (mg/dL)	33.94 ± 0.48 <sup>c</sup>	115.80 ± 0.22 <sup>a</sup>	45.89 ± 0.40 <sup>b</sup>	< 0.0001

\* Values are mean ± SEM. All groups, n = 6. Column not sharing a common letter are significantly different (p < 0.05)

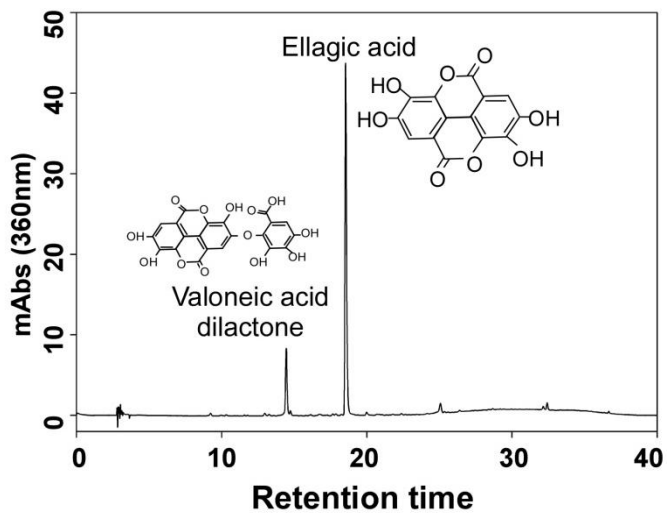


**Figure IV -1 Identification of ellagic acid and its derivatives after hydrolysis of RSF.**

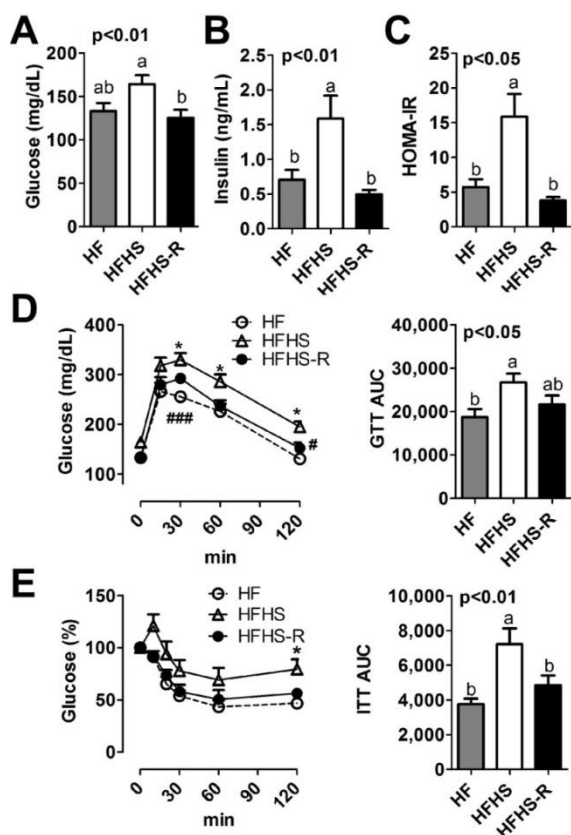


**Figure IV-2 RSF supplementation ameliorated glucose and insulin tolerance in C57BL/6 mice against HS diet.**

Eight-week old male C57BL/6 mice were fed with isocaloric HF (grey), HFHS (white), or HFHS-R (black) diet for 12 weeks ( $n = 6$  per group). (A) Fasting plasma glucose levels (mg/dL), (B) Fasting plasma insulin levels (ng/mL) quantified by ELISA, (C) HOMA-IR, (D) Glucose tolerance tests (GTT), (E) Insulin tolerance tests (ITT). Data are means expressed as mean  $\pm$  SEM ( $n = 6$ ). Bars with different letters are significantly different by one-way ANOVA.  $*P < 0.05$  (HF vs. HFHS),  $\#P < 0.01$ , and  $\###P < 0.0001$  (HFHS vs. HFHS-R) by Student's *t*-test.

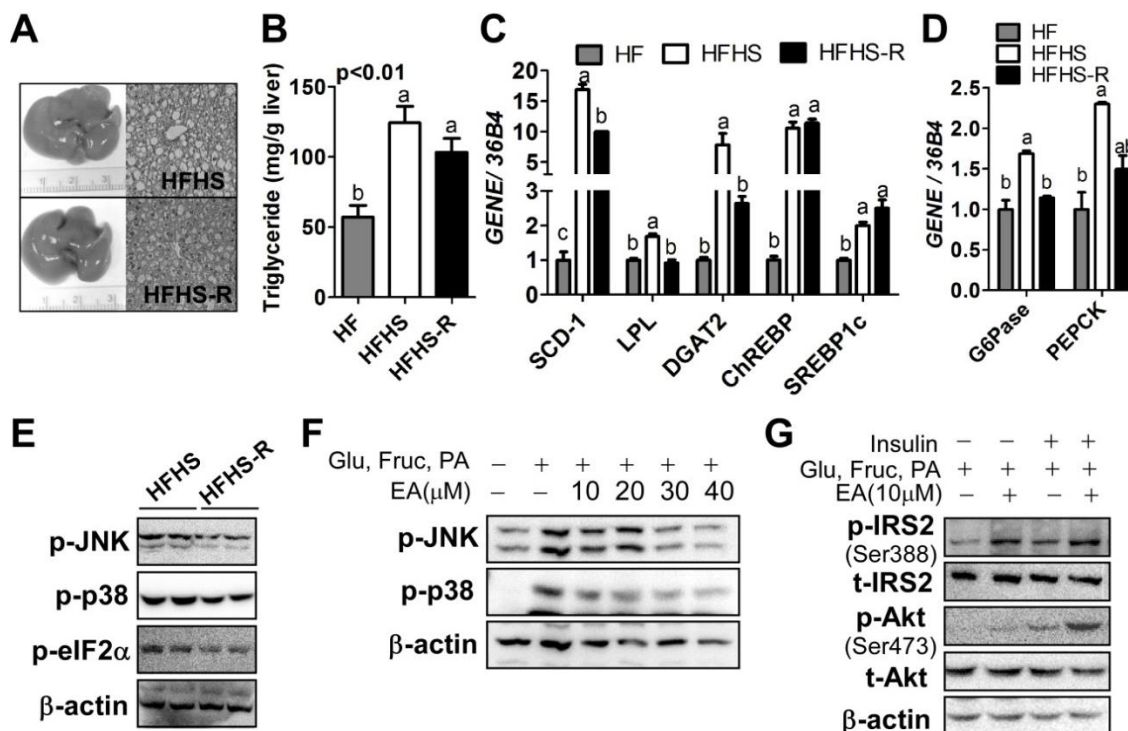


**Figure IV -3 RSF supplementation attenuated hepatic ER stress and insulin sensitivity against HS diet.**

Eight-week old male C57BL/6 mice were fed with isocaloric HF (grey), HFHS (white), or HFHS-R (black) diet for 12 weeks (n=6 per group) (A-E). (A). Gross images and representative microscopic images of liver revealed by H&E staining after 12 weeks of feeding with HFHS or HFHS-R, (B) Hepatic TG contents (mg/g liver), (C) Hepatic mRNA expression of SCD-1, LPL, DGAT2, ChREBP and SREBP1c by qPCR, (D). Hepatic mRNA expressions of gluconeogenic genes of G6Pase and PEPCk by qPCR, (E). Western blot analysis of phosphorylation of JNK, p38, and eIF2α in liver fed with either HFHS or HFHS-R. Huh7 cells were pre-incubated with either DMSO or EA before stimulation with the mixture of glucose (Glc), fructose (Fr) and palmitate (PA) (F, G). (F) Phosphorylation of JNK, and p38 expression by western blot. (G) Phosphorylation of

IRS2 and Akt by western blot with and without insulin (100 nM) treatment.  $\beta$ -actin was used for loading control. Data are expressed as mean  $\pm$  SEM (n = 6). Bars with different letters are significantly different by one-way ANOVA.

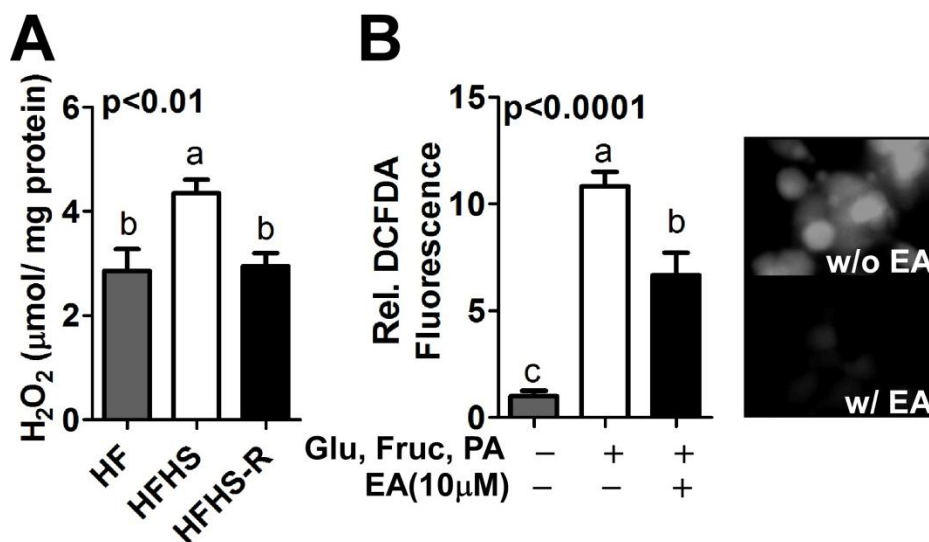


**Figure IV -4 RSF supplementation reduced hepatic oxidative stress against HS diet.** Eight week-old male C57BL/6 mice were fed with HF (grey), HFHS (white), or HFHS-R (black) diet for 12 weeks (n=6 per group). (A) H<sub>2</sub>O<sub>2</sub> level (μmol/ mg protein) in liver sample. (B) Relative ROS production in huh 7 cells with or without EA using DCFDA fluorescence as molecular probe for detecting ROS production (Left). DCF fluorescence was visualized by fluorescence microscopy (Right). Data are expressed as mean ± SEMs. Bars with different letters are significantly different by one-way ANOVA.

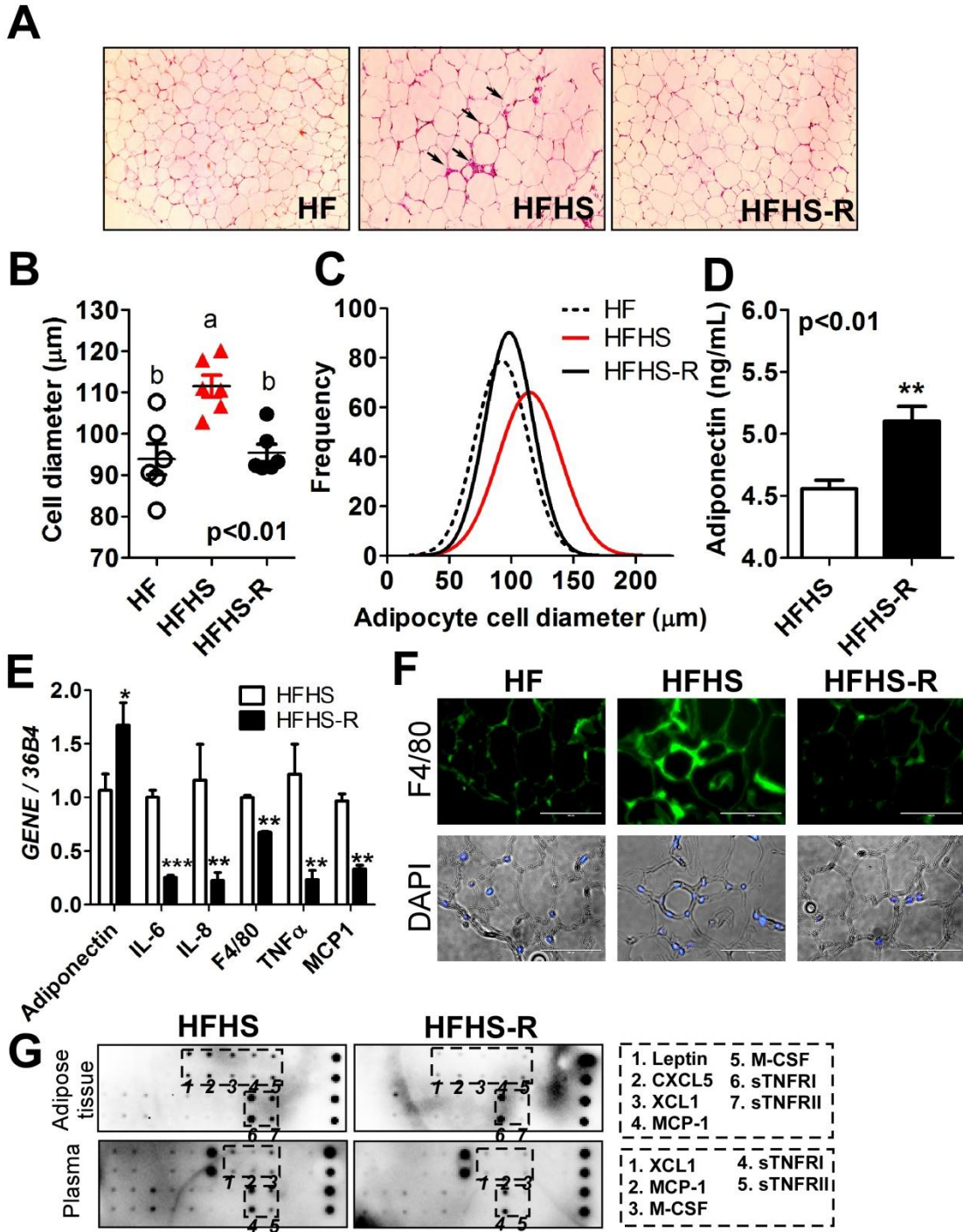


Figure IV -5 RSF supplementation attenuated visceral adipocyte hypertrophy and adipose inflammation against HS diet.

Eight week-old male C57BL/6 mice were fed with HF, HFHS, or HFHS-R diet for 12 weeks (n=6 per group). (A) Representative microscopic images of epididymal adipose tissue by H&E staining. Arrows indicate macrophage infiltration, (B) Average size (diameter) of epididymal adipocytes (n=6 mice per group), (C) Adipocyte size distribution, The line of best fit is shown (Gaussian curve fitting), (D) Plasma adiponectin levels (ng/mL) quantified by ELISA, (E) mRNA expression levels of adiponectin, IL-6, IL-8, F4/80, TNF $\alpha$  and MCP1 in epididymal adipose tissue quantified by qPCR. (F) Immunofluorescent staining of F4/80 (Green). The nuclei counterstained by DAPI (Blue) and phase contrast images were overlapped. (G) Homogenized epididymal adipose tissue and plasma (pooled sample n=6 per group) from HFHS or HFHS-R fed mice were used for simultaneous detection of multiple inflammatory cytokines using mouse inflammatory array C1. Data are expressed as mean  $\pm$  SEMs. Bars with different letters are significantly different by one-way ANOVA. \*\* $P$  < 0.01, \*\*\* $P$  < 0.001 (HFHS vs. HFHS-R) by Student's  $t$ -test.

**Supplemental Table 1.** Dietary composition of isocaloric HF diet, HFHS diet, and HFHS diet containing different ingredients fed to male C57BL/6J mice for 12 weeks<sup>1</sup>.

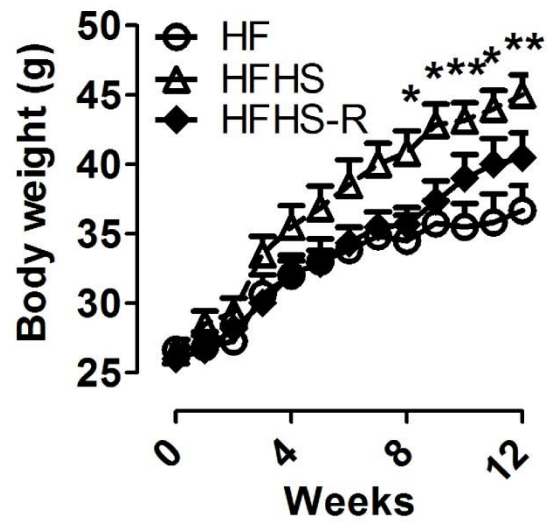
Ingredients	<b>HF diet</b>	<b>HFHS diet</b>	<b>HFHS-R diet</b>
	<i>g/kg</i>	<i>g/kg</i>	<i>g/kg</i>
Casein	195	195	195
L-Cystine	3	3	3
Sucrose	0	435	435
Corn Starch	435	0	0
Maltodextrin	50	50	50
Lard	175	175	175
Soybean oil	39	39	39
Cellulose	40	40	10
HPMC	10	10	10
Mineral Mix	35	35	35
Calcium Carbonate	4	4	4
Vitamin Mix	10	10	10
Choline bitartrate	2	2	2
RSF	0	0	30
<b>Total</b>	<b>998</b>	<b>998</b>	<b>998</b>
	<i>Kcal (%)</i>	<i>Kcal (%)</i>	<i>Kcal (%)</i>
Carbohydrate	42.2	42.2	42.2
(Sucrose)	(0.0)	(37.0)	(37.0)
Protein	16.9	16.9	16.9
Fat	41.0	41.0	41.0
<b>Kcal/g</b>	<b>4.7</b>	<b>4.7</b>	<b>4.7</b>

**Supplemental Table 2.** Primer sequences for qPCR

<b>Gene</b>	<b>Forward/Reverse</b>	<b>Sequence (5'-3')</b>
mAdiponectin	Forward	ACAATGGCACACCAGGCCGT
	Reverse	TGCCAGGGGTTCCGGGGAAG
mChREBP	Forward	ATATCTCCGACACACTCTTCACC
	Reverse	GTCAGGTCTGGCTGGATCATG
mDAGT2	Forward	CCGCAAAGGCTTTGTGAAG
	Reverse	GGAATAAGTGGGAACCAGATCA
mF4/80	Forward	CTTTGGCTATGGGCTTCCAGTC
	Reverse	GCAAGGAGGACAGAGTTTATCGTG
mG6Pase	Forward	CGACTCGCTATCTCCAAGTGA
	Reverse	GTTGAACCAGTCTCCGACCA
mIL-6	Forward	CTGCAAGAGACTTCCATCCAGTT
	Reverse	AGGGAAGGCCGTGGTTGT
mIL-8	Forward	GGTCTGCTACGGGCTCACA
	Reverse	CCCGGTGTTTCTGCCTCAT
mLPL	Forward	CATCTCATTCCCTGGATTAGCAGAC
	Reverse	CCGATACAACCAGTCTACTACAATG
mLXR $\alpha$	Forward	AACCTCAAGATGCAGGAGACC
	Reverse	GACTCCAACCCTATCCCTAAAGC
mMCP1	Forward	AGGTCCCTGTCATGCTTCTG
	Reverse	GCTGCTGGTGATCCTCTTGT

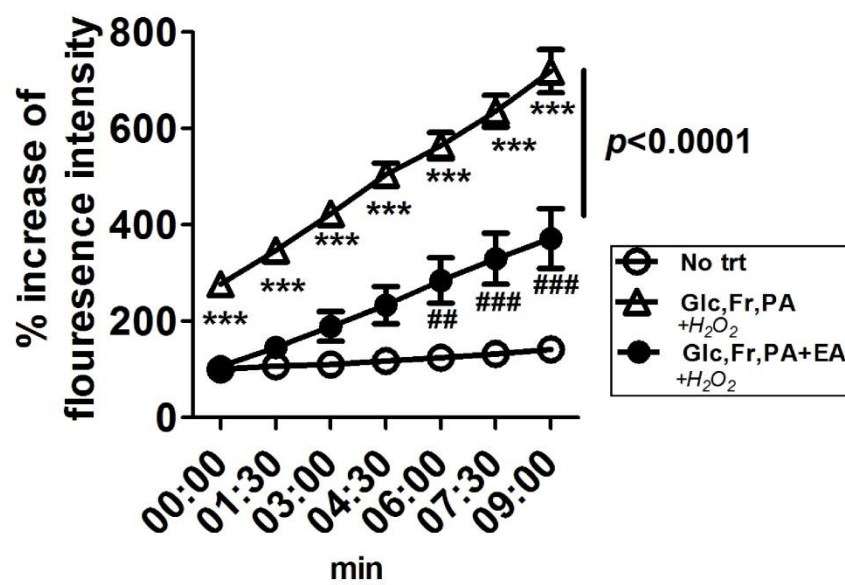
mPEPCK	Forward	CTGCATAACGGTCTGGACTTC
	Reverse	CAGCAACTGCCCGTACTCC
mSCD-1	Forward	GGGACAGATATGGTGTGAAACTATG
	Reverse	TTACAGACACTGCCCTCAAC
mSREBP1c	Forward	GTGAGCCTGACAAGCAATCA
	Reverse	GGTGCCTACAGAGCAAGAGG
mTNF $\alpha$	Forward	GGCTGCCCCGACTACGT
	Reverse	ACTTTCTCCTGGTATGAGATAGCAA AT

## Supplemental Fig 1



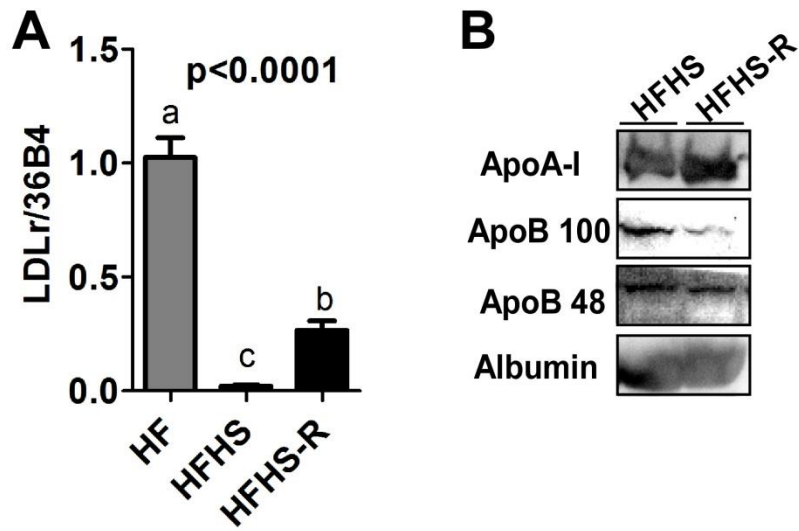
Supplemental Fig. 1. Changes in BW were monitored by weekly of all mice.

## Supplemental Fig 2



**Supplemental Fig. 2.** Kinetic productions of ROS were monitored by measuring fluorescence intensity up to 10 min in Huh7 cells.

## Supplemental Fig 3



**Supplemental Fig. 3.** (A) Hepatic LDLr gene expressions in HF, HFHS, and HFHS-R fed mice. (B) Plasma levels of apoA-I and apoB by western blot.

## References

- [1] Greenberg AS, Obin MS. Obesity and the role of adipose tissue in inflammation and metabolism. *Am J Clin Nutr* 2006;83:461s-5s.
- [2] Kubota N, Terauchi Y, Miki H, Tamemoto H, Yamauchi T, Komeda K, et al. PPAR gamma mediates high-fat diet-induced adipocyte hypertrophy and insulin resistance. *Mol Cell* 1999;4:597-609.
- [3] Cani PD, Bibiloni R, Knauf C, Waget A, Neyrinck AM, Delzenne NM, et al. Changes in gut microbiota control metabolic endotoxemia-induced inflammation in high-fat diet-induced obesity and diabetes in mice. *Diabetes* 2008;57:1470-81.
- [4] Malik VS, Popkin BM, Bray GA, Despres JP, Hu FB. Sugar-sweetened beverages, obesity, type 2 diabetes mellitus, and cardiovascular disease risk. *Circulation* 2010;121:1356-64.
- [5] Parks EJ, Hellerstein MK. Carbohydrate-induced hypertriglycerolemia: historical perspective and review of biological mechanisms. *Am J Clin Nutr* 2000;71:412-33.
- [6] Carden TJ, Carr TP. Food availability of glucose and fat, but not fructose, increased in the U.S. between 1970 and 2009: analysis of the USDA food availability data system. *Nutr J* 2013;12:130.
- [7] Malik VS, Schulze MB, Hu FB. Intake of sugar-sweetened beverages and weight gain: a systematic review. *Am J Clin Nutr* 2006;84:274-88.
- [8] Stanhope KL, Schwarz JM, Keim NL, Griffen SC, Bremer AA, Graham JL, et al. Consuming fructose-sweetened, not glucose-sweetened, beverages increases visceral adiposity and lipids and decreases insulin sensitivity in overweight/obese humans. *J Clin Invest* 2009;119:1322-34.
- [9] Lee JH, Johnson JV, Talcott ST. Identification of ellagic acid conjugates and other polyphenolics in muscadine grapes by HPLC-ESI-MS. *J Agric Food Chem* 2005;53:6003-10.
- [10] Vasudev SS, Ahmad FJ, Khar RK, Bhatnagar A, Kamal YT, Talegaonkar S, et al. Validated HPLC method for the simultaneous determination of taxol and ellagic acid in a Punica granatum fruit extract containing combination formulation. *Pharmazie* 2012;67:834-8.
- [11] Adams LS, Zhang Y, Seeram NP, Heber D, Chen S. Pomegranate ellagitannin-derived compounds exhibit antiproliferative and antiaromatase activity in breast cancer cells in vitro. *Cancer Prev Res (Phila)* 2010;3:108-13.
- [12] Losso JN, Bansode RR, Trappey A, Bawadi HA, Truax R. In vitro anti-proliferative activities of ellagic acid. *J Nutr Biochem* 2004;15:672-8.
- [13] Aiyer HS, Gupta RC. Berries and ellagic acid prevent estrogen-induced mammary tumorigenesis by modulating enzymes of estrogen metabolism. *Cancer Prev Res (Phila)* 2010;3:727-37.

- [14] Park SH, Kim JL, Lee ES, Han SY, Gong JH, Kang MK, et al. Dietary ellagic acid attenuates oxidized LDL uptake and stimulates cholesterol efflux in murine macrophages. *J Nutr* 2011;141:1931-7.
- [15] Hseu YC, Chou CW, Senthil Kumar KJ, Fu KT, Wang HM, Hsu LS, et al. Ellagic acid protects human keratinocyte (HaCaT) cells against UVA-induced oxidative stress and apoptosis through the upregulation of the HO-1 and Nrf-2 antioxidant genes. *Food Chem Toxicol* 2012;50:1245-55.
- [16] Umesalma S, Sudhandiran G. Differential inhibitory effects of the polyphenol ellagic acid on inflammatory mediators NF-kappaB, iNOS, COX-2, TNF-alpha, and IL-6 in 1,2-dimethylhydrazine-induced rat colon carcinogenesis. *Basic Clin Pharmacol Toxicol* 2010;107:650-5.
- [17] Okla M, Kang I, Kim dM, Gourineni V, Shay N, Gu L, et al. Ellagic acid modulates lipid accumulation in primary human adipocytes and human hepatoma Huh7 cells via discrete mechanisms. *J Nutr Biochem* 2015;26:82-90.
- [18] Kang I, Okla M, Chung S. Ellagic acid inhibits adipocyte differentiation through coactivator-associated arginine methyltransferase 1-mediated chromatin modification. *J Nutr Biochem* 2014;25:946-53.
- [19] Garcia-Villalba R, Espin JC, Aaby K, Alasalvar C, Heinonen M, Jacobs G, et al. Validated Method for the Characterization and Quantification of Extractable and Nonextractable Ellagitannins after Acid Hydrolysis in Pomegranate Fruits, Juices, and Extracts. *J Agric Food Chem* 2015;63:6555-66.
- [20] Friedewald WT, Levy RI, Fredrickson DS. Estimation of the concentration of low-density lipoprotein cholesterol in plasma, without use of the preparative ultracentrifuge. *Clin Chem* 1972;18:499-502.
- [21] Chen HC, Farese RV, Jr. Determination of adipocyte size by computer image analysis. *J Lipid Res* 2002;43:986-9.
- [22] Zhao L, Kang I, Fang X, Wang W, Lee MA, Hollins RR, et al. Gamma-tocotrienol attenuates high-fat diet-induced obesity and insulin resistance by inhibiting adipose inflammation and M1 macrophage recruitment. *Int J Obes (Lond)* 2015;39:438-46.
- [23] Kosmala M, Zdunczyk Z, Juskiewicz J, Jurgonski A, Karlinska E, Macierzynski J, et al. Chemical composition of defatted strawberry and raspberry seeds and the effect of these dietary ingredients on polyphenol metabolites, intestinal function, and selected serum parameters in rats. *J Agric Food Chem* 2015;63:2989-96.
- [24] Kelley GL, Allan G, Azhar S. High dietary fructose induces a hepatic stress response resulting in cholesterol and lipid dysregulation. *Endocrinology* 2004;145:548-55.
- [25] Zhang C, Chen X, Zhu RM, Zhang Y, Yu T, Wang H, et al. Endoplasmic reticulum stress is involved in hepatic SREBP-1c activation and lipid accumulation in fructose-fed mice. *Toxicol Lett* 2012;212:229-40.
- [26] Bhandary B, Marahatta A, Kim HR, Chae HJ. An involvement of oxidative stress in endoplasmic reticulum stress and its associated diseases. *Int J Mol Sci* 2012;14:434-56.

- [27] Landete J. Ellagitannins, ellagic acid and their derived metabolites: a review about source, metabolism, functions and health. *Food Research International* 2011;44:1150-60.
- [28] González-Sarriás A, García-Villalba R, Núñez-Sánchez MA, Tomé-Carneiro J, Zafrilla P, Mulero J, et al. Identifying the limits for ellagic acid bioavailability: A Crossover pharmacokinetic study in healthy volunteers after consumption of pomegranate extracts. *J Funct Foods* 2015 Doi: 10.1016/j.jff.2015.09.019.
- [29] Larrosa M, Gonzalez-Sarrias A, Yanez-Gascon MJ, Selma MV, Azorin-Ortuno M, Toti S, et al. Anti-inflammatory properties of a pomegranate extract and its metabolite urolithin-A in a colitis rat model and the effect of colon inflammation on phenolic metabolism. *J Nutr Biochem* 2010;21:717-25.
- [30] Ishimoto H, Shibata M, Myojin Y, Ito H, Sugimoto Y, Tai A, et al. In vivo anti-inflammatory and antioxidant properties of ellagitannin metabolite urolithin A. *Bioorg Med Chem Lett* 2011;21:5901-4.
- [31] Tomas-Barberan FA, Garcia-Villalba R, Gonzalez-Sarrias A, Selma MV, Espin JC. Ellagic acid metabolism by human gut microbiota: consistent observation of three urolithin phenotypes in intervention trials, independent of food source, age, and health status. *J Agric Food Chem* 2014;62:6535-8.
- [32] Ouyang X, Cirillo P, Sautin Y, McCall S, Bruchette JL, Diehl AM, et al. Fructose consumption as a risk factor for non-alcoholic fatty liver disease. *J Hepatol* 2008;48:993-9.
- [33] Caton PW, Nayuni NK, Khan NQ, Wood EG, Corder R. Fructose induces gluconeogenesis and lipogenesis through a SIRT1-dependent mechanism. *J Endocrinol* 2011;208:273-83.
- [34] Anhe FF, Roy D, Pilon G, Dudonne S, Matamoros S, Varin TV, et al. A polyphenol-rich cranberry extract protects from diet-induced obesity, insulin resistance and intestinal inflammation in association with increased *Akkermansia* spp. population in the gut microbiota of mice. *Gut* 2015;64:872-83.
- [35] Jaroslawska J, Juskiewicz J, Wroblewska M, Jurgonski A, Krol B, Zdunczyk Z. Polyphenol-rich strawberry pomace reduces serum and liver lipids and alters gastrointestinal metabolite formation in fructose-fed rats. *J Nutr* 2011;141:1777-83.
- [36] Yoshimura Y, Nishii S, Zaima N, Moriyama T, Kawamura Y. Ellagic acid improves hepatic steatosis and serum lipid composition through reduction of serum resistin levels and transcriptional activation of hepatic ppara in obese, diabetic KK-A(y) mice. *Biochem Biophys Res Commun* 2013;434:486-91.
- [37] Torronen R, Sarkkinen E, Tapola N, Hautaniemi E, Kilpi K, Niskanen L. Berries modify the postprandial plasma glucose response to sucrose in healthy subjects. *Br J Nutr* 2010;103:1094-7.
- [38] Kam A, Li KM, Razmovski-Naumovski V, Nammi S, Shi J, Chan K, et al. A comparative study on the inhibitory effects of different parts and chemical constituents of pomegranate on alpha-amylase and alpha-glucosidase. *Phytother Res* 2013;27:1614-20.

- [39] Havel PJ. Dietary fructose: implications for dysregulation of energy homeostasis and lipid/carbohydrate metabolism. *Nutr Rev* 2005;63:133-57.
- [40] Mayes PA. Intermediary metabolism of fructose. *Am J Clin Nutr* 1993;58:754s-65s.
- [41] Galano A, Francisco Marquez M, Perez-Gonzalez A. Ellagic acid: an unusually versatile protector against oxidative stress. *Chem Res Toxicol* 2014;27:904-18.
- [42] Winand J, Schneider YJ. The anti-inflammatory effect of a pomegranate husk extract on inflamed adipocytes and macrophages cultivated independently, but not on the inflammatory vicious cycle between adipocytes and macrophages. *Food Funct* 2014;5:310-8.
- [43] Jeong MY, Kim HL, Park J, An HJ, Kim SH, Kim SJ, et al. Rubi Fructus (*Rubus coreanus*) Inhibits Differentiation to Adipocytes in 3T3-L1 Cells. *Evid Based Complement Alternat Med* 2013;2013:475386.
- [44] Wang L, Li L, Ran X, Long M, Zhang M, Tao Y, et al. Ellagic Acid Reduces Adipogenesis through Inhibition of Differentiation-Prevention of the Induction of Rb Phosphorylation in 3T3-L1 Adipocytes. *Evid Based Complement Alternat Med* 2013;2013:287534.

**V. CHAPTER IV: Urolithin A, C and D, but not iso-Urolithin A and Urolithin B, attenuate triglyceride accumulation in primary cultures of human adipocytes**

<sup>1</sup>Inhae Kang, <sup>1</sup>YongEun Kim, <sup>2</sup>Francisco A. Tomás-Barberán, <sup>2</sup>Juan Carlos Espín, and  
<sup>1</sup>Soonkyu Chung<sup>§</sup>

<sup>1</sup>Department of Nutrition and Health Sciences, University of Nebraska-Lincoln, Nebraska

<sup>2</sup>Department of Food Science and Technology, CEBAS-CSIC, Murcia, Spain

<sup>§</sup>**Address correspondence:** Soonkyu Chung, PhD, Department of Nutrition and Health Sciences, University of Nebraska-Lincoln, 316G Ruth Leverton Hall, P.O. Box 830806, Lincoln, NE, 68583, Fax: (402) 472-1587, E-mail: [schung4@unl.edu](mailto:schung4@unl.edu)

**Running title:** Urolithins attenuate lipid accumulation

**Abbreviations:** AMPK, AMP-activated protein kinase; ATGL, Adipose triglyceride lipase; C/EBP $\alpha$ , CCAAT/enhancer binding protein  $\alpha$ ; EA, ellagic acid; ET, ellagitannin; FA, fatty acid; Fas, fatty acid synthase; hASCs, human adipose-derived stem cells; OA, oleic acid; PPAR $\gamma$ , peroxisome proliferator-activated receptor gamma; SCD1, Stearoyl-CoA desaturase-1; TG, triglyceride; Uro, urolithins

**Key words:** ellagic acid, urolithins, adipogenesis, lipogenesis, AMP-activated protein kinase, obesity

## Abstract

**Scope:** Urolithins (Uro) are ellagic acid (EA)-derived metabolites produced by gut microbes. There is a growing interest in the biological activities of Uro. Our aim was to evaluate the impacts of Uro on regulating triglyceride (TG) accumulation using primary cultures of human adipocytes.

**Methods and Results:** UroA, B, C, D, and iso-UroA, were used to determine the effect of Uro on adipogenesis and lipogenesis. Individual Uro (30  $\mu$ M) were added to human adipogenic stem cells (*hASCs*) during differentiation. UroA, C and D, but not iso-UroA and UroB, significantly inhibited new fat cell formation by decreasing TG accumulation and adipogenic protein and gene expressions. The regulation of TG synthesis by Uro was investigated via metabolic chasing with radiolabeled precursors. UroA, C, and D attenuated the conversion of [ $^3$ H]-acetate into [ $^3$ H]-TG as well as [ $^{14}$ C]-oleic acid (OA) into [ $^{14}$ C]-TG, while increasing the conversion of [ $^3$ H]-OA to [ $^3$ H]-H<sub>2</sub>O (FA oxidation). Furthermore, UroC, D and A promoted the phosphorylation of AMP-activated protein kinase (AMPK), implicating that Uro may alter energy-sensing metabolic pathways in primary human adipocytes.

**Conclusions:** Taken together, our results demonstrated that UroA, C, and D reduce TG accumulation and increase FA oxidation via AMPK-associated mechanisms in primary cultures of human adipocytes.

## 1 Introduction

Ellagitannins (ETs) and ellagic acid (EA) derivatives are naturally occurring polyphenols found in pomegranate, berries, and nuts. It has been reported that EA exerts various health benefits including free radical scavenger activity and anti-proliferative effects in various types of cancer in vivo and in vitro [1-3]. There is a substantial body of evidence that supplementation with pure EA alone or consumption of EA-enriched fruits and nuts attenuates body fat mass and liver lipids [4-6], suggesting that EA possesses lipid-lowering characteristics. Supporting this, our group has recently reported that EA reduces adipogenesis through the inhibition of co-activator arginine methyltransferase 1 (CARM1) in primary human adipogenic stem cells (*hASCs*) [7], alters lipid mechanisms both in human adipocytes and hepatocytes [8], and normalizes high sugar-mediated metabolic dysfunction (under review).

Likewise to many other health-promoting polyphenolic compounds, low bioavailability of EA remains paradoxical. Oral administration of pure EA or EA-containing products in both rodents and humans showed that  $\sim 1 \mu\text{M}$  of EA can be found in plasma or tissues [9, 10]. This is attributed to the fact that EA undergoes extensive metabolic transformation prior to absorption [11]. In the intestinal lumen, EA is extensively metabolized by gut microbes producing a series of metabolites called urolithins (Uro). Uro are characterized by a common 6H-dibenzo[b,d]-pyran-6-one nucleus and a decreasing number of phenolic hydroxyl groups (UroD  $\rightarrow$  UroC  $\rightarrow$  UroA or iso-UroA  $\rightarrow$  UroB) (Fig. 1A) [12]. Among Uro species, UroA is the major metabolite observed in humans while Iso-UroA and UroB conjugates are also observed in some, but

not all, humans. As the result of microbial actions, EA is converted into bioavailable Uro which can reach significant concentrations in plasma and tissues [12-15].

Recently, several studies have demonstrated that Uro have metabolic characteristics of EA showing anti-inflammatory [16], anti-cancer [17, 18], anti-glycative [19] and anti-oxidant [20] properties. However, it is largely unknown if Uro have TG-lowering effects by altering lipid metabolism. To address this issue, we investigated the effects of individual Uro on lipid metabolism in human adipocytes and confirmed augmented fatty acid (FA) oxidation in human hepatoma Huh7 cells. Here, we are the first to report that Uro (30  $\mu$ M) possess biological activities to downregulate adipogenesis and lipogenesis similar to EA in human adipocytes. We also demonstrated that Uro alter lipid metabolism via AMPK activation.

## **2 Materials and methods**

### *2.1 Chemical reagents*

All cell culture supplies were purchased from Fisher Scientific. Fetal bovine serum (FBS) and penicillin-streptomycin were purchased from Cellgro Mediatech, Inc. (Herndon, VA). Rosiglitazone (BRL49653) was purchased from Cayman Chemical (Ann Arbor, MI). EA was purchased from Sigma-Aldrich (St. Louis, MO). UroA, B, C, D and iso-UroA were obtained as described elsewhere [21]. All other chemicals and reagents were purchased from Sigma Chemical Co (St. Louis, MO), unless otherwise stated.

### *2.2 Cell culture*

All protocols and procedures were approved by the Institutional Review Board at the University of Nebraska-Lincoln. For isolation of human adipogenic stem cells (hASCs), abdominal adipose tissue was obtained from females with a body mass index (BMI) of ~30 during liposuction or abdominal plastic surgeries. Isolation of hASCs and differentiation of adipocytes was conducted as we described previously [7, 8]. Each independent experiment was repeated at least three times using a pool of hASCs from three or four human subjects to avoid individual variation. Huh7 cells were maintained in Dulbecco's modification of Eagle's medium (DMEM) containing 1% L-glutamine, 10% fetal bovine serum, 100 units/ml penicillin, 100 g/ml streptomycin in 5% CO<sub>2</sub> at 37°C. The medium was changed every 3 days.

### *2.3 Cell viability assay*

The cytotoxic effects of Uro and EA were determined using the XTT Cell Viability Kit (Cell Signaling Technology, Danvers, MA) according to the manufacturer's protocol. Briefly, undifferentiated hASCs, fully differentiated hASCs, and Huh7 cells were cultured in 96-well plates using a seeding density of ~20,000 cells per well. Cells were incubated with either dimethyl sulfoxide (DMSO) or increasing concentrations of Uro and EA for 24 hours (Fig. 2, 5). Culture medium was then replaced with fresh medium containing XTT solution for 3 hours at 37°C before measurement of OD 450 nm using a Synergy™ H1 hybrid plate reader (BioTek, Winooski, VT).

### *2.4 Lipid accumulation*

To measure the lipid accumulation in human adipocytes, cells were fixed with 10% formalin and stained with Oil Red O (ORO). Bright field images were taken by EVOS®

XL microscope (AMG), or ORO dye was extracted by isopropanol to quantify relative TG accumulation (at OD 500 nm).

### *2.5 [14C]-oleic acid (OA) and [3H]-acetate incorporation into FA and TG*

The measurement of TG esterification rate and de novo lipid synthesis in cultures of mature adipocytes or human hepatoma Huh7 cells was conducted as described previously [8]. Briefly, cells were incubated with serum-free low glucose (1,000 mg/L d-(+)-glucose) overnight before the experiment. [14C]-OA (final concentration of 0.5  $\mu$ Ci/mL, Perkin Elmer) and [3H]-acetate (final concentration of 0.5  $\mu$ Ci/mL, Perkin Elmer) were mixed with conditioned media or sodium oleate (Sigma)-Bovine Serum Albumin (BSA, fatty acid free, Sigma) complex, then added to cells for 3 hours. After 3 hours incubation with [14C]-OA and [3H]-acetate, medium (containing unincorporated isotope) was removed by washing with phosphate-buffered saline (PBS). Cellular lipids were extracted using the Bligh and Dyer method [22]. Next, thin layer chromatography was performed to fractionate FA and TG, and the [14C] and [3H] radioactivity was measured by liquid scintillation counting (Tri-Carb 2000TR, Packard). Radioactivity was normalized by protein concentration quantified by bicinchoninic acid (BCA) colorimetric assay (Pierce, Rockford, IL).

### *2.6 Fatty acid oxidation rate using [3H]-OA*

To measure the FA oxidation rate in cultures of mature adipocytes or human hepatoma Huh7 cells, we followed previously published methods [23]. Briefly, cells were incubated with serum-free low glucose (1,000 mg/L d-(+)-glucose) before the experiment. [3H]-OA (final concentration of 0.5  $\mu$ Ci/mL, Perkin Elmer) was mixed with sodium oleate-BSA complex, and then added to cells for 2 hours. [3H] radioactive containing

medium was harvested, and precipitated using trichloroacetic acid (TCA) solution. After precipitation, 6N NaOH was added to reach a final concentration of 0.8-1.0N, resulting in an alkaline supernatant. Next, supernatant was put through columns filled with Dowex™ ion-exchange resin (ACROS Organics™) to capture [3H]-H<sub>2</sub>O. Finally, radioactivity was measured by liquid scintillation counting.

### *2.7 qPCR*

Gene-specific primers for qPCR were obtained from Integrated DNA Technologies (Chicago, IL). Total RNA was isolated using TRIzol® reagent (Invitrogen). To remove any potential genomic DNA contamination, mRNA was treated with DNase (Mediatech), and 2 µg of mRNA was converted into cDNA in a total volume of 20 µl (iScript™ cDNA Synthesis Kit, Bio-Rad). Gene expression was determined by real-time qPCR (ABI7300, Applied Biosystems), and relative gene expression was normalized by 36B4 (primer sequences available in Supplemental Table 1).

### *2.8 Western blot analysis*

To prepare total cell lysates, monolayers of hASC cultures and fully differentiated adipocytes were scraped with ice cold radioimmune precipitation assay (RIPA) buffer (Thermo Scientific) containing protease inhibitors (Sigma) and phosphatase inhibitors (2 mM Na<sub>3</sub>VO<sub>4</sub>, 20 mM β-glycerophosphate and 10 mM NaF). Proteins were fractionated using 8 or 10% SDS-PAGE, transferred to PVDF membranes, and incubated with the relevant antibodies. Chemiluminescence from ECL (Western Lightning) solution was detected using a FluorChem E Imaging System (Cell Biosciences). Polyclonal or monoclonal antibodies targeting phospho-AMP-activated protein kinase (AMPK) (Ser473, #4060), total AMPK (#9279), CCAAT/enhancer binding protein α (C/EBPα

(#2295), fatty acid synthase (Fas) (#3180), and  $\beta$ -actin (#4967) were purchased from Cell Signaling Technology. The mouse monoclonal antibodies for fatty acid binding protein 4 (aP2) (sc-271529) and PPAR $\gamma$  (sc-7273) were purchased from Santa Cruz Biotechnology (Dallas, TX).

### *2.9 Statistical analysis*

Results are presented as means  $\pm$  SEM. The data were statistically analyzed using one-way ANOVA with Tukey's multiple comparison tests. All analyses were performed with GraphPad Prism 5 (Version 5.04).

## **3 Results**

### *3.1. Urolithins do not affect the viability of primary human adipogenic stem cells (hASCs) at concentrations of 0-30 $\mu$ M*

Currently, it is unknown whether Uro affect the cell viability of human adipocytes. To address this question, cytotoxic effects of individual Uro were determined both in undifferentiated hASCs and fully differentiated adipocytes. UroA, B, C, D, iso-UroA and EA were incubated with either hASCs or mature adipocytes for 24 hours before XTT assay. Similar to EA, Uro treatment slightly affected cell bioavailability (~80%) but no specific cytotoxic effects were observed in up to 30  $\mu$ M concentrations (Fig. 1B-G). Based on these results, for the remaining experiments we used the 30  $\mu$ M of Uro in order to augment the potential action but without causing cellular damage.

### *3.2 Urolithins inhibit adipogenesis in hASCs*

We previously demonstrated that EA suppressed adipogenic differentiation in hASCs [7, 8]. To determine whether Uro were able to inhibit adipogenesis, 30  $\mu$ M individual Uro was added to hASCs during differentiation (Fig. 2A). The presence of Uro, but not iso-UroA, caused a significant reduction of TG accumulation measured by ORO staining (Fig. 2A, B). The rank order of anti-adipogenic potential was UroA, C, D  $\gg$  UroB  $>$  iso-UroA as assessed by TG accumulation using ORO staining. To further confirm the anti-adipogenic effects of Uro, adipogenic gene and protein expression levels were determined by qPCR and Western blot. Consistent with reduced TG accumulation, Uro treatment, except for iso-UroA, significantly suppressed adipogenic gene expression including PPAR $\gamma$  and Fas (Fig. 2C). Adipogenic protein expression including aP2, Fas, PPAR $\gamma$ , and C/EBP $\alpha$  were also dramatically reduced in cultures treated with UroC and D and to a lesser magnitude with iso-UroA (Fig. 2D). To gain insight into whether Uro alter epigenetic marks similar to their parent compound EA [7], histone 3 arginine 17 methylation (H3R17me<sub>2</sub>), and histone acetylation (AcH3) levels were examined. Interestingly, only UroC incubation, but no other Uro treatment, markedly suppressed the epigenetic markers (Supplemental Fig. 1).

Several phytochemicals are known to inhibit adipogenesis through the mechanism related to AMPK activation [24-27]. AMPK is a major energy-sensor triggering a variety of catabolic processes and suppressing anabolic pathways simultaneously [28]. Treatment with EA increased AMPK phosphorylation dose-dependently (Fig. 2E). To further identify whether Uro are also able to regulate AMPK activation, we examined phosphorylated and total AMPK levels. Interestingly, UroA, C, and D increased

phosphorylated AMPK levels (Fig. 2F), which is consistent with the trend of the anti-adipogenic role of Uro.

### *3.3 Urolithins attenuate lipid accumulation in cultures of human adipocytes*

Next, we asked whether Uro could antagonize adipocyte hypertrophy. To examine this, fully differentiated cultures of human adipocytes were exposed to Uro for seven days based on the experimental design (Fig. 3A, upper). Exposure to 30  $\mu$ M Uro for seven days caused a significant reduction of TG accumulation, but not UroB and iso-UroA, as measured by ORO staining (Fig. 3A, below). To test whether the reduction of TG accumulation was aligned with lipogenic transcriptional inhibition, we measured mRNA expressions. Uro treatment (A, C, and D) decreased lipogenic-specific gene expression including PPAR $\alpha$ , Fas, adipose triglyceride lipase (ATGL) and steroyl-CoA desaturase-1 (SCD-1) compared to vehicle control (Fig. 3B). UroC and D are potent EA-derived metabolites in upregulating AMPK activation in fully differentiated adipocytes (Fig. 3C).

### *3.4 Urolithins regulate lipid metabolisms in cultures of human adipocytes*

We then investigated whether lipid-lowering effects of Uro are due to an alteration of lipogenic pathways. Fully differentiated adipocytes were incubated with radioactive precursors of [3H]-acetate and [14C]-OA to measure their conversion into [3H]-TG (de novo synthesis of TG) and [14C]-TG (esterification of TG). The conversion of [3H]-acetate into [3H]-TG was significantly dampened in UroA and UroD treated adipocytes (Fig. 4A). Consistently, UroA and D incubation was associated with a significant decrease of conversion of [14C]-OA into [14C]-TG, indicating a decrease of TG esterification by UroA and D (Fig. 4B). To determine whether FA oxidation is

involved in lipid-lowering effects of Uro, we measured FA oxidation rate in Uro-treated adipocytes. FA oxidation by determining [3H]-H<sub>2</sub>O release from [3H]-OA clearly showed that UroA, C, and D markedly increased FA oxidation, but not in iso-UroA and UroB treated adipocytes (Fig. 4C). Taken together, these data implicate that the inhibition of de novo synthesis of TG and FA esterification are accompanied by transcriptional regulation of lipogenic gene expression in Uro-treated human adipocytes.

### *3.5 Urolithins regulate lipid metabolism in Huh7 cells*

We further examined the effects of Uro on TG esterification, de novo synthesis and FA oxidation in human hepatoma Huh7 cells. Prior to analysis of lipid metabolism, we first measured the cytotoxic effects of individual Uro in Huh7 cells. The concentrations (0-30  $\mu$ M) of UroA, B, C, D, iso-UroA and EA treatment slightly affected cell bioavailability (~80%) but no specific cytotoxic effects were observed in up to 30  $\mu$ M concentrations (Fig. 5A). Next, to test whether Uro alter the lipogenic pathways, radiolabeled precursors were incubated with Huh7 cells, as with human adipocytes. Incorporation of [3H]-acetate into [3H]-FA and [3H]-TG were markedly decreased with UroC and D (Fig. 5B and C). Conversion of [14C]-OA into [14C]-TG was clearly inhibited by UroC treatment (Fig. 5D). FA oxidation rate was increased by UroA and C treated Huh7 cells, which was confirmed by [3H]-H<sub>2</sub>O release from [3H]-OA (Fig. 5E).

## **4 Discussion**

Uro are gut microbiota-derived metabolites of EA and ETs. Different types of Uro (Fig. 1A) are produced by intestinal microbes, which may reflect the metabolic health status of hosts [29]. Although it has long been known that Uro may be critical

determinants of the effectiveness of EA supplementation, it is largely unknown whether different species of Uro possess different biological activities in humans. Recently, a number of studies have reported the unique role of Uro species by evaluating their efficacy in various cancer [17, 30], and inflammatory diseases [16, 31]. One recent study [29] and other unpublished observation correlate a higher prevalence of the metabotype producing iso-UroA and UroB in overweight and obese individuals, while UroA is associated with healthy individuals. However, no studies have been conducted to determine the function of individual Uro in human obesity. The present study was specifically designed to assess the role of individual Uro species in manipulating lipid metabolism using primary human adipocytes. Here we demonstrated that UroA, C and D are effective in attenuating TG accumulation and increasing FA oxidation through AMPK-dependent mechanisms in primary human adipocytes as well as in Huh7 cells. These results may provide a novel insight into a ‘structure and function’ relationship among Uro, which may lead to a unique therapeutic design to control adiposity.

An accumulating body of evidence suggests that the gut microbial community affects the host’s energy homeostasis by altering energy metabolism [32-34]. To corroborate this concept, production of different Uro may comprise a part of the mechanism in which gut microbes regulate the host’s energy metabolism. In other words, metabolically healthy subjects may possess microbiota that are able to generate mainly active Uro such as UroA (i.e. subjects belonging to the so-called ‘metabotype A’ [29]). In contrast, metabolically unhealthy humans may have bacterial communities producing UroA but also other less active urolithins such as iso-UroA and UroB (i.e., subjects with ‘metabotype B’ [29]). García-Villalba et al. reported that there were compositional

differences in the gut microbiome between human subjects who produce UroA (effective Uro) and who produce iso-UroA and B (less active Uro) [11]. Also, subjects who have a higher risk of chronic illness produce iso-UroA and UroB [29], the two inactive EA metabolites in our experimental setting (Fig. 2-4). Recently, *Gordonibacter urolithinifaciens sp. nov.* has been identified as a novel bacterial species responsible for converting EA into UroM5 and UroC [35]. This bacterium belongs to the family *Coriobacteriaceae* a family that is associated with benefits in obesity [36]. Since the bacterial phylum that specifically transform EA or its intermediate metabolites into UroA vs. iso-UroA/UroB have not yet been identified, it could be of interest for future studies.

Numerous studies in animals and humans have demonstrated that free EA can be found in no more than 100 nM concentrations after oral administration of EA or ET-containing foods [9, 10]. The low bioavailability of EA is largely due to limited solubility and its rapid metabolism into Uro by the gut microbiome [10]. As a metabolic consequence, Uro can reach relevant concentrations in the blood stream and human colon microenvironment [12, 13]. Although Uro might not be accumulated in metabolic tissues, i.e., adipose tissue, liver or muscle, a few reports have shown that Uro are able to circulate enterohepatically [37]. In terms of cytotoxicity, 50-150  $\mu\text{M}$  of Uro have exhibited anti-cancer properties by inhibiting cell proliferation and cell cycle progression in various carcinoma cell lines [17, 38]. In this study, we first assessed the cytotoxicity of 30  $\mu\text{M}$  concentration in hASCs as well as differentiated cultures of adipocytes. However, Uro treatment does not seem to affect cell viability in non-carcinogenic cells [31], implying that Uro might induce apoptosis in malignant tumor cells but not in mitogenically quiescent cells. Consistently, our results showed that 30  $\mu\text{M}$  Uro

treatments showed no sign of cytotoxicity in time frames of both early- and terminal-stages of adipogenesis. The anti-adipogenic and anti-lipogenic effects of Uro in our study were not due to the apoptotic property of Uro (Fig. 1B-G). Thus, we regarded 30  $\mu$ M of Uro as a non-toxic concentration to assess potency of individual Uro in regulating lipid metabolism in human adipocytes. In our study, Uro treatment in adipocytes was associated with at least three metabolic outcomes: 1) attenuating adipogenesis, 2) inhibiting TG accumulation, and 3) increasing AMPK activation.

The major distinctive metabolic consequences that we immediately noticed was that Uro differentially impacted adipogenesis in hASCs. UroA, C and D treatment, but not iso-UroA or UroB, interfered with adipogenic differentiation (Fig. 2). Recently, estrogen receptor  $\alpha$  (ER $\alpha$ ) has been proposed as a negative regulator of adipocyte development in preadipocytes [39]. Interestingly, Larrosa et al. showed that UroA possesses higher ER $\alpha$  binding affinity than UroB in breast cancer cells suggesting that UroA plays a role as a phytoestrogen (ER binding affinity of UroA:  $\alpha > \beta$ ) [40]. In terms of structural differences, EA, UroA, C and D have common hydroxyl position at number 8 carbon (-OH at C8) compared to iso-UroA or UroB. González-Sarrías et al. also proposed that phase II phenolic enzymatic activities are crucially affected by reactive moieties such as hydroxyl groups [17]. This interpretation aligns with our results showing that the absence of -OH moiety at C8 position of Uro, due to isomerism (iso-UroA) or metabolic loss (UroB) is inversely correlated with the ability to downregulate adipogenic differentiation. Thus, it may also be reasonable to assume that -OH moiety at C8 position might affect binding affinity to ER. Further studies are necessary to validate the aforementioned structure-function relationship in adipogenic differentiation. The other

possible mechanism of Uro's anti-adipogenic effect could be explained by its ability to alter epigenetic marks. We have previously shown that EA modified histone methyltransferase (CARM1) enzyme activities during adipogenesis [7]. Consistently, we were able to observe that UroC downregulated histone arginine 17 methylation during adipogenesis (Supplemental Fig. 1). UroC was also reported to reduce TNF $\alpha$ -induced inflammation through inhibition of histone acetyltransferase (HAT) activity in the monocyte cell [41]. At this point, we speculate UroC may have stronger DNA binding affinity comparable to EA [42, 43] than the other Uro intermediates, conferring ability to edit epigenetic codes such as histone methylation and/or acetylation. Collectively, differential regulation of adipogenesis by Uro likely originates from their structural difference of Uro. Future studies are required to scrutinize the metabolic contribution of C8 hydroxyl moiety of Uro to ER binding affinity, CARM1 activity, and AMPK activation.

Subsequently, we examined the potential role of Uro in regulating lipid metabolism in fully differentiated adipocytes and hepatoma Huh7 cells. Previously, we showed that EA modulates global lipid metabolism by attenuating TG accumulation in both adipocytes and hepatocytes [8]. This TG-lowering effect seems to be conserved in mammalian cells [8] and even in yeasts (data not shown). In this current research setting, we found that Uro effectively reduced de novo synthesis and TG esterification and enhanced FA oxidation in adipocytes (Fig. 3, 4). These data revealed that EA apparently gradually lost its ability to downregulate lipid accumulation while EA is successively metabolized by gut microbes until its conversion to the least effective UroB. Therefore, the potency of Uro in regulating TG metabolism could be ranked as earlier metabolites

(UroC and D) > intermediate metabolite (UroA) > later metabolite (UroB). Agreeing to the fact that EA shows a global impact in lowering lipids in various cells, Uro were also effective in attenuating TG accumulation in Huh7 cells (Fig. 5). The simultaneous lipid-lowering action in both adipocytes and hepatocytes is one of the ultimate goals for weight loss as dietary intervention agents. To accomplish this goal, upregulation of FA oxidation is critical; otherwise the failure of FA accumulation in adipose tissue triggers lipotoxicity and hepatic steatosis. It is interesting that UroC was more potent in modulating TG accumulation than UroD in hepatocytes. More noticeably, UroA, C and D significantly elevated FA oxidation ( $[3H]\text{-OA} \rightarrow [3H]\text{-H}_2\text{O}$ ) in hepatocytes, satisfying the criteria for effective dietary supplementation to mitigate lipid accumulation both in adipocytes and hepatocytes. Further studies should be conducted to determine the efficacy of UroC, D and A in vivo.

Lastly, we have found AMPK activation could be a link mediating anti-adipogenic and anti-lipogenic effects of Uro. AMPK is an energy sensor that shuts down anabolic pathways [44]. Phosphorylation of AMPK inhibits transcriptional activation for adipogenesis, TG synthesis, and FA oxidation [45]. Here, we showed EA promotes AMPK activation during adipogenesis of hASC (Fig. 2E); Wang et al. also showed the implication of AMPK activation by EA in 3T3-L1 cells [46]. Consistently, our results showed that upregulation of AMPK phosphorylation by UroA, C, and D attenuated: i) adipogenesis (Fig. 2); ii) de novo lipogenesis (gene expressions and metabolic conversion of radiolabeled precursors) and TG esterification (Fig. 3, 4, 5); and iii) FA oxidation (Fig. 4, 5). Our in vivo data also supports that ET-containing raspberry seed flour supplementation promotes AMPK activation in adipose tissue against high fat and high

sugar fed C57BL/6 mice (under review), thereby leading to attenuation of adiposity. Consistently, the recent animal study showed that punicalagin (ET)-enriched pomegranate consumption prevents obesity associated-cardiac metabolic disorders through AMPK activation [47]. The regulation of AMPK by the structural specificity of EA and Uro will be of interest for future study to further elucidate the ultimate role of EA in regulating lipid metabolism.

In our study, we revealed the previously unknown function of Uro, gut metabolites of EA, as potential regulators of lipid metabolism in adipocytes. We also compared whether individual Uro could exert a differential impact on lipogenesis and FA oxidation in adipocytes and hepatocytes. We identified that UroA, C, and D are more plausible to reduce TG accumulation, but not iso-UroA and UroB. Whether the differential impact of Uro in lipid metabolism is dictated by structural differences of Uro, and these initial findings *in vitro* will be confirmed *in vivo*, must await future studies. Also, following studies should define whether the mode of action from the tentative mixtures of Uro (that are pertinent to human physiology) would be additive, synergistic and/or counteractive. Nevertheless, we believe that our study sheds new insight into Uro, gut metabolites of EA, as new dietary strategies to attenuate adiposity by activation of AMPK.

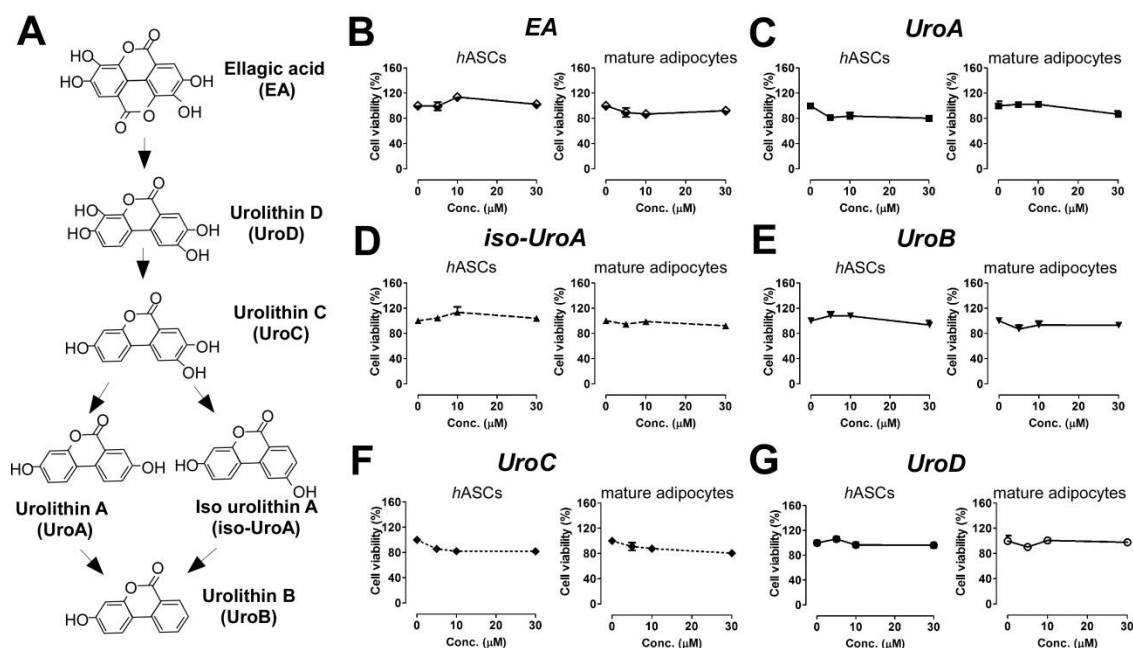


**Figure V -1 Metabolism of EA to produce Uro and the effects of Uro on cell viability in primary human adipocytes.**

(A) Microbial enzymatic transformation to produce a series of Uro metabolites from EA. Chemical structures of test compounds are shown. Culture of *hASCs* containing undifferentiated and differentiated cells were treated with either 10 μM EA (B) or 30 μM UroA (C), iso-Uro A (D), UroB (E), UroC (F), and UroD (G) for 24 hours. XTT reagent was added 3 hours before measurement of OD 450nm. Data are expressed as a percentage of the vehicle control (DMSO). Each data point represents the mean ± S.E.M (n=3).

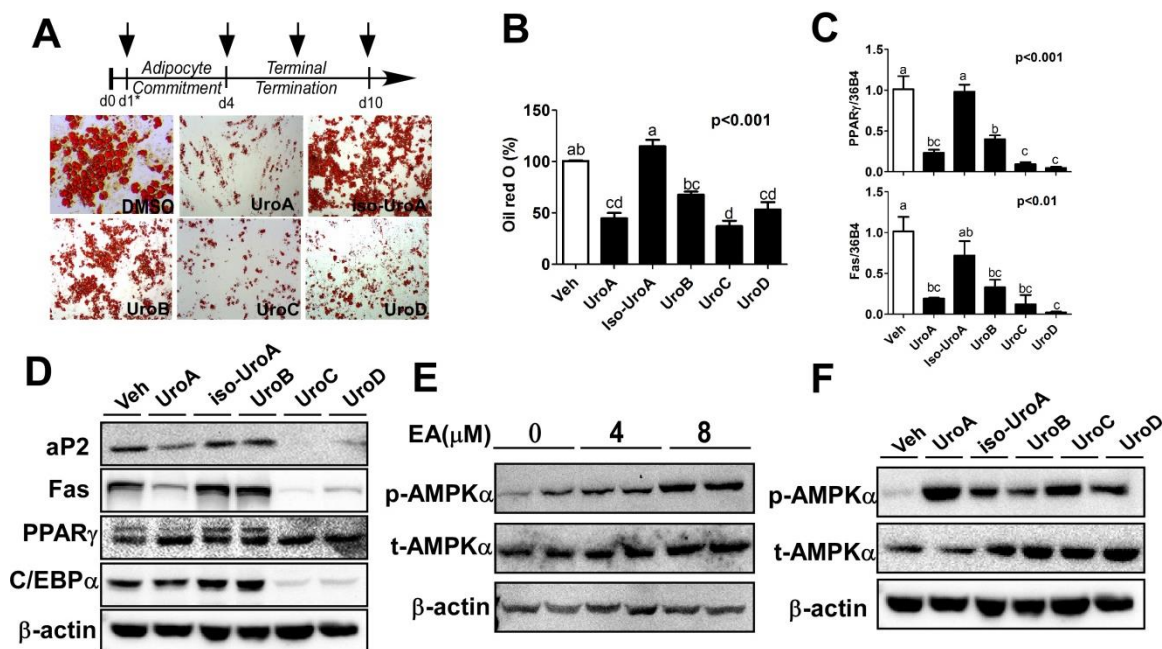


**Figure V -2 Uro, but not iso-UroA, suppressed adipogenesis in *h*ASCs.**

(A, upper) Experimental Scheme: *h*ASCs were seeded the day before differentiation (d0). Cultures of *h*ASCs were induced to differentiation (d1\*) in the presence of either DMSO (vehicle control) or 30  $\mu$ M Uro for 10 days. (A, below) Triglyceride accumulation was visualized by Oil Red O staining and representative images from three separate experiments are shown. (B) Extracted staining was quantified (OD 500 nm) and relative TG accumulations to the DMSO control are shown. (C) Adipogenic gene expression of PPAR $\gamma$ , and Fas by qPCR. (D) Adipogenic protein expressions of aP2, Fas, PPAR $\gamma$ , and C/EBP $\alpha$  by Western blot analysis. (E) Culture of *h*ASCs was differentiated for 2 days in the presence or absence of 0, 4, and 8  $\mu$ M EA. Total cell extracts were immunoblotted with phosphor or total antibodies targeting AMPK. (F) Immunoblot of phosphor or total antibodies targeting AMPK in Uro treated *h*ASCs. All values are presented as the mean  $\pm$ S.E.M. Bars with different letters are significantly different by one-way ANOVA.

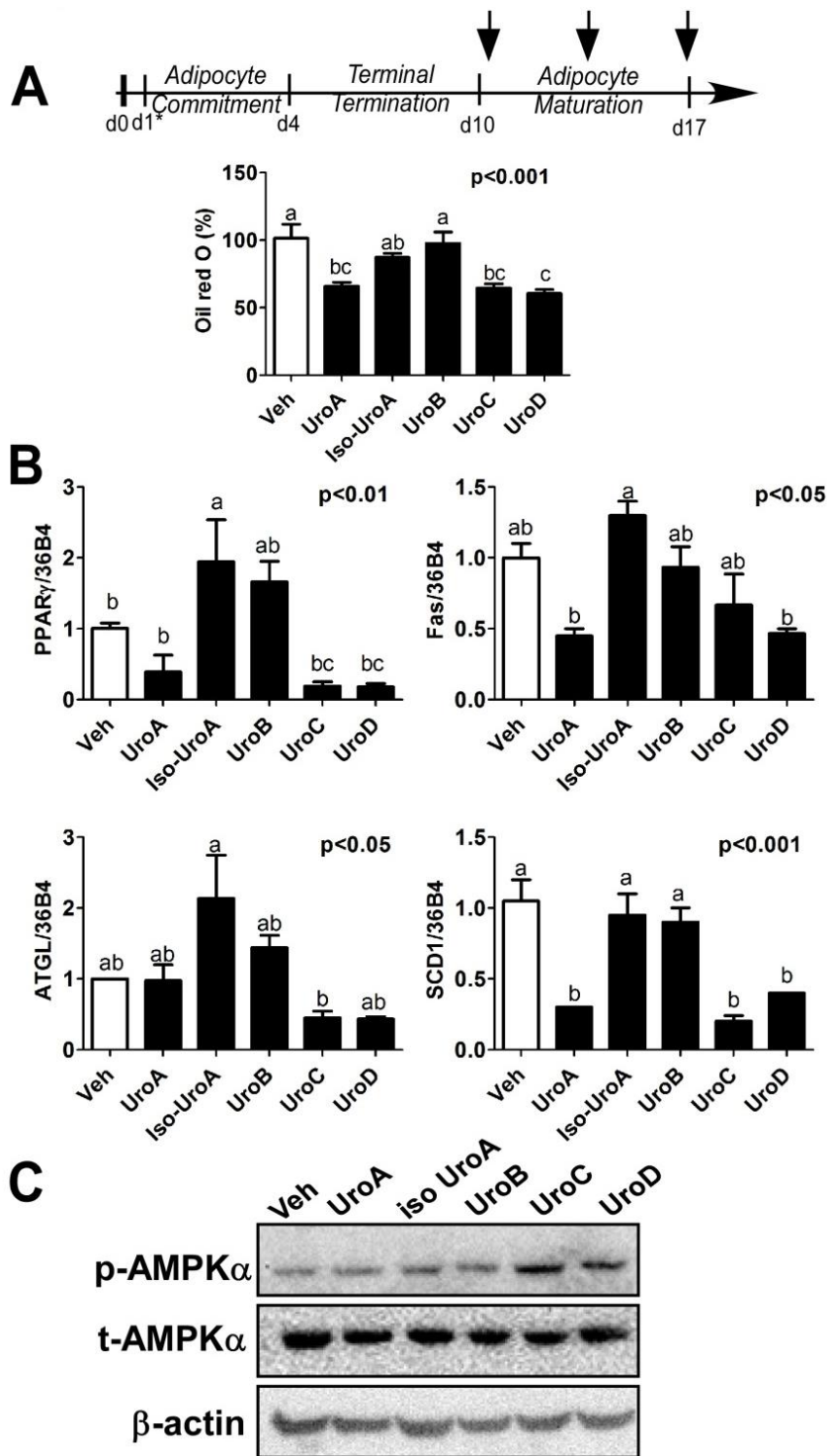


**Figure V -3 Uro, but not iso-UroA, suppressed lipogenesis in mature human adipocytes.**

(A, upper) Experimental Scheme: *hASCs* were seeded the day before differentiation (d0) and induced to differentiation (d1\*). *hASCs* were kept differentiated into fully differentiated adipocytes until d10. 30  $\mu\text{M}$  Uro was added to the fully differentiated human adipocytes (d10) and incubated for 7 days. (A, below) Relative TG accumulations stained by Oil Red O. (B) Relative gene expressions levels of PPAR $\gamma$ , Fas, ATGL and SCD1 by qPCR. (C) Cultures of fully differentiated adipocytes were treated with 30  $\mu\text{M}$  Uro for 3 days. Total cell extracts were immunoblotted with phosphor or total antibodies targeting AMPK. All values are presented as the mean  $\pm$ S.E.M. Bars with different letters are significantly different by one-way ANOVA.

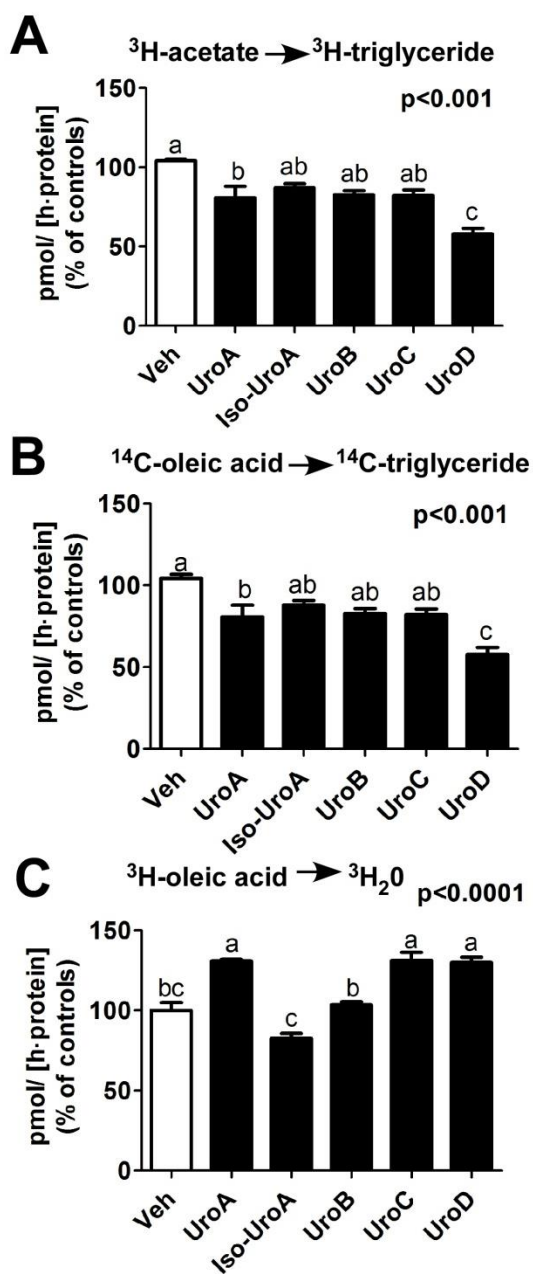


**Figure V -4 Uro regulated lipid metabolisms in human adipocytes.**

Uro (30  $\mu\text{M}$ ) was added to the differentiated human adipocytes (d10) and incubated for 3 days.

(A) Conversion of [ $^3\text{H}$ ]-acetate into [ $^3\text{H}$ ]-TG.

(B) Conversion of [ $^{14}\text{C}$ ]-OA into [ $^{14}\text{C}$ ]-TG.

(C) [ $^3\text{H}$ ]-OA into [ $^3\text{H}$ ]- $\text{H}_2\text{O}$ . All values are presented as the mean  $\pm$ S.E.M. Bars with different letters are significantly different by one-way ANOVA.

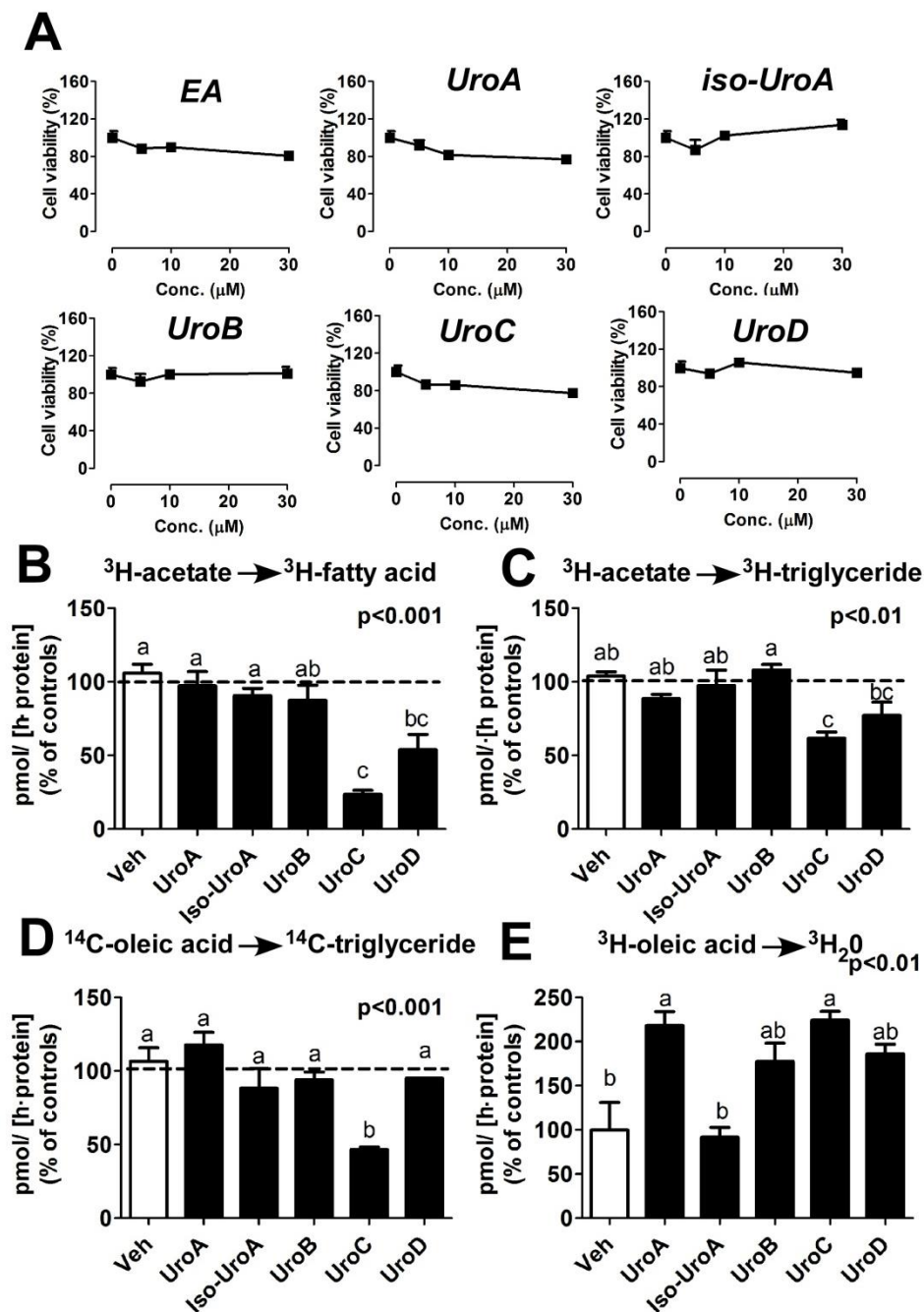
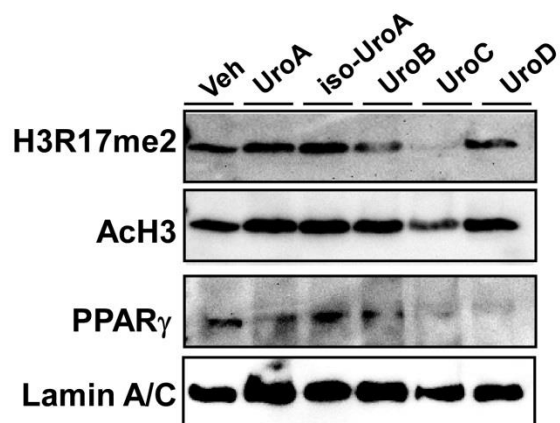


**Figure V -5 Uro, but not iso-UroA, regulated lipid mechanisms in human hepatoma Huh7 cells.**

(A) Cultures of Huh7 cells were treated with either 10  $\mu\text{M}$  EA or 30  $\mu\text{M}$  UroA, iso-UroA, UroB, UroC, and UroD for 24 hours. XTT reagent was added 3 hours before

measurement of OD 450nm. Huh7 cells were pre-incubated with Uro (30  $\mu$ M) for 48 hours and 0.4 or 0.8 mM BSA-OA complex was loaded for 3 hours with radiolabeled precursors ( $[^3\text{H}]$ -acetate,  $[^{14}\text{C}]$ -OA,  $[^3\text{H}]$ -OA). (B) Conversion of  $[^3\text{H}]$ -acetate into  $[^3\text{H}]$ -FA. (C) Conversion of  $[^3\text{H}]$ -acetate into  $[^3\text{H}]$ -TG. (D) Conversion of  $[^{14}\text{C}]$ -OA into  $[^{14}\text{C}]$ -TG. (E) Conversion of  $[^3\text{H}]$ -OA into  $[^3\text{H}]$ -H<sub>2</sub>O. All values are presented as the mean  $\pm$ S.E.M. Bars with different letters are significantly different by one-way ANOVA.

## Supplemental Figure 1



**Supplemental Fig. 1.** Cultures of *hASCs* were induced to differentiation (d1) in the presence of either DMSO (vehicle control) or 30  $\mu$ M Uro for 10 days. Nuclear extracts from Uro treated *hASCs* were immunoblotted for histone modification enzyme (H3R17me2, AcH3, and PPAR $\gamma$ ).

## Supporting Information

**Supplemental Table 1.** Primer sequences for qPCR

<b>Gene</b>	<b>Forward/Reverse</b>	<b>Sequence (5'-3')</b>
h36B4	Forward	GAAGGCTGTGGTGCTGATG
	Reverse	GTGAGGTCCTCCTTGGTGAA
hATGL	Forward	CTGACCACCCTCTCCAACAT
	Reverse	ACCAGGTAAGTGGCAGATGCT
hFas	Forward	GGCAAGCTGAAGGACCTGTCTA
	Reverse	AATCTGGGTTGATGCCTCCGT
hPPAR $\gamma$	Forward	TGCTGTTATGGGTGAAACTCTG
	Reverse	TCAAAGGAGTGGGAGTGGTC
hSCD1	Forward	GGGTGAGGGCTTCCACAATA
	Reverse	CGGCCATGCAATCAATGAA

## References

- [1] Yu, Y. M., Chang, W. C., Wu, C. H., Chiang, S. Y., Reduction of oxidative stress and apoptosis in hyperlipidemic rabbits by ellagic acid. *J.Nutr.Biochem.* 2005, 16, 675-681.
- [2] Park, S. H., Kim, J. L., Lee, E. S., Han, S. Y., et al., Dietary ellagic acid attenuates oxidized LDL uptake and stimulates cholesterol efflux in murine macrophages. *J.Nutr.* 2011, 141, 1931-1937.
- [3] Losso, J. N., Bansode, R. R., Trappey, A., Bawadi, H. A., Truax, R., In vitro anti-proliferative activities of ellagic acid. *J.Nutr.Biochem.* 2004, 15, 672-678.
- [4] Panchal, S. K., Ward, L., Brown, L., Ellagic acid attenuates high-carbohydrate, high-fat diet-induced metabolic syndrome in rats. *Eur J.Nutr.* 2013, 52, 559-568.
- [5] Lei, F., Zhang, X. N., Wang, W., Xing, D. M., et al., Evidence of anti-obesity effects of the pomegranate leaf extract in high-fat diet induced obese mice. *Int.J.Obes.(Lond)* 2007, 31, 1023-1029.
- [6] Gourineni, V., Shay, N. F., Chung, S., Sandhu, A. K., Gu, L., Muscadine Grape ( *Vitis rotundifolia* ) and Wine Phytochemicals Prevented Obesity-Associated Metabolic Complications in C57BL/6J Mice. *J.Agric.Food Chem.* 2012, 60, 7674-7681.
- [7] Kang, I., Okla, M., Chung, S., Ellagic acid inhibits adipocyte differentiation through coactivator-associated arginine methyltransferase 1-mediated chromatin modification. *J.Nutr.Biochem.* 2014, 25, 946-953.
- [8] Okla, M., Kang, I., Kim, d. M., Gourineni, V., et al., Ellagic acid modulates lipid accumulation in primary human adipocytes and human hepatoma Huh7 cells via discrete mechanisms. *J.Nutr.Biochem.* 2015, 26, 82-90.
- [9] Seeram, N. P., Lee, R., Heber, D., Bioavailability of ellagic acid in human plasma after consumption of ellagitannins from pomegranate (*Punica granatum* L.) juice. *Clin.Chim.Acta.* 2004, 348, 63-68.
- [10] González-Sarrías, A., García-Villalba, R., Núñez-Sánchez, M. Á., Tomé-Carneiro, J., et al., Identifying the limits for ellagic acid bioavailability: A crossover pharmacokinetic study in healthy volunteers after consumption of pomegranate extracts. *J.Funct.Foods.*2015, 19, Part A, 225-235.
- [11] Garcia-Villalba, R., Beltran, D., Espin, J. C., Selma, M. V., Tomas-Barberan, F. A., Time course production of urolithins from ellagic acid by human gut microbiota. *J.Agric.Food Chem.* 2013, 61, 8797-8806.
- [12] Espin, J. C., Larrosa, M., Garcia-Conesa, M. T., Tomas-Barberan, F., Biological significance of urolithins, the gut microbial ellagic Acid-derived metabolites: the evidence so far. *Evid.Based Complement.Alternat.Med.* 2013, 2013, 270418.
- [13] Cerda, B., Espin, J. C., Parra, S., Martinez, P., Tomas-Barberan, F. A., The potent in vitro antioxidant ellagitannins from pomegranate juice are metabolised into bioavailable but poor antioxidant hydroxy-6H-dibenzopyran-6-one derivatives by the colonic microflora of healthy humans. *Eur J.Nutr.* 2004, 43, 205-220.

- [14] Seeram, N. P., Henning, S. M., Zhang, Y., Suchard, M., et al., Pomegranate juice ellagitannin metabolites are present in human plasma and some persist in urine for up to 48 hours. *J.Nutr.* 2006, 136, 2481-2485.
- [15] Nunez-Sanchez, M. A., Garcia-Villalba, R., Monedero-Saiz, T., Garcia-Talavera, N. V., et al., Targeted metabolic profiling of pomegranate polyphenols and urolithins in plasma, urine and colon tissues from colorectal cancer patients. *Mol. Nutr. Food Res.* 2014, 58, 1199-1211.
- [16] Larrosa, M., Gonzalez-Sarrias, A., Yanez-Gascon, M. J., Selma, M. V., et al., Anti-inflammatory properties of a pomegranate extract and its metabolite urolithin-A in a colitis rat model and the effect of colon inflammation on phenolic metabolism. *J.Nutr.Biochem.* 2010, 21, 717-725.
- [17] Gonzalez-Sarrias, A., Gimenez-Bastida, J. A., Nunez-Sanchez, M. A., Larrosa, M., et al., Phase-II metabolism limits the antiproliferative activity of urolithins in human colon cancer cells. *Eur J.Nutr.* 2014, 53, 853-864.
- [18] Adams, L. S., Zhang, Y., Seeram, N. P., Heber, D., Chen, S., Pomegranate ellagitannin-derived compounds exhibit antiproliferative and antiaromatase activity in breast cancer cells in vitro. *Cancer Prev.Res.(Phila)* 2010, 3, 108-113.
- [19] Verzelloni, E., Pellacani, C., Tagliazucchi, D., Tagliaferri, S., et al., Antiglycative and neuroprotective activity of colon-derived polyphenol catabolites. *Mol. Nutr. Food Res.* 2011, 55 Suppl 1, S35-43.
- [20] Bialonska, D., Kasimsetty, S. G., Khan, S. I., Ferreira, D., Urolithins, intestinal microbial metabolites of Pomegranate ellagitannins, exhibit potent antioxidant activity in a cell-based assay. *J.Agric.Food Chem.* 2009, 57, 10181-10186.
- [21] Garcia-Villalba, R., Espin, J. C., Tomas-Barberan, F. A., Chromatographic and spectroscopic characterization of urolithins for their determination in biological samples after the intake of foods containing ellagitannins and ellagic acid. *J. Chromatogr. A.* 2015. doi: 10.1016/j.chroma.2015.08.044.
- [22] Bligh, E. G., Dyer, W. J., A rapid method of total lipid extraction and purification. *Can. J. Biochem. Physiol.* 1959, 37, 911-917.
- [23] Olpin, S. E., Manning, N. J., Pollitt, R. J., Clarke, S., Improved detection of long-chain fatty acid oxidation defects in intact cells using [9,10-3H]oleic acid. *J. Inherit. Metab. Dis.* 1997, 20, 415-419.
- [24] Hwang, J. T., Park, I. J., Shin, J. I., Lee, Y. K., et al., Genistein, EGCG, and capsaicin inhibit adipocyte differentiation process via activating AMP-activated protein kinase. *Biochem. Biophys. Res. Commun.* 2005, 338, 694-699.
- [25] Jeong, M. Y., Kim, H. L., Park, J., An, H. J., et al., Rubi Fructus (*Rubus coreanus*) Inhibits Differentiation to Adipocytes in 3T3-L1 Cells. *Evid.Based Complement.Alternat.Med.* 2013, 2013, 475386.
- [26] Chen, S., Li, Z., Li, W., Shan, Z., Zhu, W., Resveratrol inhibits cell differentiation in 3T3-L1 adipocytes via activation of AMPK. *Can J. Physiol. Pharmacol.* 2011, 89, 793-799.
- [27] Choi, H. S., Jeon, H. J., Lee, O. H., Lee, B. Y., Dieckol, a major phlorotannin in *Ecklonia cava*, suppresses lipid accumulation in the adipocytes of high-fat diet-fed

- zebrafish and mice: Inhibition of early adipogenesis via cell-cycle arrest and AMPK $\alpha$  activation. *Mol. Nutr. Food Res.* 2015, 59, 1458-1471.
- [28] Hardie, D. G., Ross, F. A., Hawley, S. A., AMPK: a nutrient and energy sensor that maintains energy homeostasis. *Nat. Rev. Mol. Cell. Biol.* 2012, 13, 251-262.
- [29] Tomas-Barberan, F. A., Garcia-Villalba, R., Gonzalez-Sarrias, A., Selma, M. V., Espin, J. C., Ellagic acid metabolism by human gut microbiota: consistent observation of three urolithin phenotypes in intervention trials, independent of food source, age, and health status. *J.Agric.Food Chem.* 2014, 62, 6535-6538.
- [30] Gonzalez-Sarrias, A., Espin, J. C., Tomas-Barberan, F. A., Garcia-Conesa, M. T., Gene expression, cell cycle arrest and MAPK signalling regulation in Caco-2 cells exposed to ellagic acid and its metabolites, urolithins. *Mol. Nutr. Food Res.* 2009, 53, 686-698.
- [31] Piwowarski, J. P., Kiss, A. K., Granica, S., Moeslinger, T., Urolithins, gut microbiota-derived metabolites of ellagitannins, inhibit LPS-induced inflammation in RAW 264.7 murine macrophages. *Mol. Nutr. Food Res.* 2015.
- [32] Backhed, F., Ding, H., Wang, T., Hooper, L. V., et al., The gut microbiota as an environmental factor that regulates fat storage. *Proc.Natl.Acad.Sci.U.S.A* 2004, 101, 15718-15723.
- [33] Backhed, F., Manchester, J. K., Semenkovich, C. F., Gordon, J. I., Mechanisms underlying the resistance to diet-induced obesity in germ-free mice. *Proc.Natl.Acad.Sci.U.S.A* 2007, 104, 979-984.
- [34] Turnbaugh, P. J., Ley, R. E., Mahowald, M. A., Magrini, V., et al., An obesity-associated gut microbiome with increased capacity for energy harvest. *Nature.* 2006, 444, 1027-1031.
- [35] Selma, M. V., Beltran, D., Garcia-Villalba, R., Espin, J. C., Tomas-Barberan, F. A., Description of urolithin production capacity from ellagic acid of two human intestinal *Gordonibacter* species. *Food Funct.* 2014, 5, 1779-1784.
- [36] Clavel, T., Desmarchelier, C., Haller, D., Gérard, P., et al., Intestinal microbiota in metabolic diseases. *Gut Microbes.* 2014, 5, 544-551.
- [37] Espin, J. C., Gonzalez-Barrio, R., Cerda, B., Lopez-Bote, C., et al., Iberian pig as a model to clarify obscure points in the bioavailability and metabolism of ellagitannins in humans. *J.Agric.Food Chem.* 2007, 55, 10476-10485.
- [38] Cho, H., Jung, H., Lee, H., Yi, H. C., et al., Chemopreventive activity of ellagitannins and their derivatives from black raspberry seeds on HT-29 colon cancer cells. *Food Funct.* 2015, 6, 1675-1683.
- [39] Pedram, A., Razandi, M., Blumberg, B., Levin, E. R., Membrane and nuclear estrogen receptor  $\alpha$  collaborate to suppress adipogenesis but not triglyceride content. *FASEB J.* 2015.
- [40] Larrosa, M., Gonzalez-Sarrias, A., Garcia-Conesa, M. T., Tomas-Barberan, F. A., Espin, J. C., Urolithins, ellagic acid-derived metabolites produced by human colonic microflora, exhibit estrogenic and antiestrogenic activities. *J.Agric.Food Chem.* 2006, 54, 1611-1620.

- [41] Kiss, A. K., Granica, S., Stolarczyk, M., Melzig, M. F., Epigenetic modulation of mechanisms involved in inflammation: Influence of selected polyphenolic substances on histone acetylation state. *Food. Chem.* 2012, 131, 1015-1020.
- [42] Teel, R. W., Ellagic acid binding to DNA as a possible mechanism for its antimutagenic and anticarcinogenic action. *Cancer. Lett.* 1986, 30, 329-336.
- [43] Mandal, S., Shivapurkar, N. M., Galati, A. J., Stoner, G. D., Inhibition of N-nitrosobenzylmethylamine metabolism and DNA binding in cultured rat esophagus by ellagic acid. *Carcinogenesis.* 1988, 9, 1313-1316.
- [44] Canto, C., Gerhart-Hines, Z., Feige, J. N., Lagouge, M., et al., AMPK regulates energy expenditure by modulating NAD<sup>+</sup> metabolism and SIRT1 activity. *Nature.* 2009, 458, 1056-1060.
- [45] Kahn, B. B., Alquier, T., Carling, D., Hardie, D. G., AMP-activated protein kinase: ancient energy gauge provides clues to modern understanding of metabolism. *Cell. Metab.* 2005, 1, 15-25.
- [46] Wang, L., Li, L., Ran, X., Long, M., et al., Ellagic Acid Reduces Adipogenesis through Inhibition of Differentiation-Prevention of the Induction of Rb Phosphorylation in 3T3-L1 Adipocytes. *Evid.Based Complement.Alternat.Med.* 2013, 2013, 287534.
- [47] Cao, K., Xu, J., Pu, W., Dong, Z., et al., Punicalagin, an active component in pomegranate, ameliorates cardiac mitochondrial impairment in obese rats via AMPK activation. *Sci. Rep.* 2015, 5, 14014.

## Supporting Information

**Supplemental Table 1.** Primer sequences for qPCR

<b>Gene</b>	<b>Forward/Reverse</b>	<b>Sequence (5'-3')</b>
h36B4	Forward	GAAGGCTGTGGTGCTGATG
	Reverse	GTGAGGTCCTCCTTGGTGAA
hATGL	Forward	CTGACCACCCTCTCCAACAT
	Reverse	ACCAGGTACTGGCAGATGCT
hFas	Forward	GGCAAGCTGAAGGACCTGTCTA
	Reverse	AATCTGGGTTGATGCCTCCGT
hPPAR $\gamma$	Forward	TGCTGTTATGGGTGAAACTCTG
	Reverse	TCAAAGGAGTGGGAGTGGTC
hSCD1	Forward	GGGTGAGGGCTTCCACAATA
	Reverse	CGGCCATGCAATCAATGAA

## OUTLOOK

The results indicated that 10  $\mu$ M of EA inhibits adipogenic conversion as well as hypertrophic lipid accumulation in *h*ASCs. Distinctive mechanisms are involved for reduction of lipid accumulation by EA in adipocytes. 1) During adipogenesis, EA reduced CARM1 activity results in a decrease of H3R17me2 levels, which may interrupt consecutive histone remodeling steps for adipocyte differentiation including histone acetylation and HDAC9 dissociation from chromatin. 2) During the mature stage of adipogenesis, EA reduced TG levels, glucose uptake and conversion of acetyl CoA to TG, but no significant impact on FA uptake or FA conversion to TG. Consistently, EA reduced TG contents in Huh7 hepatoma cells, which was accompanied by reduction of FA uptake, FA esterification into TG, *de novo* synthesis of TG as well as augmentation of FA oxidation. These lipid-lowering effects of EA *in vitro* were further confirmed *in vivo* by using C57BL6/J mice. EA supplementation by RSF (3% in diet) significantly reduced HFHS diet-induced body weight gain and dyslipidemia and improved insulin resistance. Furthermore, EA supplementation ameliorated fructose-induced hepatic toxicity through inhibition of ER/oxidative stress, which indirectly attenuated adipose/systemic inflammation. Lastly, we found the evidence that gut microbiota-derived metabolites, Uro, might resemble anti-adipogenic/lipogenic effects of EA. UroA, C, and D were biologically active metabolites to reduce lipid accumulation in both adipocyte and hepatocytes, which was comparable with EA treatment. Overall, these data suggested that EA is a potent dietary factor to attenuating obesity and Uro may be used as novel metabolites mediating EA's effects on obesity and metabolic disorders.

These outcomes describe the association between EA treatment/ intake and outcomes in reducing obesity and obesity-associated complications. Mechanistic studies should be conducted to investigate EA's anti-obesity effect. Secondly, dose-reponse studies in animal studies will be needed to determine the efficacy and safety ranges of EA dose. Determination of tissue distribution and plasma peak concentration of EA and EA-metabolites after consumption of EA will be informative. As emerging evidence indicates that Uro may potentiate or nullify the health benefits of EA, the health beneficial results of EA will be compared between control conventional mice and germ-free mice and/or anti-biotic treated model (no Uro produced group). This experiment is also significant in defining a potential role of gut microbiome ecology in lipid metabolisms. Regarding epigenetic regulation, as CARM1 is a key regulator to control adipogenesis by EA in adipose tissue, determine the adipose tissue-specific role of CARM1 in obesity-related disease would be of interest. Lastly, for practical applications the effects of EA fortification on the physical and chemical properties of the food products should be determined.